Multi-decker assemblies from porphyrin derivatives

Reem Ali Al-Yami

This thesis is submitted in partial fulfilment of the requirements of the degree of Doctor of Philosophy at the University of East Anglia

Supervised by Prof Andrew N. Cammidge

March 2025

Declaration

The research described in this thesis is, to the best of my knowledge, original and my own work except where due reference has been made.

Reem Al-Yami

Abstract

There has been a huge development in the study of sandwich-type complexes over the past few decades. The work set out in this thesis focuses on the synthesis and investigations of linked heteroleptic triple-deckers (TDs) based on porphyrin-porphyrin-porphyrin. They are interesting materials because of the potential applications of the lanthanide-bridged triple deckers in single-molecule magnets (SMM) and in thin-film transistors (OTFT). This thesis describes various methods for the synthesis of lanthanide mixed-porphyrin triple-decker complexes. These triple-deckers are formed from a symmetrical dyad containing two porphyrin molecules linked together by a flexible decyl or dodecyl chain. The optimisation of the synthesis of these dyads, and the precursor monohydroxyphenyl porphyrin (TPPOH), took significant time and the improvements are discussed in detail. Triple-decker synthesis focused mostly on the use of commercially available octaethylporphyrin (OEP). Unlike the smooth synthesis of related triple deckers employing phthalocyanine as the third ring, reported by our group and found to exclusively produce the symmetrical TD with the phthalocyanine in the middle, syntheses using OEP were more challenging. Conditions for the synthesis were eventually achieved, and they are discussed. Most interestingly, the isolated TD has a different structure to that previously observed with phthalocyanine, in that OEP is found to occupy an external site in the sandwich (BAA structure). Complexes with La, Nd, and Pr were successfully prepared and characterised, and crystals suitable for XRD analysis were obtained to prove the assignment of the BAA arrangement. Other porphyrins (octamethyl porphyrin, tetraphenyl porphyrin, protoporphyrin) were briefly examined and gave mixed results. While inconclusive, the results demonstrate scope for further development of this triple-decker chemistry to deliver a range of heteroleptic complexes where the order of assembly is controlled by (presumably) steric factors.

Access Condition and Agreement

Duplication or sale of all or part of any of the Data Collections is not permitted, except that material may be duplicated by you for your research use or for educational purposes in electronic or print form. You must obtain permission from the copyright holder, usually the author, for any other use. Exceptions only apply where a deposit may be explicitly provided under a stated licence, such as a Creative Commons licence or Open Government licence.

Electronic or print copies may not be offered, whether for sale or otherwise to anyone, unless explicitly stated under a Creative Commons or Open Government license. Unauthorised reproduction, editing or reformatting for resale purposes is explicitly prohibited (except where approved by the copyright holder themselves) and UEA reserves the right to take immediate 'take down' action on behalf of the copyright and/or rights holder if this Access condition of the UEA Digital Repository is breached. Any material in this database has been supplied on the understanding that it is copyright material and that no quotation from the material may be published without proper acknowledgement.

Dedication

This thesis is dedicated to my late father, Ali Al-Yami, who was the light of my life and whose unexpected passing on November 2, 2023, left an indelible void in my heart, and my grand-mother, Noura Al-Dubaikhi, who was equally dear to me and whose unexpected passing on November 24, 2019, profoundly impacted my life.

Additionally, I dedicate this work to my beloved children, Rawan, Raghad, Abdullah, and Osama Al-Shammari, whose kindness and love inspire me daily and everyone. I extend this dedication to my cherished mother and my two incredible sisters, Anwar and Norah Al-Yami, whose unwavering support has been a source of strength throughout this journey. Lastly, I dedicate this work to my brother Mohammed Al-Yami and to everyone who loves me.

Acknowledgements

I express my deepest gratitude to Allah for guiding me throughout my career, granting me health and safety, and providing me with the strength to overcome challenges, and I pray for continued blessings in all aspects of my life. I would like to extend a heartfelt thank you to Professor Andrew Cammidge. Meeting him has been a great privilege, and his unwavering support over the years has been invaluable to me. Also, his leadership, support, and friendship have been crucial to the completion of this thesis, and his help and encouragement were always present. The thesis was made possible by the invaluable support and guidance of the supervisor, Andy, who provided motivation, insightful feedback, and constant support. I would like to extend my thanks to my second supervisor, Dr. Isabelle Fernandes, for her valuable comments and support. I also thank Dr. Joseph Wrigh, Dr. Isabelle Fernandes and Dr. David Hughes for the X-ray crystallography service. Also, thank Dr Maria Paz, and Chris Richards. Also, Faisal Alqahtani, Jake, Jack, Mamdouh Al-Shammari, James, the storage workers, (cleaners for their honesty and keeping my valuables items), and the University of East Anglia staff, particularly David Hughes and Joseph Wright. David provided incredible support, while Joseph's invaluable expertise in X-ray analysis of compounds significantly contributed to my work. Faisal's moral support and encouragement were greatly appreciated, and Jake and Jack were both kind in providing the necessary equipment. I am also grateful to Jacob for his helpful nature and to Nora Farhan for her friendship and moral support during the challenging times in the lab. I am deeply thankful to my parents for their unwavering support, as well as to Colin and Matthew for their assistance. I extend my appreciation to Vasily Oganesyan and Steve Meech for helping me understand some specific aspects of the application part that were unclear, and to Mamdouh Al-Shammari for his invaluable IT support. The University of East Anglia provided a welcoming and supportive environment, with staff always ready to aid and assist whenever needed. Additionally, I am immensely grateful to the University of Hail for granting me the opportunity to pursue a PhD in organic chemistry in the UK. Finally, I would like to express my admiration and appreciation for the friendly and welcoming British people of Norwich, whose warmth and kindness made my experience even more memorable. I would also like to thank the Saudi Culture Bureau and Hail University, who provided full funding for this work.

Table of Contents

List of Tables

Chapter 1

Chapter 2

List of Figures

Chapter 1

Chapter 2

List of Schemes

Chapter 1

Chapter 2

List of Abbreviations

Abbreviation	Meaning
AC_2O	Acetic anhydride
acac	Acetylacetonate
brs	Broad Singlet
°C	Degrees Celsius
cm	Centimetre
COSY	Correlation spectroscopy
d	Doublet
DBU	1,8-Diaza bicyclo[5-4-0] undec-7-ene
DCC	*N*,*N*'-Dicyclohexylcarbodiimide
DCM	Dichloromethane
DD	Double-decker
dd	Doublet of doublet
DDQ	2,3-Dichloro-5,6-dicyano-1,4-benzoquinone
DIC	*N*,*N*′-Diisopropylcarbodiimide
DM	Diamagnetic
DMAP	4-Dimethylaminopyridine
DMF	N-DimethylFormamide
DMSO	Dimethyl sulfoxide
dq	Doublet of quartets
eq	Equivalent
Et_3N	Triethylamine

EtOAc	Ethyl acetate
g	Gram
HOMO	Highest occupied molecular orbital
hrs	Hours
HZ	Hertz
IPA	Isopropyl Alcohol
J	Coupling constant
K	Kelvin
La	Lanthanum
Ln	Lanthanide
LUMO	Lowest unoccupied molecular orbital
m	Multiplet
M (in structures)	Metal (any)
m.p.	Melting point
MALDI-TOF-MS	Matrix-assisted laser desorption/ionization (time of flight)
Me	Methyl
MEK	Methyl Ethyl Ketone
MeOH	Methanol
mi	Meta-inside
min	Minutes
ml	Millilitres
mmol	Millimole
mo	Meta-outside

N_2	Nitrogen
Nd	Neodymium
nm	Nanometres
NMR	Nuclear Magnetic Resonance
OEP	Octaethylporphyrin
oi	Ortho-inside
OMP	Octamethylporphyrin
oo	Ortho-outside
OTFT	Organic thin-Film-transistors
Pc	Phthalocyanine
P-Chloranil	Tetrachloro-p-benzoquinone
$Pd(pph_3)_4$	Tetrakis(triphenylphosphine)Palladium
Pet-ether	Petroleum
PIDA	Phenyl iodine (III) diacetate
PIFA	Phenyl iodine bis (trifluoro acetate)
PM	Paramagnetic
Pn	Porphyrin
ppm	Parts per million
PPN	Protoporphryin (IX)
Pr	Praseodymium
q	Quartet
RBF	Round bottom flask
Rf	Retention factor

s	Singlet
t	Triplet
TBPP	5,10,15,20-tetrakis[(4-tert-butyl) porphyrinate
TCB	1,2,4-Trichlorobenzene
TCE	Trichloroethylene
TCPP	5,10,15,20-tetrakis(4-cyanophenyl) porphyrinate
TD	Triple-decker
THF	Tetrahydro furan
TLC	Thin Layer Chromatography
TPP	Tetraphenyl porphyrin
TPP-OH	5,10,15-tris-phenyl-20-(p-hydroxyphenyl) porphyrin
UV-vis	Ultraviolet-visible spectroscopy
δ	Chemical Shift
ε	Extinction coefficient

Chapter (1): Introduction

1. Porphyrins and phthalocyanines

Porphyrins and phthalocyanines have been extensively used as organic dyes and pigments because of their strong light absorption in the visible and ultraviolet regions. These materials have shown great chemical and thermal stability since they were originally synthesised in the early 20th century.[1,2] Furthermore, porphyrins and synthetic phthalocyanines have potential scientific and technological applications in chemistry and photochemistry due to their high efficiency in producing free radicals and excited state species, potentially serving as catalysts or photosensitisers.[3,4]

1.1 Introduction and history of the pigment of life (Pn):

Porphyrins are pigments and the name comes from the Greek word *porphura*, referring to its "purple-colour" as shown in Figure 1.1. Porphyrins are present naturally and may be synthesised. They are intensely coloured.[5] Surprisingly, when Küster proposed the porphyrin's macrocyclic structure in 1912, no one believed him, even Hans Fischer the "father of modern porphyrin chemistry" who assumed that such a big ring would be highly unstable. He came around to this structure in 1929 when he and his Munich school of chemists successfully synthesised heme, the iron porphyrin in haemoproteins, from pyrrolic starting materials.[6]

Figure 1.1: Purple colour of porphyrins.

1.1.1 Porphyrins in biological systems:

Iron-containing porphyrins found as heme and magnesium porphyrins found as chlorophyll are the greatest examples of biological molecules (Figure 1.2).[7] Understanding these systems and their excited states is essential for understanding many biological processes, including oxygen binding, electron transfer, catalysis and the first photochemical step in photosynthesis.[8,9]

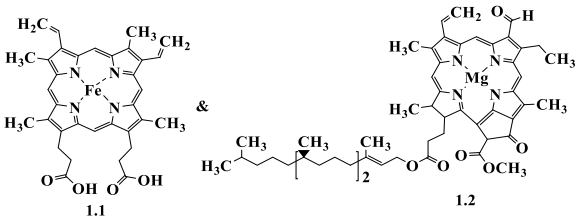

Figure 1.2: Structures of heme (left) and chlorophyll (right)

1.1.2 Structure and properties of porphyrins:

Porphyrins form a wide family of highly coloured red or purple compounds because they have conjugated double bonds (aromatic) that make them absorb light. Porphyrins contain a substituted aromatic macrocyclic ring composed of four pyrrole-type groups joined by four methine bridges as shown in Figure 1.3.[10]

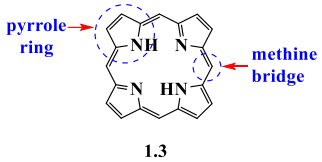

Figure 1.3: Structure of free-base porphyrin.

1.1.3 Fischer's nomenclature of porphyrins:

There was a numbering system for the macrocyclic ring in Fischer's nomenclature, as shown in Figure 1.4, in which each possible site for a substituent on the pyrrole fragments was designated as a beta-carbon and given a number from 1 to 8, while each nitrogen was unnumbered. The pyrrole positions adjacent to the nitrogen atoms were referred to as alpha-carbons.[11]

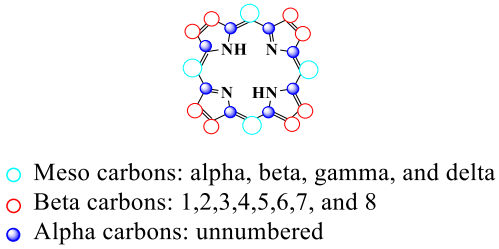

Figure 1.4: Fischer's numbering system.

When the eight positions on the pyrrole have the same functional group, the naming of porphyrins is simple; for example, eight ethyl-groups attached to beta positions gives octaethylporphyrin (OEP) **1.4** (Figure 1.5). Octamethylporphyrin **1.5**, has eight methyl groups attached in the beta position, and another example of a symmetrical porphyrin is tetraphenylporphyrin (TPP) **1.6** with a phenyl group on each meso-position. When the meso-position has three phenyl rings attached and one hydroxyphenyl porphyrin, as shown in Figure 1.6, it is called

TPPOH **1.7**. When beta positions have more than one type of substituent, naming becomes more difficult, such as with protoporphyrin (IX) **1.8**.[5]

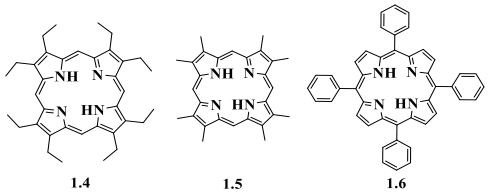

Figure 1.5: Octaethyl porphyrin **1.4** (OEP), octamethyl porphyrin **1.5** (OMP), and tetraphenyl porphyrin **1.6** (TPP).

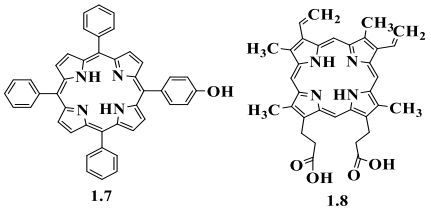

Figure 1.6: TPPOH **1.7** and unsymmetrical porphyrin protoporphyrin (IX) **1.8**.

1.1.4 IUPAC nomenclature for porphyrins:

IUPAC nomenclature of porphyrins was established in 1979 and completed in 1987 and assigns a number from 1–24 to each atom in the macrocyclic tetrapyrrolic system, as shown in Figure 1.7. The two nitrogen atoms linked to the hydrogen atoms are designated 21 and 23. The beta positions are numbered 2, 3, 7, 8, 12, 13, 17, and 18, whereas the alpha positions are numbered 1, 4, 6, 9, 11, 14, 16, and 19, while meso-positions are numbered 5, 10, 15, and 20. Porphyrin has two distinct sites where electrophilic substitution can occur with varying reactivity. The replacement may have an impact on the classification of porphyrins as symmetric or asymmetric as seen in Figure 1.8.[5,11]

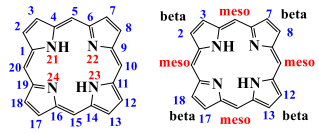

Figure 1.7: IUPAC system of porphyrins and description of porphyrin numeration.

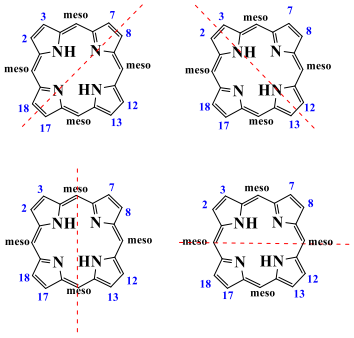

Figure 1.8: The potential for a symmetrical environment is shown by the axes.

1.2 Porphyrin properties:

1.2.1 Aromatic properties of porphyrins:

According to Hückel's rule (4n+2= 18, n= 4), although porphyrins possess 22 π-electrons, only 18 of them are involved in the formation of an aromatic system.[5] The porphyrin macrocycle is a highly conjugated molecule; it has several resonance pathways with 18 π-electrons delocalised in the ring, as seen in Figure 1.9.[5,11]

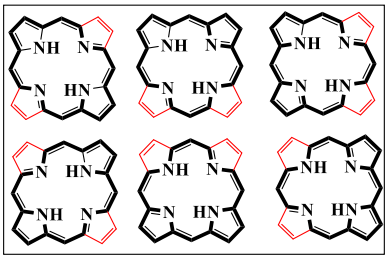

Figure 1.9: Six different aromatic delocalization pathways for the 18 π-electrons in the porphyrin ring.

1.2.2 Porphyrins' substituent positions:

Porphyrins exhibit a wide diversity due to the ability to attach various substituents at different places within the macrocycle. We may customise the macrocycle for different by altering these substituents. There are two primary patterns of porphyrin substitution.

These are porphyrins with β-substituents and porphyrins with meso-substituents, as shown in Figure 1.10. Beta-substituted porphyrins are often seen in nature, whereas meso-substituted porphyrins have generated significant attention in the field of synthetic chemistry.[12]

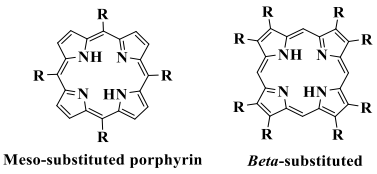

Figure 1.10: Meso and beta substitution in porphyrin rings.

1.2.3 Tautomerisation of porphyrin:

Unsubstituted porphyrin can exist in two different tautomeric structures. The tautomer in trans position has two hydrogens on two opposite pyrrole rings and is more stable than the tautomer which has two hydrogens on neighbouring pyrrole rings, according to computational and spectroscopic studies.[5,13] If the hydrogen atoms were in close proximity, they would sterically hinder each other; this means that the cis configuration is disfavoured, as shown in Figure 1.11.

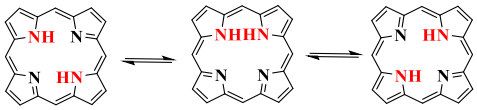

Figure 1.11: Tautomerisation of porphyrin.

1.2.4 Ring current in porphyrin and ^{1}H NMR spectra of meso-tetraphenyl porphyrin:

^{1}H NMR spectra reveal downfield shifts for peripheral protons and significant upfield shifts in inner protons on Ns, causing negative chemical shifts and highlighting the magnetic anisotropy in aromatic systems, with positive shifts external to the ring.[14,15,16]

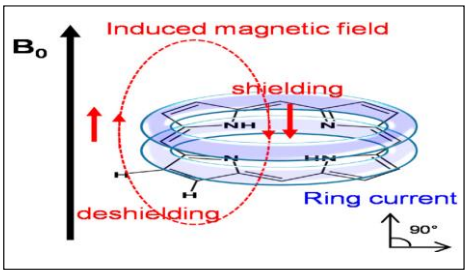

Figure 1.12: Scheme of porphyrin ring current.[15]

Reproduced from Probing the Interactions of Porphyrins with Macromolecules Using NMR Spectroscopy Techniques, no permission required, simply attribution link.

The biggest interest in synthetic chemistry has come from meso-aryl systems. They are significant in materials chemistry and can be synthesised easily. Pyrrole and aldehydes are mostly used in their production. Tetraphenylporphyrin (TPP) is a common example of a symmetrical porphyrin. The NH protons inside the porphyrin ring system moved upfield to as low as -2.00 ppm in porphyrins, while ring currents have a de-shielding impact on the proton signal of pyrrole and meso-aryl protons, as shown in Figure 1.13. [1,4,5]

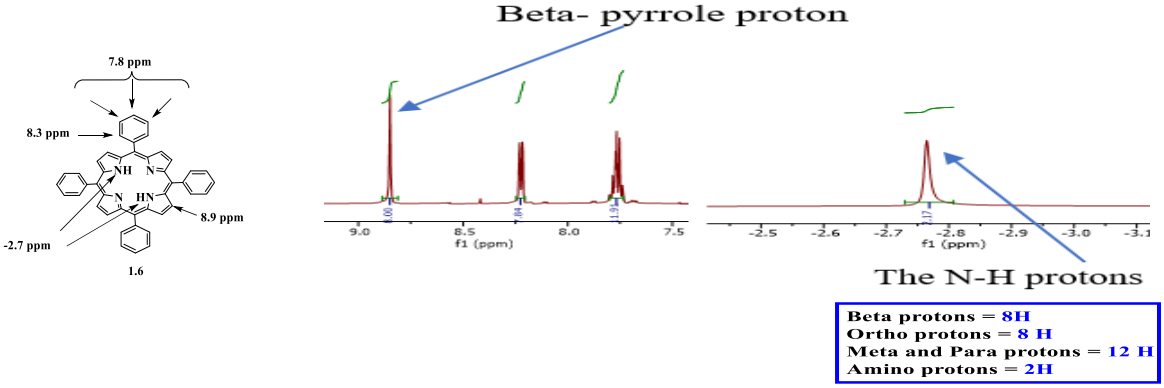

Figure 1.13: ^{1}H NMR spectrum of TPP **1.6**.

1.2.5 Metalloporphyrin:

Usually, porphyrins are made without metal ions, and these are added later. When the metal ion M^{n+} is added to the porphyrin $PorH_2$ to make Por-$M^{(n-2)+}$, the two amine protons in $PorH_2$ are lost from the two pyrrole rings as shown in the equation:

$$M^{n+} + PorH_2 \longrightarrow MPor^{(n-2)+} + 2H^+$$

Porphyrin macrocycles are large enough to accommodate most metal ions, making them ideal for the formation of M-Por, and they create molecules with metals that are important in various biological processes, such as Fe, Mg, Zn, and Co. The best radii for the metal ions are between 55 and 80 pm, corresponding to the cavity in the porphyrin (Figure 1.14-a), while the sitting-atop (SAT) metalloporphyrins result when the radii of the metal ions are very large, in the range of 81–90 pm, and the metals are located out of the ligand-plane (Figure 1.14-b).[16,17]

Figure 1.14: Schematic representation of (a) regular and (b) SAT metalloporphyrins.

1.2.6 UV-vis. spectroscopy of porphyrin:

As previously mentioned in the introduction describing the characteristics of porphyrins, these structures include a highly conjugated π-electron system, which explains their intensity and colouration. Many studies on porphyrins have shown that changes in the conjugation and compound symmetry may affect the UV-vis absorption spectra. They may absorb light in two different areas of the visible spectrum, one near the UV and the other in the visible range.[18] To investigate porphyrin absorption spectra, Gouterman developed a model of four orbitals (the two highest occupied π orbitals (HOMOs) and the two lowest π* orbitals (LOMOs)).[19]

In this theory, transitions between the two HOMOs and the two LUMOs produce the absorption bands seen in porphyrin spectra. The energies of these transitions alter in the presence of substituents on the ring and the identities of the coordinating metal (Figure 1.15).

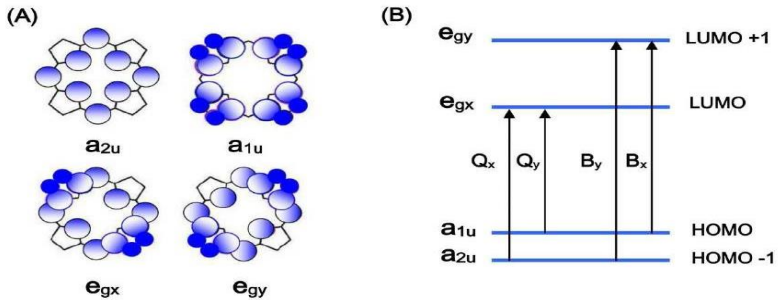

Figure 1.15: Porphyrin HOMOs/LUMOs, in Gouterman's orbital energy level model.[19]
Reproduced with permission from (1.15).

The electronic absorption spectra of a free base porphyrin with D_{2h} symmetry display two different regions. The transition from the ground state to the second excited state (S_0 to S_2) is referred to as the B band, and the absorbance ranges between 380 and 500 nm, dependent on β- or meso- substitution. The Q-bands indicate the secondary region, characterised by a less strong transition to the first excited state (S_0 to S_1), including a wavelength range of 500-700 nm,[19,20,21] as seen in Figure 1.16.

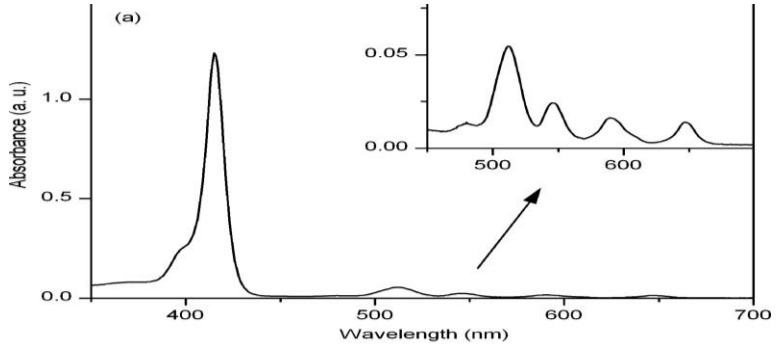

Figure 1.16: UV-Vis. spectrum of metal-free porphyrin and an expanded view of the Q-band region.[21] Reproduced with permission from (1.16).

Metalloporphyrin and metal-free porphyrins differ in their spectra due to their different symmetry point groups, D_{2h} and D_{4h}, which cause degenerate energy levels and decrease the number of Q bands as shown in Figure 1.17.[20,21,22]

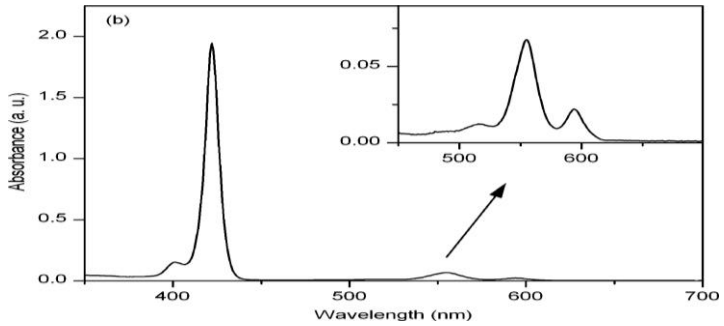

Figure 1.17: UV-vis spectrum of metalloporphyrin and view of the Q-band region.[21] Reproduced with permission from (1.17).

1.3 Synthesis of symmetrical porphyrins:

1.3.1 Synthesis of meso-substituted porphyrins:

For the synthesis of porphyrin, several different techniques have been documented; these processes have evolved through time to achieve greater yields with fewer unwanted by-products. The preparation of porphyrin is most often done using the Rothemund, Adler, and Lindsey procedures, which are summarised in the following paragraphs.

1.3.2 Rothemund's and Adler–Longo's syntheses:

There are many techniques for synthesising porphyrins, ranging from a straightforward one-step reaction involving pyrrole and an aldehyde to a more intricate multistep synthesis. Each approach has its own set of merits and drawbacks. Rothemund in 1935 emerged as a trailblazer in this area of investigation.[23] The synthesis of meso-tetramethyl porphyrin, together with its copper and iron complexes, was achieved by Rothemund[24] by the reaction of acetaldehyde with pyrrole in methanol. The resulting product was obtained as a crystalline solid. Subsequently, the researchers extended the scope of their investigation to include a diverse range of aldehydes, so generating an extensive compendium of porphyrins that had undergone substitution at the meso-position. They reacted pyrrole and benzaldehyde in pyridine in a covered flask at 150 °C for 24 hrs in a one-step reaction, as shown in Scheme 1.1. Low yield resulted, and meso-substituted chlorin was a primary by-product of benzaldehyde conversion to substituted porphyrin. The enhancement in porphyrin production was observed by Calvin *et al*. with the addition of zinc acetate, resulting in the formation of the zinc complex of the porphyrin. This resulted in an increase in the mean yield of meso-tetraphenyl porphyrin from around 4–5% to 10%.

Adler and Longo's[25] approach (Scheme 1.1) led to a significant transformation in the synthesis of meso-substituted porphyrins during the mid-1960s. It has been shown that subjecting pyrrole to acidic conditions in an oxygen-rich environment gives significant enhancement in the resulting yields. Alternative acids, including acetic acid, have been explored for their potential to provide improved yields for some aldehydes. However, propionic acid is typically preferred in this context. The isolation of these porphyrins is often straightforward and comprises filtering and washing procedures. However, it should be noted that crystallisation may not always occur in some instances.[23,24,25]

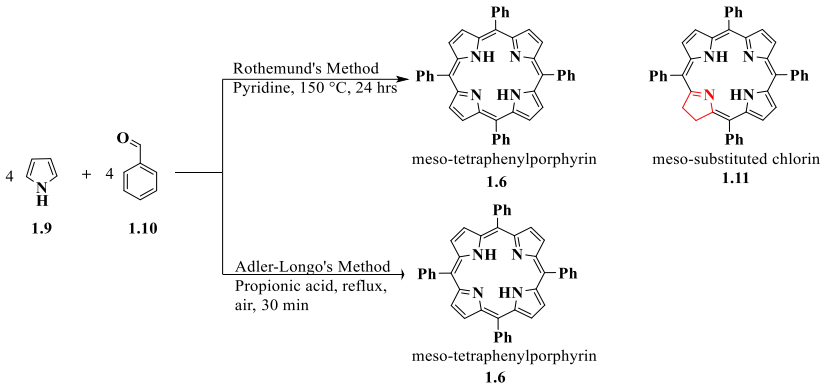

Scheme 1.1: Rothemund's and Adler–Longo's classic synthetic methods for porphyrins.

1.3.3 Lindsey's method:

Lindsey *et al*. noted that the reactivity of pyrrole and aldehydes indicates that the high reaction temperatures often used in the Adler–Longo method may be unnecessary. In nature, the synthesis of porphyrins involves a series of consecutive phases characterised by condensation and oxidation processes. As a result of this, Lindsey embarked on a research endeavour over a period of seven years, leading to the development of a novel methodology. The researchers discovered that by subjecting pyrrole to a reaction with benzaldehyde in dichloromethane at ambient temperature, by treating it with trifluoroacetic acid for about 60 minutes, followed by the addition of an equimolar quantity of an oxidising agent such as DDQ, a yield of 35–40% could be obtained (Scheme 1.2).[26,27]

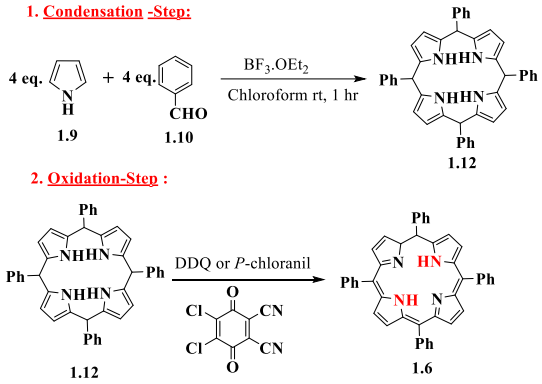

Scheme 1.2: Synthesis of meso-tetraphenyl porphyrin (TPP) **1.6** by Lindsey.

In summary, there are three primary approaches of synthesising meso-substituted porphyrins: the Rothemund technique, the Alder method, and the Lindsey method. The Rothemund approach is without any obvious benefits compared to the other two approaches; hence the selection of method often comes down to a decision between the Alder and Lindsey methods. The Alder method is more effective in synthesising porphyrins from stable aldehydes, but it is less suitable for porphyrins derived from aldehydes that cannot withstand refluxing propionic acid. Additionally, it is not effective for aliphatic aldehydes and aldehydes that yield porphyrins that do not precipitate from propionic acid. The Lindsey technique exhibits the least severe reaction conditions and often generates larger yields compared to other procedures. It is very effective in synthesising porphyrins from aldehydes. A major limitation of this approach is that the purifying process often entails chromatography. If this situation presents a challenge, it could be more advantageous to use the Alder technique.

1.3.4 Synthesis of octaethylporphyrin (OEP):

OEP has eight ethyl groups in beta position, and it is a symmetrical molecule. This core is used as an element of triple-decker porphyrins in this project. Although it can be synthesised according to the procedure described below, OEP was purchased for the purpose of this work. The procedure to synthesise OEP involves the reaction of propionaldehyde **1.13** with 1-nitropropane **1.14** in IPA using KF as a catalyst to obtain 4-nitrohexan-3-ol **1.15** followed by its acylation by reaction with acetic anhydride to produce **1.16**. Cyclisation reaction of **1.16** with ethyl 2-isocyanoacetate in THF/IPA using DBU as a strong base affords pyrrole **1.17**. Compound **1.17** undergoes basic hydrolysis and decarboxylation to give 3,4-diethyl-1*H*-pyrrole **1.18**, which can be condensed with formaldehyde in benzene/*p*-TsOH followed by oxidation to form target OEP **1.4** as shown in Scheme 1.3.[28]

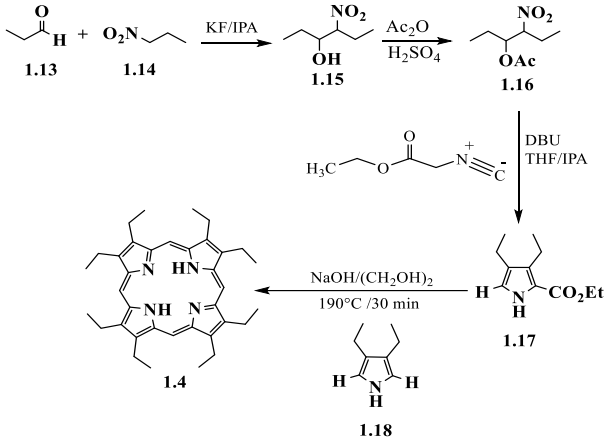

Scheme 1.3: Synthesis of octaethylporphyrin **1.4**.

1.4 Synthesis of unsymmetrical porphyrins:

The investigation of porphyrins continues, with new improvements in synthetic methodologies yielding functionalised porphyrins, particularly those with modifications at the meso-positions. ABCD-type porphyrins, characterised by four unique substituents at the meso-positions, show a typical unsymmetrically meso-substituted porphyrin.

To synthesise an ABCD porphyrin, Senge and colleagues developed the procedures shown in Schemes 1.4 and 1.5. Alkylation of monoalkylated porphyrin **1.19** by lithium alkyl gave the two isomers **1.21** (17 %) and **1.20** (7 %) when R_2= *n*-Bu.[29,30]

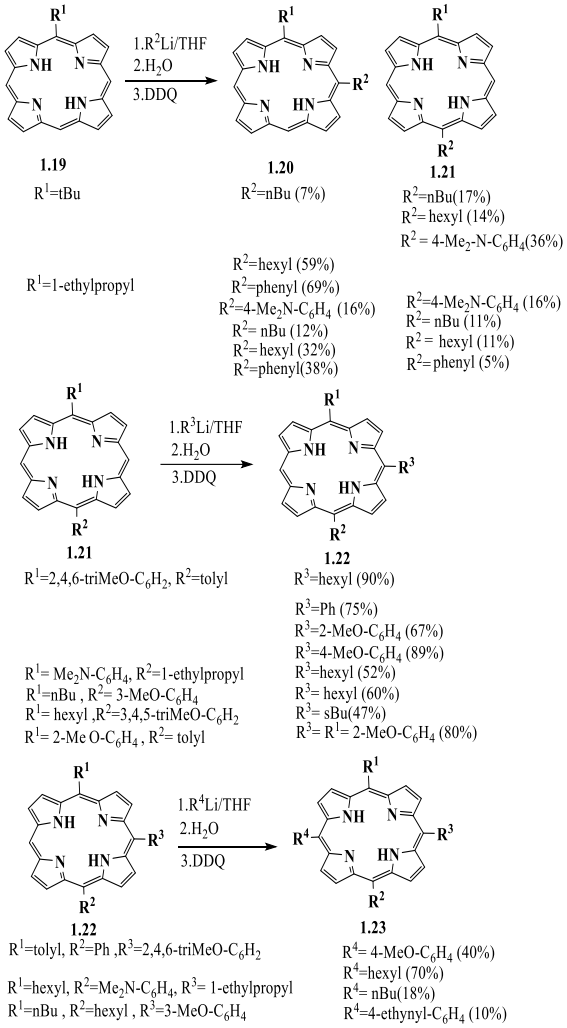

Scheme 1.4: Synthesis of ABCD-type of porphyrin.

Palladium catalysts are commonly used for substituting meso- and β-locations in (C-C) coupling processes, which often involve the transformation of halogenated porphyrins. Ruthenium, cobalt, nickel, and tin complexes are also employed.[30,31,32]

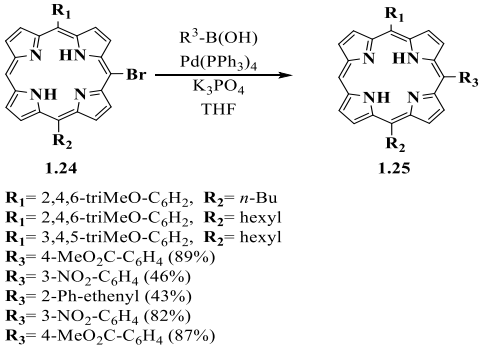

Scheme 1.5: Synthesis of ABC-type porphyrin by Suzuki reactions.

The synthesis of ABC- and ABCD-type porphyrins entails the bromination of porphyrin intermediates followed by Pd-catalysed C-C coupling reactions. The reaction's efficacy is notable,

although the yields exhibit significant variation depending on the specific porphyrin and boron coupling partner used (Schemes 1.5 and 1.6).[30,31,32]

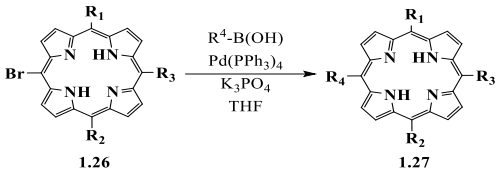

R_1= hexyl, R_2= 3-NO_2-C_6H_4, R_3= 3,4,5-triMeO-C_6H_2
R_1= hexyl, R_2= *n*-Bu, R_3= 3,4,5-triMeO-C_6H_2
R_4 = 4-MeO_2C-C_6H_4 (67%)
R_4 = *n*-Bu (10%)
R_4 = 4-MeN-C_6H_4 (22%)
R_4 = 4-HO-C_6H_4 (70%)
R_4 = 4-Br-C_6H_4 (45%)
R_4 = 3-Br-pyridyl (47%)
R_4 = 2,4,6-triMe-C_6H_2 (53%)

Scheme 1.6: Synthesis of ABCD-type porphyrin by Suzuki reactions.

1.5 Introduction to phthalocyanine:

1.5.1 General introduction of Pc:

Phthalocyanines (Pcs) are compounds with unique chemistry, and the basic structure **1.28** is shown in Figure 1.18.[33,34] Phthalocyanine is classified as a tetrapyrrole macrocycle, characterised by a structure that consists of a ring of alternating nitrogen and carbon atoms. This class comprises phthalocyanines and porphyrazines, and it has a cavity that accepts around 70 metals in the Pc ring.[35] It is only made in the lab (prepared artificially).[36]

Pc is dark blue, and its name comes from the Greek word, *cyanine* (blue). Properties include exceptional thermal, chemical, and optical stability, and unique electrochemical, photochemical, and photophysical characteristics, which have led to various applications such as photodynamic therapy in cancer treatment, chemical sensors, and solar cells. The bright blue/green colour of Pc comes from the delocalised π-electron system of four rings connected by azamethine bridges. Popular metals include zinc and copper.[33-36]

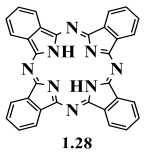

Figure 1.18: Structure of H_2Pc.

1.5.2 Synthesis of Pc:

The general procedure to produce Pc was developed by Galanin and Shaposhnikov, and this method gave a high yield of product in a short time of reaction as shown in Scheme 1.7.

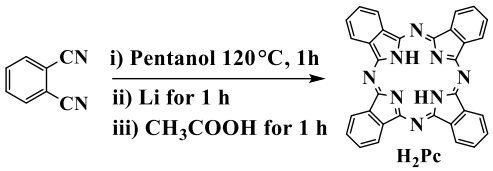

Scheme 1.7: General synthesis for metal-free Pc.

Pc synthesis is straightforward and yields around 40%. Phthalonitrile **1.29** reacts with lithium pentanolate in refluxing pentanol to produce Pc **1.28**. Acetic acid removes metal to produce phthalocyanines as shown in Scheme 1.8.[33,34]

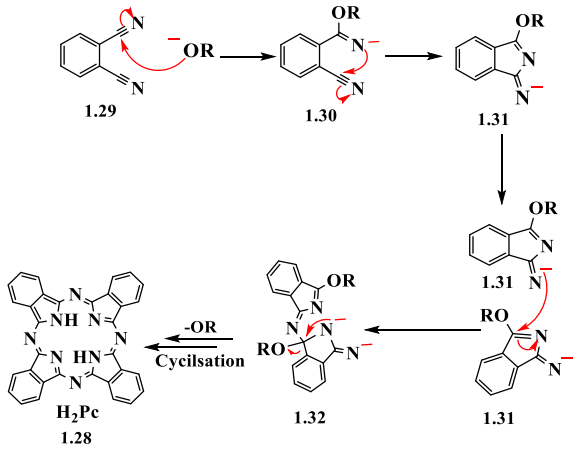

Scheme 1.8: Mechanism of metal-free phthalocyanine formation.

1.5.3 Absorption spectra of metal-free phthalocyanine 1.28:

Phthalocyanines show different ultraviolet-visible (UV-vis) spectra, involving a prominent absorption peak in the red end of the visible region known as the Q-band, which occurs around 650–720 nm. This is responsible for the intense colour of the phthalocyanine, and its position is largely influenced by the central metal and the substituents on the Pc ring as transitions occur from (π - π*) orbitals. In addition, a second band known as the B-band is seen as a wide band with a wavelength range of 300–400 nm.[35,36] Gouterman's four-orbital model is shown in Figure 1.19.

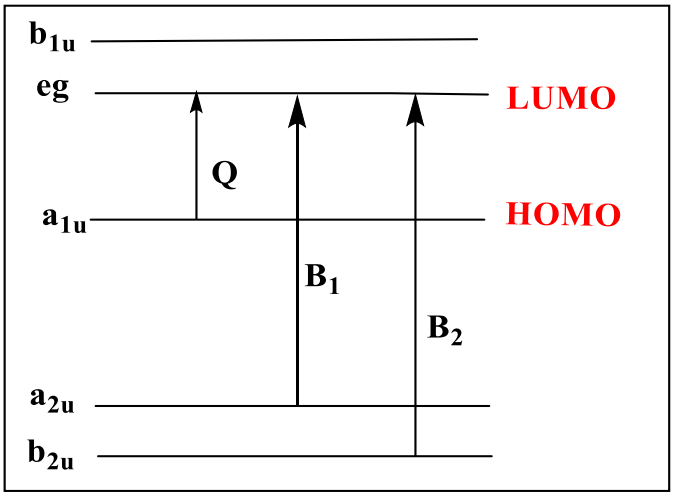

Figure 1.19: Energy level diagram of phthalocyanine showing transitions that give rise to absorption bands.

The symmetry of metal phthalocyanine (MPc) results in degenerate orbitals, and it exhibits a single main Q band.[35,36] However, in the case of metal-free phthalocyanine, the absence of molecular symmetry results in nondegenerate orbitals and causes it to have two distinct main Q-bands, as seen in Figure 1.20.

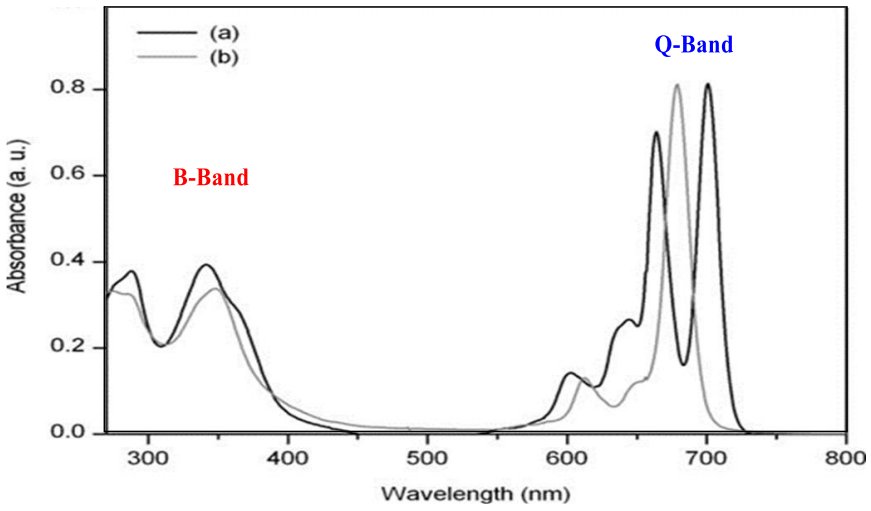

Figure 1.20: Standard UV–Visible spectra for a phthalocyanine in two forms: (a) as a free-base and (b) as a metal complex.[35]
Reproduced with permission from (1.20).

1.6 Porphyrin and phthalocyanine arrays:

Over recent years there has been a lot of interest in porphyrin and phthalocyanine molecules both because of how special they are when it comes to electronics and optics and for the chemical properties they possess. These molecules have served as building blocks for creating structures that have found various uses in materials science applications, like linear arrays and multidecker complexes. Linear arrays are often used in applications that involve wires and collecting

light efficiently for transferring electrons. Linkers can play a role in connecting core units and forming double- or triple-decker sandwich compounds known as dyads and triads. The intramolecular interactions can significantly influence the spectroscopic and physical properties of the materials while also affecting their electrochemical characteristics. Porphyrins can get involved in electrophilic substitution reactions to form new compounds; further steps may provide complex structures, such as dimers and triads, by linking porphyrin molecules with hydrocarbon chains at the meso or β locations.[37,38,39,40] Intramolecular (π-π) and (f-f) interactions affect the attributes and physical properties of complexes, as well as their spectroscopic and electrochemical features. Triple-decker sandwich structures display multiple oxidation states that render them ideal for information storage,[41] applications in molecular magnets,[42] sensors,[43] and field-effect transistors.[44]

1.6.1 Dyads, triads, and sandwich-type complexes:

1.6.2 Definition:

The porphyrin dyad is a chemical structure consisting of two porphyrin rings connected by a linker, [37,38,39,40] while the triad comprises three porphyrin units attached by a linker, such as an alkane chain. Sandwich complexes are structures in which a metal ion is coordinated by two rings (Figure 1.21).

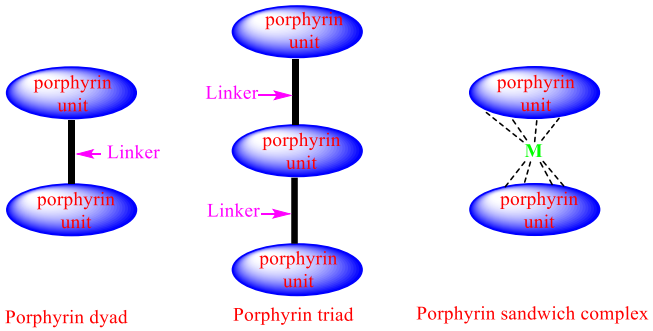

Figure 1.21: General structures of porphyrin dyad, triad, and sandwich complexes.

Conjugated pairs of porphyrin molecules exhibit electronic properties that make them useful in various applications. Furthermore, scientists have examined porphyrin pairs that incorporate both electron acceptor and donor elements. These pairs are crafted to replicate processes of electron and energy transfer, providing insights into photosynthesis, where light energy is transformed into chemical energy.[45] The process comprises two steps. The first is the absorption of energy by molecules, at a particular wavelength. After light excites the system, in a process called photoinduced electron transfer (PET), it generates charges in the reaction centre

area.[46] To be effective a light gathering system employs arrays of chromophores made up of porphyrin compounds linked to either electron donors or acceptors.

In one example,[47] the Sonogashira cross-coupling method (Scheme 1.9) connected two sets of palladium (II) β octaethylporphyrin to nickel (II) meso diphenylporphyrin and methyl pyropheophorbide a using a butenyne bridge, **1.36** and **1.37**. The optical properties of the two sets differed significantly from their components, suggesting electronic interaction between the units in both their normal and excited states facilitating fast energy transfer between the chromophores. Dyads **1.36** and **1.37** show absorption across the visible spectrum, like panchromatic dyes, and could be useful as photosensitisers for converting solar light into energy systems. Certain porphyrin dyads with a donor and acceptor unit in an unsymmetrical setup are also used in this system, as shown in Figure 1.22.[47]

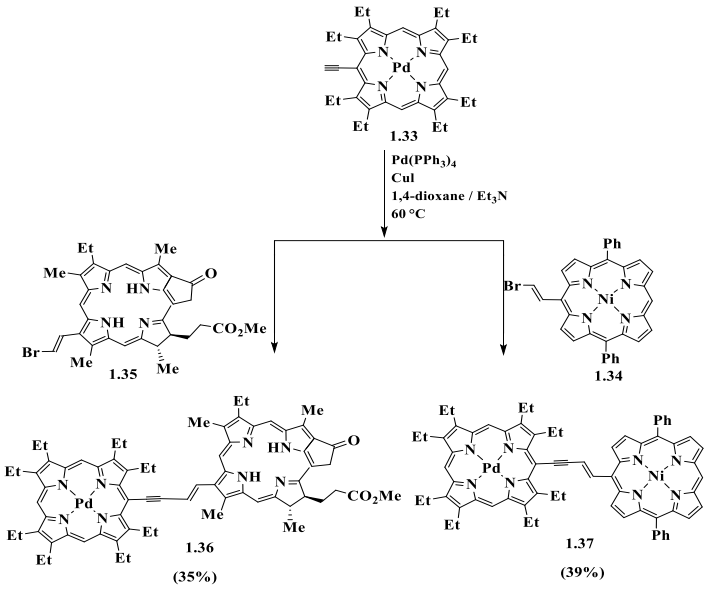

Scheme 1.9: Synthesis of dyads **1.36** and **1.37**.

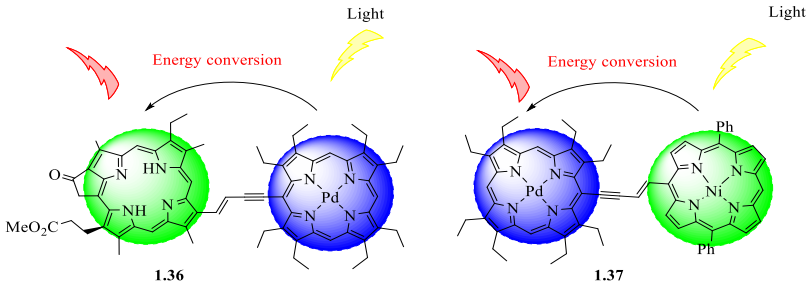

Figure 1.22: Porphyrins act as electron donor-acceptor pairs.

1.6.3 Types of arrays:

1.6.3.1 Homo-arrays of porphyrins:

In 1994, Therien and his colleagues[48] produced a novel category of porphyrin arrays, meso-meso ethyne-linked linear porphyrin arrays, as shown in Figure 1.23; within these arrays, porphyrin chromophores are connected by individual ethynyl bridges at the meso-location.

Porphyrin dyad **1.38**, which includes a single ethyne bridge, and porphyrin triads **1.39**, have been created by the combination of 5-bromo-10,20-diphenylporphyrinatozinc and ethyne-elaborated porphyrin synthons using palladium-catalysed coupling. Acetylene-linked porphyrins exhibit unique photophysical and electrochemical properties due to their excellent electronic interactions with chromophores. [48]

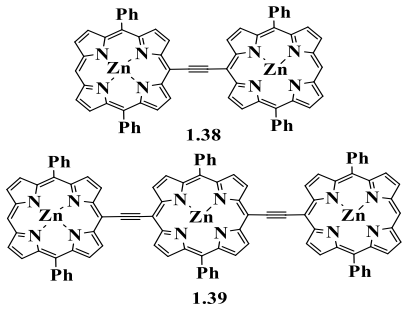

Figure 1.23: Meso-meso ethyne-linked (**1.38**) and di-ethyne-linked (**1.39**) linear porphyrin arrays.

There are potential applications of directly meso-meso connected linear porphyrin arrays in nanotechnology and optoelectronic devices. Various techniques have been used to directly produce linear arrays of porphyrins that are coupled at the meso-meso positions. For instance, a Zn porphyrin array **1.40** has been produced using oxidative coupling with silver salts to bring the porphyrin monomers closer together, facilitating fast energy transfer (Figure 1.24). [49,50]

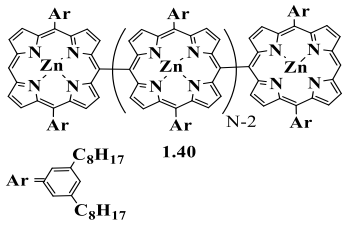

Figure 1.24: Directly meso-meso-linked linear Zn porphyrin arrays **1.40**.

Jin, Chen *et al*. successfully synthesised 10–12 linear porphyrin arrays using iodine (III) reagents [bis(trifluoroacetoxy)iodo] benzene (PIFA), $PhI(OCOCF_3)_2$, or (Diacetoxyiodo)benzene (PIDA), $PhI(OAc)_2$ as shown in Scheme 1.10.[51]

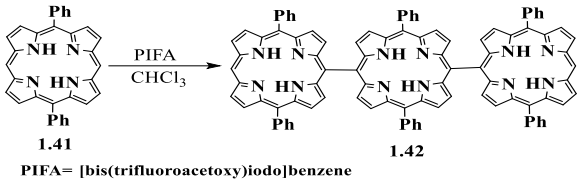

Scheme 1.10: Synthesis of meso-meso-linked linear porphyrins **1.42**.

Jiblaoui *et al*. [52] successfully prepared porphyrin dimer **1.43** at high yield (75%) using PIFA as the iodine (III) reagent, as shown in Figure 1.25.

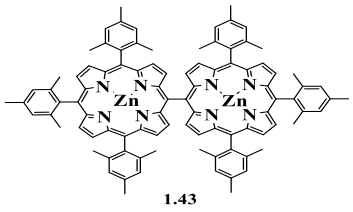

Figure 1.25: Molecular structure of meso-meso-linked porphyrin dimer **1.43**.

The Cammidge group[53,54] successfully produced a porphyrin dyad by reacting 2 eq. of TPPOH **1.7** with 0.5 eq. 1,10-dibromodecane and excess K_2CO_3. The mixture was added in a sealed tube and heated in dry acetone at 70 °C for 72 hrs, and the yield of **1.44** obtained was 12–57%. Also, they prepared the derivative from 1,12-dibromododecane following the same conditions and dyad **1.45** was obtained in 27–38% yield, as shown in Scheme 1.11.

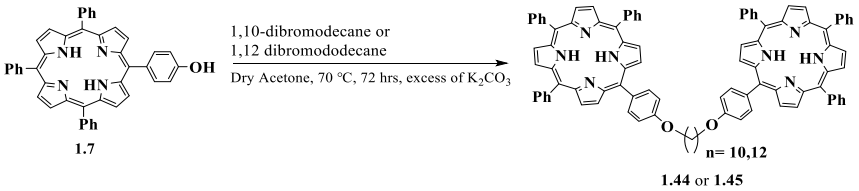

Scheme1.11: Synthesis of Porphyrin C_{10} dyad (TPP-O-$(CH_2)_{10}$-O-TPP) **1.44** and C_{12} dyad (TPP-O-$(CH_2)_{12}$-O-TPP) **1.45**.

1.6.3.2 Hetero arrays of porphyrins:

Porphyrin hetero arrays have garnered attention because of their wide-ranging applications in fields like photonics and catalysis, among others. Scientists are exploring methods to create these arrays by using coupling reactions and coordination chemistry to achieve unique molecular structures; a few examples are outlined below. An effective method involves using porphyrin boronates such as **1.46** to create connected Por - arrays like **1.48** by the Suzuki coupling technique as shown in Scheme 1.12. In this procedure, Porphyrin boronate **1.46** reacts with bromoporphyrin **1.47** using a palladium catalyst, like Pd $(PPh_3)_4$, leading to dyads of porphyrins being formed. [55]

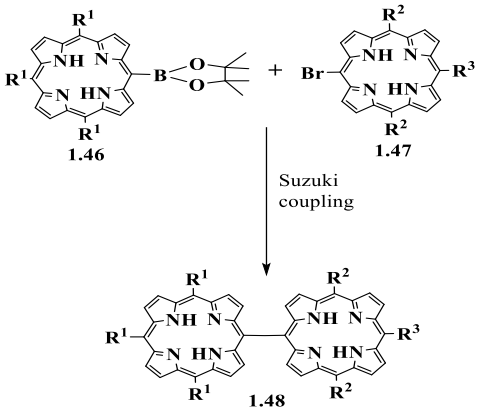

Scheme 1.12: Synthesis of meso-meso-linked porphyrin **1.48** using Suzuki coupling.

Palladium-catalysed C–C coupling has been utilised to synthesise a series of symmetrical and unsymmetrical porphyrin arrays linked by alkyne and phenyl acetylene moieties, which provide structural diversity and flexibility.

The synthesis of an exemplar asymmetrical alkyne-linked dyad is depicted in Scheme 1.13 and an example of the synthesis of linear trimers via copper-free Sonogashira coupling is shown in Scheme 1.14, which demonstrates the potential of this approach in the production of complex molecular structures. Also, Figure 1.26 further illustrates examples of unsymmetrical alkyne-linked dimers **1.55** and **1.56**.[55]

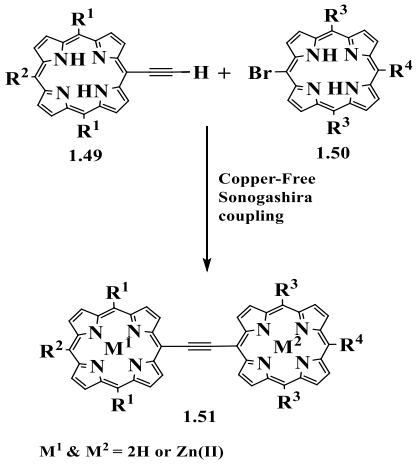

Scheme 1.13: Synthesis of asymmetrical alkyne-linked dyad.

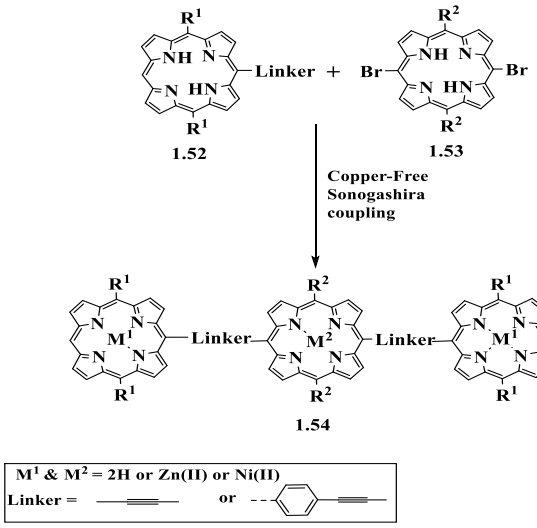

Scheme 1.14: Synthesis of linear trimers by copper-free Sonogashira coupling.

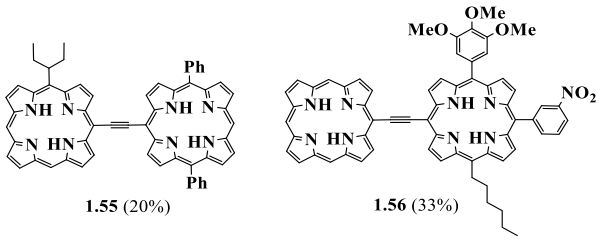

Figure 1.26: Other examples of unsymmetrical alkyne-linked dimers **1.55** and **1.56**.

Anabuki *et al.*[56] achieved the direct meso-alkynylation of β, β'-dipyridyl porphyrin using several alkynyl lithium reagents. The β, β'-dipyridyl groups significantly improve the nucleophilic addition of the reagents by multiple coordination. This method allowed the synthesis of meso-ethyne-bridged di-porphyrin **1.60**, as shown in Scheme 1.15.

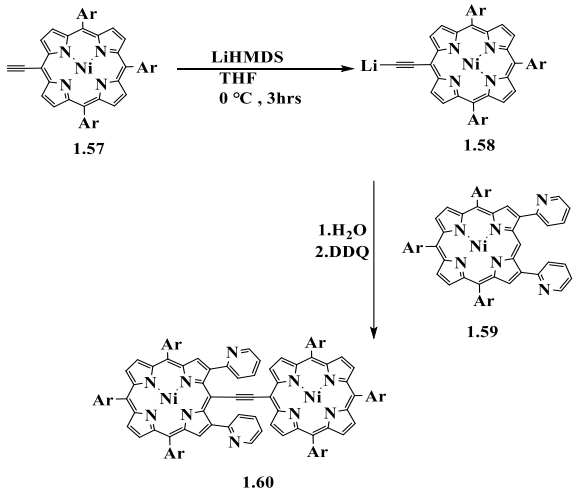

Scheme 1.15: Synthesis of meso-ethyne-bridged di-porphyrin (Ar = 3,5-di-tert-butylphenyl).

Senge and Feng[57] attempted to examine the relative reactivity of porphyrins at both the free meso and β positions with RLi. The researchers used 5,15-disubstituted free base porphyrins

(**1.61a, b**) as the starting materials, which can be readily synthesised by the reaction of dipyr-romethane with the alkyl or aryl aldehydes.

Subsequently, Senge and his colleague included these porphyrins in the RLi addition sequence, which included the hydrolysis step, resulting in the identification of 5,10,15-trisubstituted por-phyrins (**1.62**), as seen in Scheme 1.16. Senge and Feng[57] successfully synthesised meso-meso linked bis porphyrins **1.63** with a good yield, as seen in Scheme 1.17.

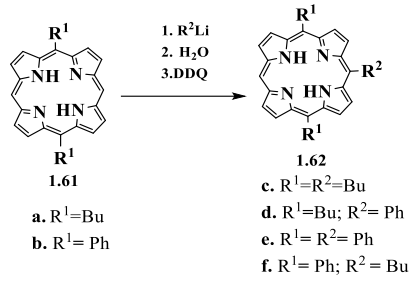

Scheme 1.16: Synthesis of 5,10,15-trisubstituted porphyrins.

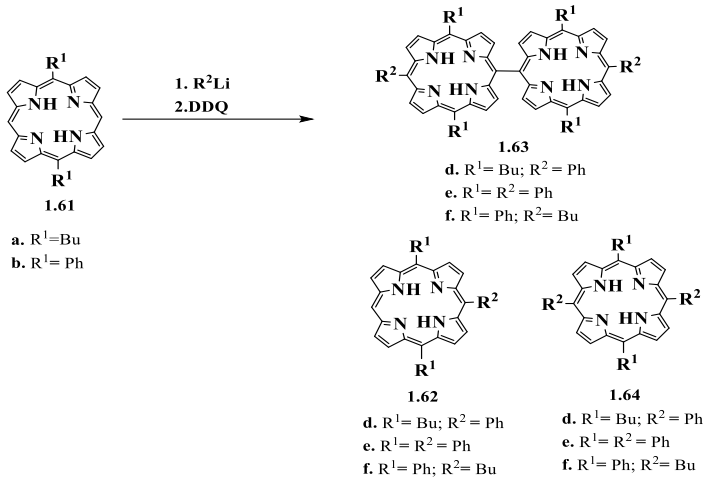

Scheme 1.17: Synthesis of directly linked dimers with mixed meso-substituted porphyrins.

Chen and colleagues created linear porphyrin arrays by synthesising them with iodine reagents, like Phl (OCOCF) (PIFA) or Phl (OAe) (PIDA), as demonstrated in Schemes 1.18 and 1.19.[58]

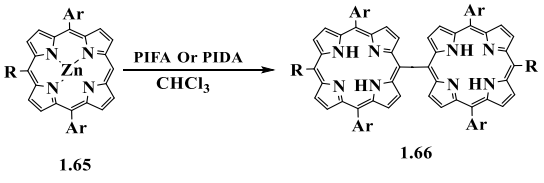

Scheme 1.18: Synthesis of meso-meso-linked linear porphyrin dyad using PIFA or PIDA.

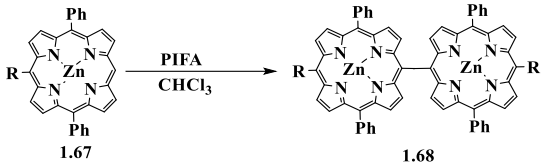

Scheme 1.19: Synthesis of dimeric porphyrins with PIFA.

1.6.3.2.1 Porphyrin–phthalocyanine combinations:

The first reported covalent bonding of porphyrins and phthalocyanines in heteroarrays was achieved by Maillard and his colleagues in 1986.[59] The synthesis process commenced by the treatment of hydroxyporphyrin **1.69** with nitrophthalonitrile **1.70**, followed by condensation with 4-tert-butylphthalonitrile **1.72** in the presence of zinc powder. This reaction produced dyads **1.73** and **1.74**, as illustrated in Scheme 1.20.[59,60]

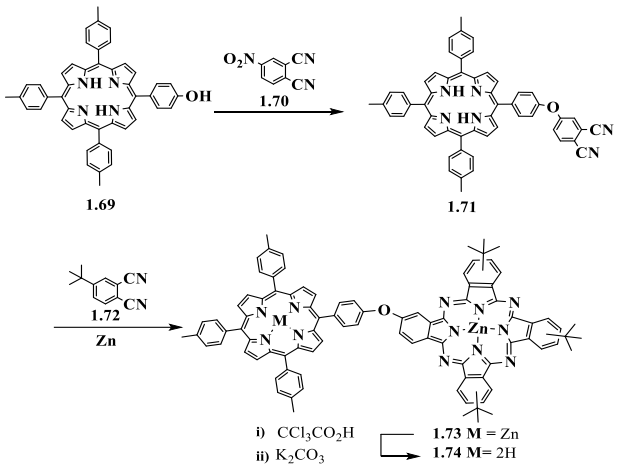

Scheme 1.20: Product of mixed porphyrin-phthalocyanine dyads **1.73** and **1.74**.

1.7 Homoleptic double- and triple-decker complexes:

1.7.1 Lanthanide metals and contraction effect:

Lanthanide characteristics are in part dictated by the size of the positive ion in an oxidation state of Ln^{+3}, which is a more common state than Ln^{+4} and Ln^{+2}. Lanthanides have been extensively studied in the creation of TDs, because they provide the necessary size and acceptable oxidation state. Numerous heteroleptic and/or homoleptic double-decker and triple-decker compounds may be produced using these rare earth metals. The lanthanides decrease in ionic radius from lanthanum (1.03 Å) to lutetium (0.86 Å), as the atomic number increases. Inner shell electrons protect outer shell electrons from nuclear charge, ensuring they remain unaffected, as shown in Figure 1.27 and Table1.1. In addition, lanthanides may also form (1:1) complexes with porphyrinoids. Lanthanide ions are bigger than the cavities of Por and Pc

ligands; therefore the metal centres are above the planar macrocycles, as shown in Figure1.28.
37,38, 61,62,63

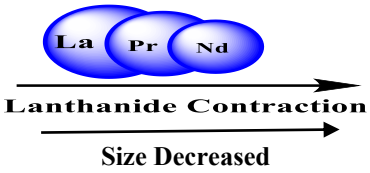

Figure 1.27: Lanthanide contraction in La, Pr and Nd; decrease in the ionic radius for each Ln^{3+} ion from left to right across the series.

Figure 1.28: Lanthanides' location on porphyrin and Pc molecules.

Table 1.1: Selected Properties of lanthanides and their ions:

Atomic Number	Name	Symbol	Neutral Valence Electrons	M^{+3} Valence Electrons	Ionic Radius (M^{+3}, Å)
57	Lanthanum	La	[Xe] $5d^16s^2$	-	1.03 Å
58	Cerium	Ce	[Xe] $4f^15d^16s^2$	$4f^1$	1.02 Å
59	Praseodymium	Pr	[Xe] $4f^35d^06s^2$	$4f^2$	0.99 Å
60	Neodymium	Nd	[Xe] $4f^45d^06s^2$	$4f^3$	0.98 Å
61	Promethium	Pm	[Xe] $4f^55d^06s^2$	$4f^4$	0.97 Å
62	Samarium	Sm	[Xe] $4f^65d^06s^2$	$4f^5$	0.96 Å
63	Europium	Eu	[Xe] $4f^75d^06s^2$	$4f^6$	0.95 Å
64	Gadolinium	Gd	[Xe] $4f^75d^16s^2$	$4f^7$	0.94 Å
65	Terbium	Tb	[Xe] $4f^95d^06s^2$	$4f^8$	0.92 Å
66	Dysprosium	Dy	[Xe] $4f^{10}5d^06s^2$	$4f^9$	0.91 Å
67	Holmium	Ho	[Xe] $4f^{11}5d^06s^2$	$4f^{10}$	0.90 Å
68	Erbium	Er	[Xe] $4f^{12}5d^06s^2$	$4f^{11}$	0.89 Å
69	Thulium	Tm	[Xe] $4f^{13}5d^06s^2$	$4f^{12}$	0.88 Å
70	Ytterbium	Yb	[Xe] $4f^{14}5d^06s^2$	$4f^{13}$	0.87 Å
71	Lutetium	Lu	[Xe] $4f^{14}5d^16s^2$	$4f^{14}$	0.86 Å

The magnetic properties of matter are defined by how atomic magnetic moments work within matter. There are three types of properties, diamagnetic (DM), ferromagnetic (FM) and paramagnetic (PM), which are distinguished by the way these atomic magnetic moments interact with each other and respond to external magnetic forces. Lanthanides stand out as a group of materials due to their electronic structures and diverse magnetic characteristics that have proven valuable for use in applications as molecular devices. When diamagnetic materials come into contact with a magnetic field, they tend to generate a magnetic field in the opposite direction. In these materials each electron is paired up within its orbit, resulting in a magnetic moment of zero in the absence of an external magnetic field.

However, when an external magnetic field is present, it triggers an opposing field within the material, leading to a weak repulsion. Accordingly, La and Lu have diamagnetic properties and serve as common examples of such materials. In contrast, ferromagnetic materials display their characteristics because they have unpaired electrons. If the magnetic field is powerful enough, the whole material could become magnetised and keep its properties even when the external field is removed, such as in gadolinium.[38] Also, the lanthanides are known to be paramagnetic because they have their 4f orbitals partially filled and hence have unpaired electrons. Paramagnetism differs along the series according to the number of 4f electrons that are unpaired.

The homoleptic porphyrins' and phthalocyanines' double- and triple-decker complexes with lanthanide metals are shown in Figure 1.29.

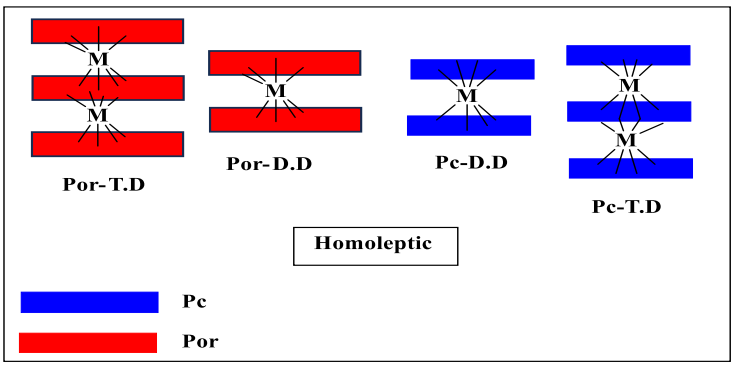

Figure 1.29: Structure of homoleptic porphyrin or phthalocyanine double- and triple-decker complexes.

1.7.2 Synthesis of homoleptic phthalocyanine double- and triple-decker complexes:

Sandwich metal bis-phthalocyanine complexes were first synthesised by Russian scientists in 1965. The synthesis of bis-phthalocyanine complexes may be classified into three groups according to the nature of the starting molecule.[59]

Homoleptic double-decker complexes are often synthesised using the template method or by metalating the uncoordinated ligand. Kirin and Moskashev[64] synthesised and characterised the first lanthanide bis-phthalocyanines. They reacted a combination of phthalonitrile and lanthanide acetates at 280–290 °C for 40–90 min, which led to the formation of bis-phthalocyanine complexes, and the yield of these complexes ranged from 10 to 15%, as shown in Scheme 1.21.

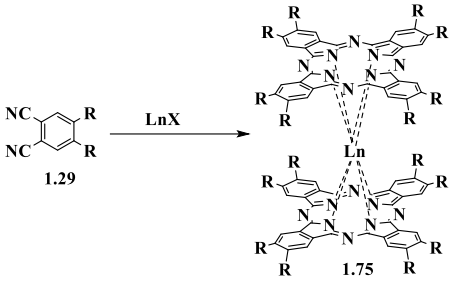

Scheme 1.21: Synthesis of homoleptic double decker **1.75**.

The homoleptic triple-decker complexes were first described by Russian researchers[65] in 1967. The study conducted at 280±290 °C for 1 to 8 hrs produced compounds with double-decker complexes, including binuclear tris-phthalocyanine complexes Pc_3Ln_2 (Ln = Pr, Nd, Er, Lu).

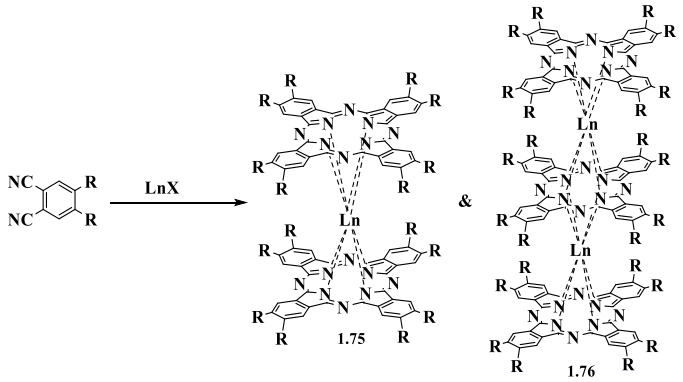

Scheme 1.22: Synthesis of homoleptic double and triple deckers **1.75** and **1.76**.

1.7.3 Synthesis of homoleptic porphyrins double- and triple-decker complexes:

Combinations of bis(2,3,7,8,12,13,17,18-octaethylporphyrinato), tris(2,3,7,8,12,13,17,18-octaethylporphyrinato) with europium (III) and cerium (III) metals were used to synthesise $Eu(OEP)_2$, $Eu_2(OEP)_3$ and $Ce(OEP)_2$, $Ce_2(OEP)_3$, homoleptic porphyrin double- and triple-decker complexes. As illustrated in Figure 1.31, Buchler *et al.* successfully synthesised these complexes by heating a solution of $H_2(OEP)$ and $Eu(acac)_3.H_2O$ in 1,2,4-trichlorobenzene (TCB) under nitrogen for 20 hrs.

The double- and triple-decker complexes were then isolated using an alumina column. $Eu(OEP)_2$ double-decker was obtained as a dark blue solid with a 79% yield, while $Eu_2(OEP)_3$

triple-decker was obtained in a lower yield of 16%.[66,67] The same process was used to synthesise $Ce(OEP)_2$ DD and $Ce_2(OEP)_3TD$. Ce $(OEP)_2$ DD was obtained with a 55% yield, while $Ce_2(OEP)_3TD$ was obtained with a 35% yield (Figure 1.30).

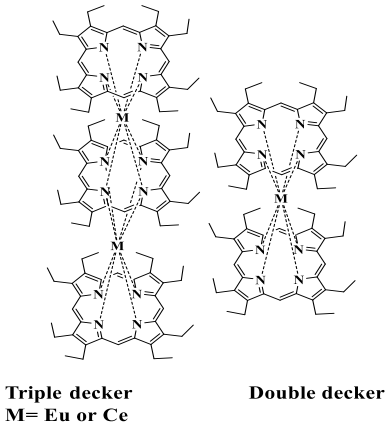

Figure 1.30: Homoleptic double and triple deckers.

1.8 Heteroleptic double- and triple-decker complexes:

Tetrapyrrole derivatives with mixed porphyrin and phthalocyanine macrocycles are called heteroleptic complexes, and different isomers are theoretically possible, as shown in Figure 1.31 for triple deckers.[68]

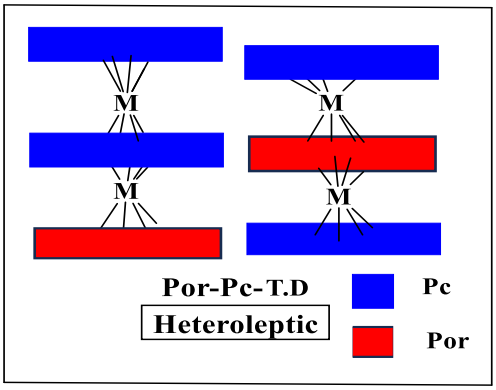

Figure 1.31: Structure of heteroleptic porphyrin-phthalocyanine triple-decker complexes.

Heteroleptic sandwich compounds with porphyrinto or phthalcayinato ligands were first reported in 1986, with increased attention since 1990. Syntheses of novel porphyrin and phthalocyanine triple-decker complexes have been achieved using various methods.

The first technique, “one-by-one deck construction of triple-decker”, includes the reaction of $Ln(acac)_3.nH_2O$ with porphyrin to form a stable complex, followed by a reaction with phthalonitrile to generate the planned double-decker complexes (Scheme 1.23).[69]

Furthermore, mixes of triple-decker complexes $[Por]_2[Pc]Ln_2$ and $[Por][Pc]_2Ln_2$ were synthesised directly from the corresponding double-decker complexes and the $[Por]Ln(acac)_3$ precursor.[70,71]

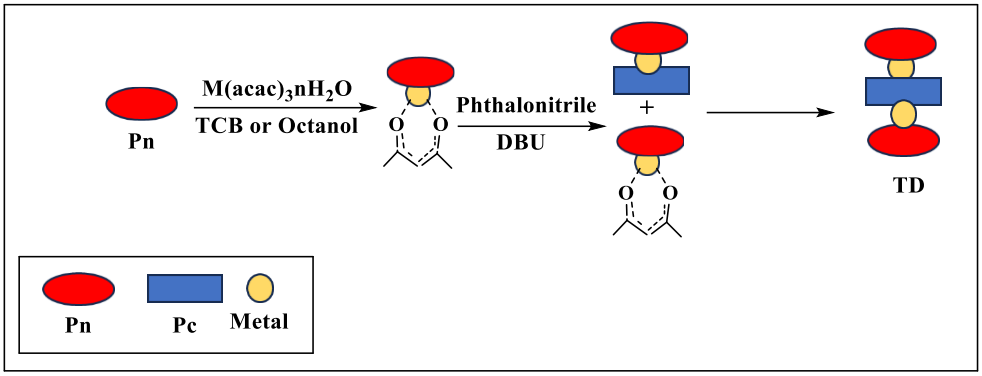

Scheme 1.23. One-pot synthesis with two steps using different starting materials.

The second method, known as the one-pot procedure, improved the synthesis of heteroleptic double- and triple-decker (porphyrinato)(phthalocyaninates) of various lanthanides (La, Eu). This method involves beginning with porphyrin, phthalonitrile, and lanthanide acetylacetonate, and utilising a high-boiling-point alcohol as the solvent. A yield of 30% was obtained by refluxing tetrakis-meso-(4-methoxyphenyl)-porphyrin, 4,5-dicyanobenzo-15-crown-5, lanthanide acetylacetonate, and DBU in 1-octanol. This leads to the symmetric heteroleptic triple-decker compound.[71,72] Whereas the double-decker complex 1.79 was synthesised as a green product with a yield of 12–35%, the triple-decker complex 1.80 was produced as a brown product with a yield of 15–30% (Scheme 1.24).

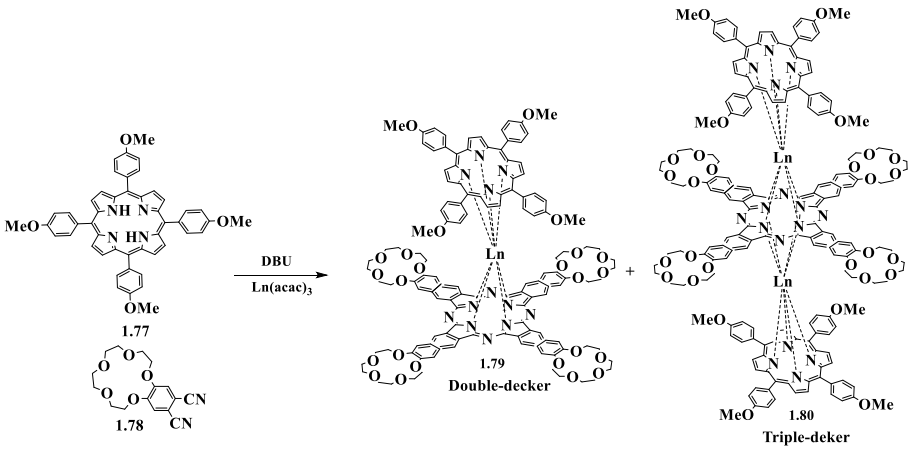

Scheme 1.24: Tsivadze and *et al.*, general protocol for TD formation.

Lu and colleagues[73] found that the yield of mixed triple-decker rare earth complexes $M_2[Por](Pc)_2$ is influenced by the metal ionic radius and successfully produced and analysed

mixed triple-deckers. The reaction of H_2[Por] and $M(acac)_3H_2O$ in TCB was monitored using UV-vis spectroscopy under N_2 reflux. The metal-free H_2[Por] was transformed into the half-sandwich rare earth complex M[Por](acac) within 4–5 hrs, resulting in a red solution.

The solution was cooled under nitrogen and then double-decker $M(Pc)_2$ was added. The mixture was heated for 12 hrs, resulting in a dark green solution, and it was purified using column chromatography and precipitated into MeOH, affording the triple-decker complex. Nine TD complexes with A_2B type structures (Scheme1.25) were synthesised, with yields up to 58% of Ln_2[Por]$(Pc)_2$ obtained for Eu, Sm, Gd, Tb, Dy and Pr, while Ce_2 and La_2 TD produced lower yields.[73]

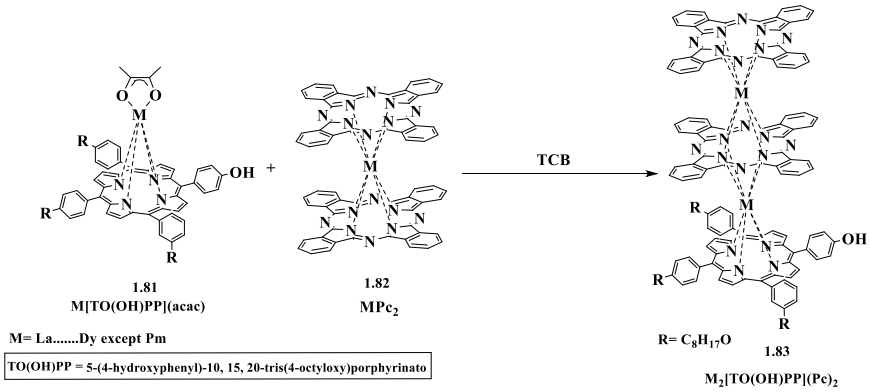

Scheme 1.25: Synthesis of new mixed rare earth triple-decker complexes with A_2B type [5-(4-hydroxyphenyl)-10,15,20-tris- (4-octyloxyphenyl) porphyrinato] and phthalocyaninato ligand.

Yang *et al.*[74] succeeded in increasing selectivity forming a terbium (III) triple-decker complex [(TNP)Tb (Pc)Tb(TNP)] by first generating the half sandwich complex Tb(III)(TNP)(acac) and reacting it with Li_2Pc in refluxing 1, 2, 4-trichlorobenzene, as shown in Scheme 1.26.

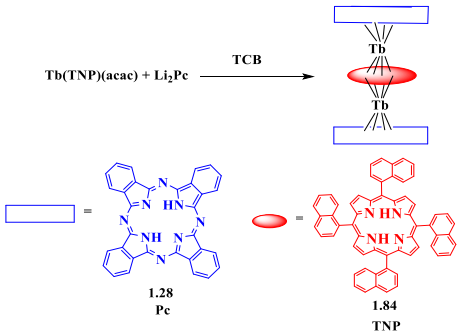

Scheme 1.26: Synthesis of a triple-decker compound of terbium (III).

The resulting compound demonstrated good solubility in common organic solvents such as chloroform ($CHCl_3$), dichloromethane (CH_2Cl_2), and toluene. It was purified through column chromatography, yielding the final product with a 20% recovery.

The single-crystal X-ray of the terbium (III) TD complex is shown in Figure 1.32 and shows that each porphyrin is a single atropisomer with the naphthalenes oriented away from the central Pc.[74]

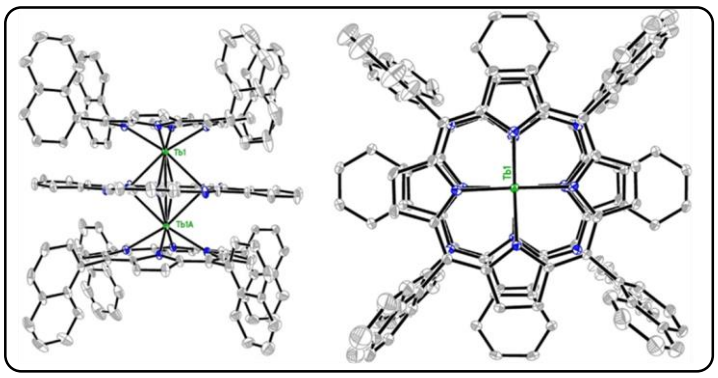

Figure 1.32: XRD crystal structure of [(TNP)Tb(Pc)Tb(TNP)].[74]
Reproduced with permission from (1.32).

Birin *et al.*[75] have described a strategy to synthesise the heteroleptic lanthanide (porphyrinato)(phthalocyanines) by allowing the free-base porphyrin, phthalonitrile, and lanthanide acetylacetonate to reflux in 1-hexanol with DBU for a day, as shown in Scheme1.27. Unsubstituted and substituted porphyrins, in addition to unsubstituted and substituted phthalocyanines, were employed (Figure 1.33).

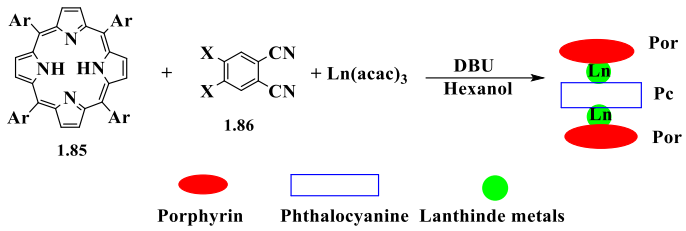

Scheme 1.27: Synthesis of heteroleptic lanthanide TD complexes.

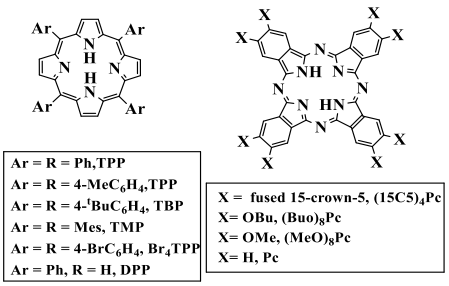

Figure 1.33: Ligand designation used by Birin *et al.*

Birin and team[75] successfully produced lanthanum and neodymium (III) triple-decker complexes, with tetra(4-bromophenyl) porphyrinato and tetra(15-crown-5) phthalocyaninato

ligands, with 63% and 55% yields respectively. Neodymium (III) triple-decker [Br_4TPP][$(BuO)_8$Pc] was obtained in 56% yield; however the Neodymium (III) triple-decker [Br_4TPP][$(MeO)_8$Pc] was obtained in only 6% yield. The reaction of unsubstituted phthalocyanine with Br_4TPP revealed that the TD was not formed in this attempt with neodymium metal salt.

The study of mixed sandwich phthalocyanine and porphyrinato europium triple-deckers, conducted by Xia Zhang, Lihong Liu *et al.*[76] proposed a TD complex as shown in Scheme 1.28. The triple-decker design was formed by coordinating Eu^{3+} ions with $Pc(OPh)_8$ molecules, refluxing metal-free tetra-pyridyl porphyrin and $Eu(acac)_3.nH_2O$ under N_2 and isolating and recrystallising the desired TD **1.89** product.

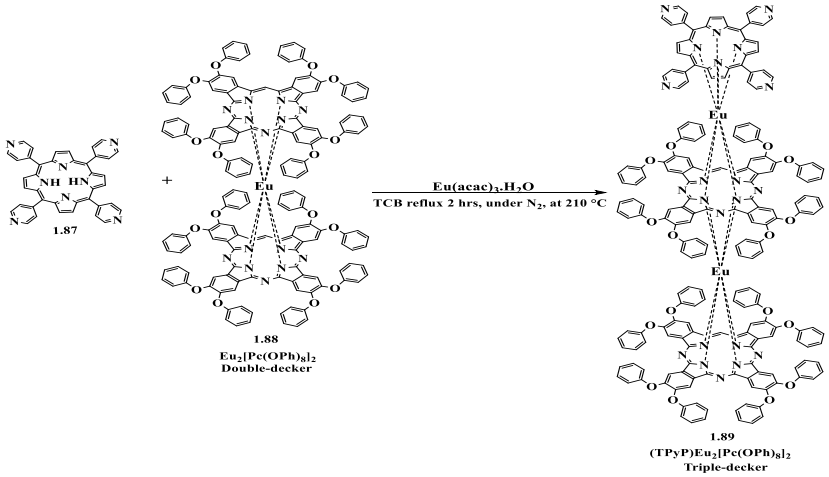

Scheme 1.28: Synthesis of (phthalocyaninato)(porphyrinato) europium complex (TPyP)Eu_2[Pc $(OPh)_8]_2$.

Xia Zhang *et al.*[77] produced Eu_2[Pc $(OPh)_8]_2$(MPyPP) following the above procedure but using a different porphyrin unit. The mixture of Eu[Pc $(OPh)_8]_2$, metal-free MPyPP, and $Eu(acac)_3.nH_2O$ was refluxed in TCB for 2 hrs under N_2, and the product **1.91** was isolated and gained in 34% yield, as shown in Scheme 1.29.

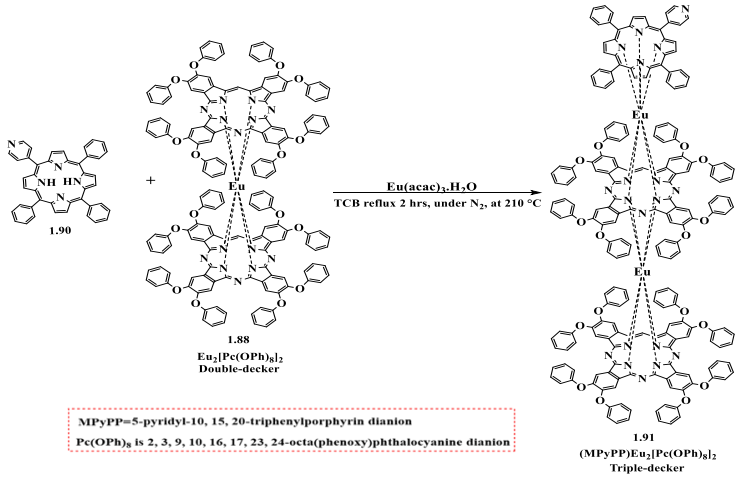

Scheme 1.29: Synthesis of TD complex (MPyPP)Eu_2[Pc $(OPh)_8]_2$ **1.91**.

The Cammidge group[53,54] has developed a methodology for producing high yields of heteroleptic triple-deckers with a bridge. This method uses a dyad intermediate to control the synthesis processes, initially linking two porphyrin units with an n-alkyl chain. For hosting unsubstituted phthalocyanine and two lanthanide atoms, n-decyl was determined as an appropriate length for creating (Por-Pc-Por "ABA") triple-decker **1.92**, as shown in Scheme 1.30.

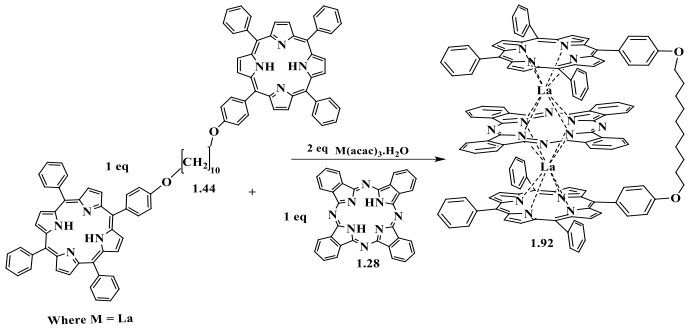

Scheme 1.30: Procedure for ABA triple-deckers incorporating unsubstituted phthalocyanine developed by Cammidge *et al.*

The Cammidge group successfully grew crystals that confirmed the ABA arrangement, as shown in Figure 1.34.

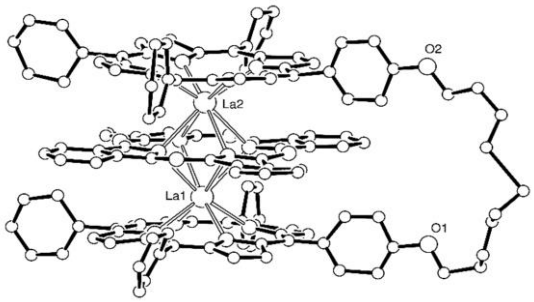

Figure 1.34: XRD structure showing the Pc located between di-porphyrin ("ABA").[53]
Reproduced with no need for permission in Figure (1.34).

1.9 The significant applications and uses of multi-decker complexes:

The characteristics of sandwich complexes can be tailored by choosing metals and macrocyclic ligands impacting their spectroscopic traits and redox properties. The versatility of TD complexes renders them appealing for uses like single-molecule magnets (SMMs) and thin-film transistors (OTFT) mentioned briefly below.

1.9.1 Application of double- and triple-decker complexes in single-molecule magnets:

Double and triple deckers have been utilised as molecular magnets due to their structural and electronic characteristics. Development of dysprosyium in single-molecule magnets (SMMs) is particularly noteworthy.[40,78] The powerful magnetic characteristics of dysprosium result from the electronic distribution; it is difficult to change the direction of magnetism (spin reversal),

and this ensures that the magnetism remains for a long period (slow relaxation). This is important to maintain stable magnetic behaviour, which is what is required in SMM applications.[79]

These factors play a role in the properties of single-molecule magnets. The characteristics of the SMM could be altered by changing the types of ligands and the structure of the complexes.[80] An analysis carried out as a case study by researchers reviewed the properties of triple-decker compounds containing yttrium and dysprosium ions, placed in-between ligands like phthalocyanine and porphyrin. These structures (dysprosyium-dysprosyium **1.93**, yttrium-dysprosyium **1.94**, and dysprosyium-ytrium **1.95**) showed properties that varied depending on how metals were paired and coordinated geometrically. Only complexes like **1.93** and **1.94** demonstrated SMM behaviour, while **1.95** complex did not display any useful traits. The group studied the structure of dysprosium compounds using X-ray crystal diffraction analysis to understand their composition and features, as shown in Figure 1.35. Interestingly, they found that the arrangement of the macrocycles impacted the properties of SMMs.[80]

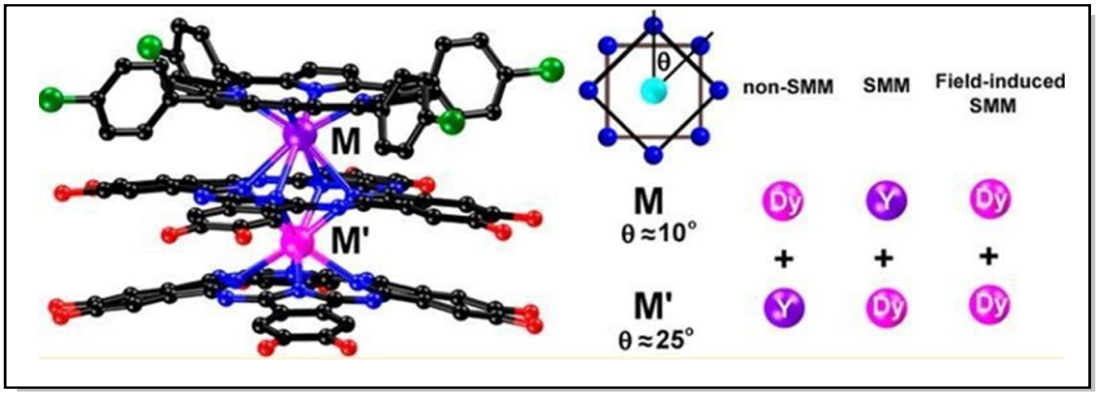

Figure 1.35: Mixed triple decker of (phthalocyaninato) (porphyrinato) with (Dy−Dy) **1.93**, (Y−Dy) **1.94**, and (Dy−Y) **1.95**.[80]

Reproduced with no need for permission in Figure (1.35).

A second example in SMM applications was the dysprosium-containing heteroleptic double-decker complexes shown in Scheme 1.31. In this study, three sandwich-type dysprosium complexes, namely Dy(Pc)(TCPP) **1.96**, Dy(Pc)(TPP) **1.97**, and Dy(Pc)(TBPP) **1.98**, consisting of a dysprosium ion between phthalocyanine and porphyrin ligands and meso-attached phenyl substituents, (e.g. cyano-phenyl, phenyl, and tert-butylphenyl groups), Dy (III) (Pc)(TCPP) **1.96**, was prepared by refluxing a mixture of H_2TCPP and Dy(acac)$_3$.nH_2O in octanol under nitrogen for 4 hrs. After a brief cooling, Li_2Pc was added, and the resulting mixture was heated to reflux for a further 4 hrs under N_2. After cooling, the solvent was removed and then purified by chromatography on a silica gel column with $CHCl_3$ as the eluent.[81]

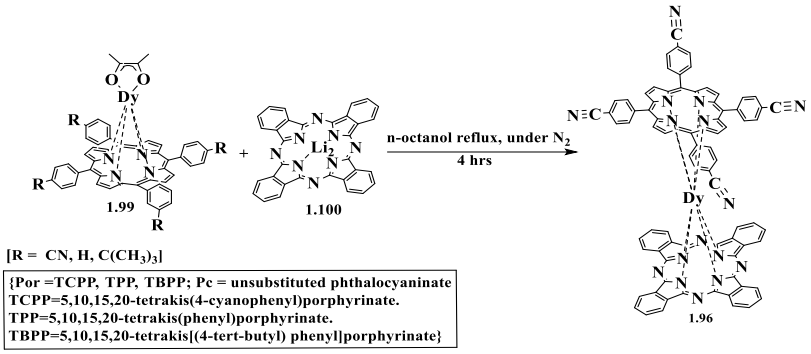

Scheme 1.31: A molecular schematic of the sandwich-type mixed (phthalocyaninato)(porphyrinato) double-decker complex **1.96**, wherein R may be (CN, H, or $C(CH_3)_3$.

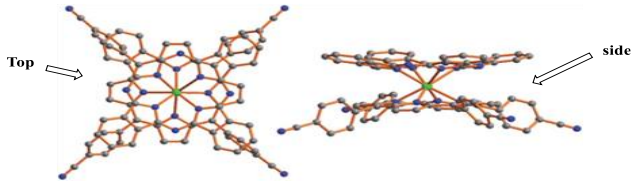

Figure 1.36: The molecule structure of Dy (Pc)(TCPP) double decker **1.96**.[81] Reproduced with permission from (1.36).

1.9.2 Utilisation of triple-decker structure in organic thin-film transistors (OTFT):

Organic thin-film transistors (OTFTs) are versatile low-cost devices used widely in applications. Using porphyrins and phthalocyanines in such transistors can boost semiconductor characteristics such as charge mobility. When they are integrated into triple-decker structures, there have been advancements observed in how electric charges move within the devices. The arrangement of the macrocycles enhances the alignment of π orbitals to facilitate the movement of charges in the semiconductor materials.[82]

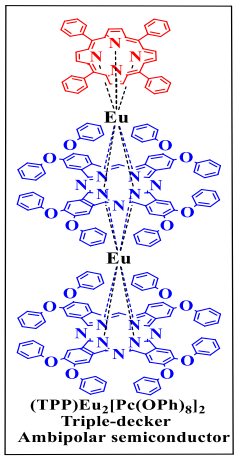

Figure 1.37: Organic thin-film transistors based on heteroleptic triple-decker structures.

References:

(1). McKeown, N.B. Phthalocyanine Materials: Synthesis, Structure and Function; Cambridge University Press, **1998**.

(2). Buchler, J.W.; Ng, D.K. Metal Tetrapyrrole Double and Triple Deckers with Special Emphasis on Porphyrin Systems. ChemInform. **2003**, 34 (44). DOI: 10.1002/chin.200344215.

(3). Ion, R.M. Porphyrins and phthalocyanines: photosensitizers and photocatalysts. **2017**, 9, pp. 189-221.

(4). Can Karanlık, C., Aguilar-Galindo, F., Sobotta, L., Guzel, E. and Erdogmus, A. Combination of light and ultrasound: exploring sono–photochemical activities of phthalocyanine-based sensitizers. Journal of Physical Chemistry C, **2023**, 127(19), pp. 9145-9153.

(5). Milgrom, L.R. The Colours of Life: An Introduction to the Chemistry of Porphyrins and Related Compounds; Oxford University Press, **1997**.

(6). With, T.K. A short history of porphyrins and the porphyrias. International Journal of Biochemistry, **1980**,11(3-4), pp.189-200.

(7). Lesage, S.; Xu, H.; Durham, L. The occurrence and roles of porphyrins in the environment: possible implications for bioremediation. Hydrological Sciences Journal, **1994**, 38 (4), 343-354.

(8). Heyes, D.J.; Ruban, A.V.; Wilks, H.M.; Hunter, C.N. Enzymology below 200 K: The kinetics and thermodynamics of the photochemistry catalysed by protochlorophyllide oxidoreductase. Proc. Natl. Acad. Sci. USA. **2002,** 99 (17), 11145-11150.

(9). Heyes, D.J.; Heathcote, P.; Rigby, S.E.J.; Palacios, M.; van Grondelle, R.; Hunter, C.N. The first catalytic step of the light-driven enzyme protochlorophyllide oxidoreductase proceeds via a charge transfer complex. Journal of Biological Chemistry, **2006**, 281 (37), 26847-26853.

(10). Falk, J.E.; Smith, K.M., Ed. Porphyrins and Metalloporphyrins: A new edition based on the original volume by J. E. Falk; Elsevier, Amsterdam, 1975.

(11). Kadish, K.M.; Smith, K.M; Guilard, R. The Porphyrin Handbook, Volume 1; Academic Press, San Diego, CA, **2000**.

(12). Moss, G. Nomenclature of tetrapyrroles (Recommendations 1986). Pure and Applied Chemistry, **1987,** 59 (6), 779-832. DOI: 10.1351/pac198759060779.

(13). Braun, J.; Limbach, H.H.; Williams, P.G.; Morimoto, H.; Wemmer, D.E. Observation of kinetic tritium isotope effects by dynamic NMR. The tautomerism of porphyrin. Journal of the American Chemical Society, **1996**, 118 (30), 7231-7232.

(14). Steiner, E. and Fowler, P.W. Ring currents in the porphyrins: a four-orbital model. ChemPhysChem, **2002**, 3(1), pp.114-116.

(15). Gjuroski, I.; Furrer, J.; Vermathen, M. Probing the interactions of porphyrins with macromolecules using NMR spectroscopy techniques. Molecules, **2021**, 26 (7), 1942.

(16). Barkigia, K.M.; Fajer, J.; Adler, A.D.; Williams, G.J.B. Crystal and molecular structure of (5,10,15,20-tetra-N-propylporphinato) lead (II): a "roof" porphyrin. Inorganic Chemistry, **1980**, 19 (7), 2057-2061.

(17). Walker, V.E.; Castillo, N.; Matta, C.F.; Boyd, R.J. The Effect of multiplicity on the size of iron (II) and the structure of iron (II) porphyrins. Journal of Physical Chemistry A, **2010**, 114 (37), 10315-10319.

(18). Gouterman, M. Spectra of porphyrins. Journal of Molecular Spectroscopy, **1961**, 6, 138-163.

(19). Giovannetti, R. The Use of Spectrophotometry UV-Vis for the Study of Porphyrins*;* In Macro to Nano Spectroscopy*;* **2012**; Vol. 6, pp 87–108.

(20). Yang, R.; Wang, K.; Long, L.; Xiao, D.; Yang, X.; Tan, W. A selective optode membrane for histidine based on fluorescence enhancement of meso-meso-linked porphyrin dimer. Analytical Chemistry, **2002**, 74 (5), 1088-1096.

(21). Rio, Y.; Rodriguez-Morgade, M. S.; Torres, T. Modulating the Electronic Properties of Porphyrinoids: A Voyage from the Violet to the Infrared Regions of the Electromagnetic Spectrum. Org. Biomol. Chem. **2008**, 6 (11), 1877–1894.

(22). Di Natale, C.; Salimbeni, D.; Paolesse, R.; Macagnano, A.; D'Amico, A. Porphyrins-based opto-electronic nose for volatile compounds detection. Sensors and Actuators B: Chemical, **2000**, 65 (1-3), 220-226.

(23). Rothemund, P. Formation of porphyrins from pyrrole and aldehydes. Journal of the American Chemical Society, **1935**, 57 (10), 2010-2011.

(24). Rothemund, P.; Menotti, A.R. Porphyrin studies. IV. 1. The synthesis of $\alpha,\beta,\gamma,\delta$-tetraphenylporphine. Journal of the American Chemical Society, **1941**, 63 (1), 267-270.

(25). a. Adler, A. D.; Longo, F. R.; Shergalis, W. Mechanistic Investigations of Porphyrin Syntheses. I. Preliminary Studies on ms-Tetraphenylporphin. Journal of the American Chemical Society, **1964**, 86 (15), 3145-3149**. b.** Adler, A. D.; Longo, F. R.; Finarelli, J. D.; Goldmacher, J.; Assour, J.; Korsakoff, L. J. A Simplified Synthesis for Meso-tetraphenylporphine. Journal of Organic Chemistry, **1967**, 32 (2), 476.

(26). Lindsey, J.S.; Schreiman, I.C.; Hsu, H.C.; Kearney, P.C.; Marguerettaz, A.M. Rothemund and Adler-Longo reactions revisited: synthesis of tetraphenylporphyrins under equilibrium conditions. Journal of Organic Chemistry, **1987**, 52 (5), 827-836.

(27). Lindsey, J.S.; MacCrum, K.A.; Tyhonas, J.S.; Chuang, Y.Y. Investigation of a synthesis of meso-porphyrins employing high concentration conditions and an electron transport chain for aerobic oxidation. Journal of Organic Chemistry, **1994**, 59 (3), 579-587.

(28). Sessler J.L.; Mozaffari A.; Johnson M.R. 3,4-diethylpyrrole and 2,3,7,8,12,13,17,18-octaethylporphyrin. Organic Synthesis, **1992**, 70, 68. DOI: 10.15227/orgsyn.070.0068

(29). Senge, M.O.; Shaker, Y.M.; Pintea, M.; Ryppa, C.; Hatscher, S.S.; Ryan, A.; Sergeeva, Y. Synthesis of meso-Substituted ABCD-Type Porphyrins by Functionalization Reactions. European Journal of Organic Chemistry, **2010**, (2), 237-258.

(30). Senge, M. O.; Plunkett, S.; Roger, L.; Moylan, C., The Synthesis of ABCD-type porphyrins. In Tetrapyrrole Discussion Group Meeting Cardiff, UK, **2011**; Vol. Br. J. Dermatol., p 1167.

(31). Leznoff, C.; Lever, A. Properties and Applications. VCH, New York, **1989**.

(32). Rio, Y.; Rodriguez-Morgade, M.S. and Torres, T. Modulating the electronic properties of porphyrinoids: a voyage from the violet to the infrared regions of the electromagnetic spectrum. Organic & Biomolecular Chemistry, **2008**, 6(11), pp.1877-1894.

(33). Yaraşır, M.N.; Kandaz, M.; Koca, A. and Salih, B. Functional alcohol-soluble double-decker phthalocyanines: synthesis, characterization, electrochemistry and peripheral metal ion binding. Journal of Porphyrins and Phthalocyanines, **2006**, 10(08), pp.1022-1033.

(34). Ghani, F.; Kristen, J. and Riegler, H. Solubility properties of unsubstituted metal phthalocyanines in different types of solvents. Journal of Chemical & Engineering Data, **2012**, 57(2), pp.439-449.

(35). Breloy, L.; Yavuz, O.; Yilmaz, I.; Yagci, Y.; Versace, D.L. Design, synthesis and use of phthalocyanines as a new class of visible-light photoinitiators for free-radical and cationic polymerizations. Polymer Chemistry, **2021**, 12 (30), 4291-4316.

(36). Chen, Y., Dini, D., Hanack, M., Fujitsuka, M. and Ito, O. Excited state properties of monomeric and dimeric axially bridged indium phthalocyanines upon UV-Vis laser irradiation. Chemical Communications, **2004**, (3), pp.340-341.

(37). Mironov, A.F. Porphyrin complexes with lanthanides. Uspekhi Khimii, **2013**, 82(4), pp.333-351.

(38). Mironov, A.F. Lanthanide porphyrin complexes. Russian Chemical Reviews, **2013**, 82(4), p.333.

(39). Lu, G.; Li, J.; Yan, S.; Zhu, W.; Ou, Z.; Kadish, K.M. Synthesis and characterization of rare earth corrole–phthalocyanine heteroleptic triple-decker complexes. Inorg.Chem, **2015**, 54 (12), 5795-5805.

(40). Jiang, J.; Ng, D.K. A decade journey in the chemistry of sandwich-type tetrapyrrolato−rare earth complexes. Accounts Chem. Res, **2009**, 42 (1), 79-88.

(41). Liu, Z.; Yasseri, A. A.; Lindsey, J. S.; Bocian, D. F. Molecular Memories that Survive Silicon Device Processing and Real-World Operation. Science, **2003**, 302, 1543–1545.

(42). Ishikawa, N.; Sugita, M.; Wernsdorfer, W. Quantum Tunneling of Magnetization inLanthanide Single-Molecule Magnets: Bis(phthalocyaninato)terbium and Bis(phthalocyaninato)dysprosium Anions. Angew. Chem., Int. Ed, **2005**, 44, 2931–2935.

(43). Gao, J., Lu, G., Chen, Y. and Bouvet, M. Solution-processed thin films based on sandwich-type mixed (phthalocyaninato)(porphyrinato) europium triple-deckers: Structures and comparative performances in ammonia sensing. Sensors and Actuators B: Chemical, **2012**, 166, pp.500-507.

(44). Chen, Y.; Su, W.; Bai, M.; Jiang, J.; Li, X.; Liu, Y.; Wang, L.; Wang, S. HighPerformance Organic Field-Effect Transistors Based on AmphiphilicTris(phthalocyaninato) Rare Earth Triple-Decker Complexes. J. Am. Chem. Soc.**2005**, 127, 15700–15701.

(45). Sun, X., Li, D., Chen, G. and Zhang, J. A series of new porphyrin dyads: The synthesis and photophysical properties. Dyes and pigments, **2006**, 71(2), pp.118-122.

(46). D'Souza, F., Smith, P.M., Zandler, M.E., McCarty, A.L., Itou, M., Araki, Y. and Ito, O. Energy transfer followed by electron transfer in a supramolecular triad composed of boron dipyrrin, zinc porphyrin, and fullerene: a model for the photosynthetic antenna-reaction center complex. Journal of the American Chemical Society,**2004**, 126(25), pp.7898-7907.

(47). Shkirdova, A. O.; Tyurin, V. S.; Chernyadyev, A. Y.; Zamilatskov, I. A., Synthesis of new porphyrinoid dyads linked with a butenyne bridge via the Sonogashira reaction. New Journal of Chemistry, **2024**, 48 (37), pp.16481-16490.

(48). Lin, V.S.Y., DiMagno, S.G. and Therien, M.J. Highly conjugated, acetylenyl bridged porphyrins: new models for light-harvesting antenna systems. Science, **1994**,264(5162), pp.1105-1111.

(49). Tait, C.E., Neuhaus, P., Peeks, M.D., Anderson, H.L. and Timmel, C.R. Transient EPR reveals triplet state delocalization in a series of cyclic and linear π-conjugated porphyrin oligomers. Journal of the American Chemical Society, **2015**, 137(25), pp.8284-8293.

(50). Senge, M.O. and Feng, X. Synthesis of directly meso-meso linked bisporphyrins using organolithium reagents. Tetrahedron letters, **1999**, 40(22), pp.4165-4168.

(51). Jin, L.M., Chen, L., Yin, J.J., Guo; and Chen, Q.Y. A Facile and Potent Synthesis of meso, meso-Linked Porphyrin Arrays Using Iodine (III) Reagents, **2005**.

(52). Jiblaoui, A., Baudequin, C., Chaleix, V., Ducourthial, G., Louradour, F., Ramondenc, Y., Sol, V. and Leroy-Lhez, S. An easy one-pot desilylation/copper-free Sonogashira cross-coupling reaction assisted by tetra-butylammonium fluoride (TBAF): synthesis of highly π-conjugated porphyrins. Tetrahedron, **2013**, 69(25), 5098-5103.

(53). González Lucas, D. Molecular machines constructed from multichromophore arrays. Ph.D. Dissertation, University of East Anglia, Norwich, **2014**.

(54). González-Lucas, D.; Soobrattee, S.C.; Hughes, D.L.; Tizzard, G.J.; Coles, S.J.; Cammidge, A.N. Straightforward and Controlled Synthesis of Porphyrin–Phthalocyanine–Porphyrin Heteroleptic Triple-Decker Assemblies. Chemistry-A European Journal, **2020**, 26 (47), 10724-10728.

(55). Ryan, A., Gehrold, A., Perusitti, R., Pintea, M., Fazekas, M., Locos, O.B., Blaikie, F. and Senge, Porphyrin dimers and arrays. M.O, **2011**, 5817-5844.

(56). Anabuki, S., Tokuji, S., Aratani, N. and Osuka, A. Direct meso-alkynylation of porphyrins doubly assisted by pyridyl coordination. Organic letters, **2012**, 14(11), 2778-2781.

(57). Senge, M. O.; Feng, X., Synthesis of directly meso-meso linked bisporphyrins using organolithium reagents. Tetrahedron Letters, **1999**, 40 (22), 4165-4168.

(58). Jin, L.M., Chen, L., Yin, J.J., Guo; and Chen, Q.Y. A Facile and Potent Synthesis of meso, meso-Linked Porphyrin Arrays Using Iodine (iii) Reagents, **2005**.

(59). Gaspard, S., Giannotti, C., Maillard, P., Schaeffer, C. and Tran-Thi, T.H. The first synthesis of covalently linked mixed dimer complexes containing phthalocyanine and porphyrin. Journal of the Chemical Society, Chemical Communications, 1986, (16), pp.1239-1241.

(60). Lo, P.C., Leng, X. and Ng, D.K. Hetero arrays of porphyrins and phthalocyanines. Coordination Chemistry Reviews, **2007**, 251(17-20), pp.2334-2353.

(61). Andrew Charles Behrle; **2012**. The Study of Lanthanides for Organometallic and Separations Chemistry (The University of Toledo).

(62). Horváth, O., Huszánk, R., Valicsek, Z. et al. Photophysics and photochemistry of kinetically labile, water-soluble porphyrin complexes. Coordination chemistry reviews, **2006**, 250(13-14), pp.1792-1803.

(63). Giovannetti, R. The use of spectrophotometry UV-Vis for the study of porphyrins. Macro to nano spectroscopy, **2012,** pp.87-108.

(64). Kirin, I.S. Formation of unusual phthalocyanines of the rare-earth elements. Russ. J. Inorg. Chem., **1965**,10, pp.1065-1066.

(65). Kirin, I.S., Moskalev, P.N. and Moskashev, Y.A. New complex compounds of phthalocyanine with rare earth elements. Zhurnal Neorganicheskoi Khimii, **1967**, 12, pp.707-712.

(66). Buchler, J. W.; Knoff, M. In Optical Spectra and Structure of Tetrapyrroles·, Blauer, G., Sund, H., Eds.; de Gruyter: West Berlin, **1985**; pp 91-105

(67). Buchler, J.W., De Cian, A., Fischer, J., Kihn-Botulinski, M. and Weiss, R. Metal complexes with tetrapyrrole ligands. 46. Europium (III) bis (octaethylporphyrinate), a lanthanoid porphyrin sandwich with porphyrin rings in different oxidation states, and dieuropium (III) tris (octaethylporphyrinate). Inorganic Chemistry, **1988**, 27(2), pp.339-345.

(68). Wang, H., Wang, K., Bian, Y., Jiang, J. and Kobayashi, N. Mixed (phthalocyaninato)(porphyrinato) heterometal complexes with sandwich quadruple-decker molecular structure. Chemical Communications, **2011**, 47(24), pp.6879-6881.

(69). K. P. Birin, K. A. Kamarova, Y. G. Gorbunova, A. Y. Tsivadze, Protection of Metals and Physical Chemistry of Surfaces, **2013**, 49, 173-180.

(70). Norah Alsaiari A. Multidecker assemblies from Porphyrin and Phthalocyanine derivatives Ph.D. Dissertation, University of East Anglia, Norwich, **2022**.

(71). Birin, K.P., Gorbunova, Y.G. and Yu. Tsivadze, A. Novel one-pot regioselective route towards heteroleptic lanthanide (phthalocyaninato)(porphyrinato) triple-decker complexes. Journal of Porphyrins and Phthalocyanines, **2009**, 13(02), pp.283-290.

(72). Birin, K.P., Gorbunova, Y.G. and Tsivadze, A.Y. NMR-based analysis of structure of heteroleptic triple-decker (phthalocyaninato)(porphyrinato) lanthanides in solutions. Magnetic Resonance in Chemistry, **2010**, 48(7), pp.505-515

(73). Lu, F.L.; Mao, Y.J.; Wang, W.D.; Xiao, C. Synthesis and characterization of new mixed rare earth triple-decker complexes with A_2B type [5-(4-hydroxyphenyl)-10, 15, 20-tris-(4-octyloxyphenyl) porphyrinato] and phthalocyaninato ligands. Dyes Pigments **2013**, 99 (3), 686-692.

(74). Yang, L.; Yu, Y.; Wang, X.; Zhu, M.; Gao, Q.; Dai, Y.; Bian, Y. Mixed (phthalocyaninato) (tetranaphthylporphyrinato) terbium triple-decker complex: Synthesis, crystal structure and magnetic properties. Inorg. Chem. Commun. **2016**, 73, 30-33.

(75). Birin, K.P.; Poddubnaya, A.I.; Gorbunova, Y.G.; Tsivadze, A.Y. Revisiting the One-Step Synthesis of Heteroleptic Lanthanide (III) (Porphyrinato)(Phthalocyaninates): Opportunities and Limitations, **2017**, 10 (4-5), 514-519.

(76). Zhang, X., Liu, L., Xiao, J., Sun, Z. and Li, P. Organic (TPyP) Eu_2 [Pc $(OPh)_8]_2$/CdS self-assembled hybrid nano-transistors with high ambipolar performance. Journal of Materials Research and Technology, **2020**, 9(6), pp.13682-13691.

(77). Zhang, X., Gao, M. and Xiao, J. A sandwich mixed (Phthalocyaninato)(Porphyrinato) Europium triple-decker: Balanced-mobility, ambipolar organic thin-film transistor. Materials Today Communications, **2021**, 29, p.103003.

(78). Christou, G., Gatteschi, D., Hendrickson, D.N. and Sessoli, R. Single-molecule magnets. MRS bulletin, **2000**, 25(11), pp.66-71.

(79). Marin, R., Brunet, G. and Murugesu, M. Shining new light on multifunctional lanthanide single-molecule magnets. Angewandte Chemie International Edition. **2021** 60(4), pp.1728-1746.

(80). Kan, J.; Wang, H.; Sun, W.; Cao, W.; Tao, J.; Jiang, J. Sandwich-Type Mixed Tetrapyrrole Rare-Earth Triple-Decker Compounds: Effect of the Coordination Geometry on the Single-Molecule-Magnet Nature. *Inorg. Chem.* **2013**, *52* (15), 8505–8510.

(81). Cao, W., Zhang, Y., Wang, H., Wang, K., & Jiang, J. Influence of porphyrin meso-attached substituent on the SMM behavior of dysprosium (III) double-deckers with mixed tetrapyrrole ligands. RSC Advances, **(2015)**, 5(23), 17732-17737.

(82). Zhang, X. and Chen, Y. A sandwich mixed (phthalocyaninato)(porphyrinato) europium triple-decker: Balanced-mobility, ambipolar organic thin-film transistor. Inorganic Chemistry Communications, **2014**, 39, pp.79-82.

Chapter (2): Results and discussion

2. Results and discussion:

2.1 Introduction to the aims of the project:

The Cammidge group successfully synthesised a series of connected multi-decker structures.[1] In the approach, two porphyrins are connected by a flexible carbon-chain spacer (decyl and dodecyl linker) selected to prevent the synthesis of intramolecular porphyrin-porphyrin double-decker complexes and then connected to phthalocyanine to form a triple decker. By using this simple method and precursor, this procedure achieved high yields (Scheme 2.1).

These complexes have properties useful for several potential applications in materials sciences, such as their optical, physical, spectroscopic, electrical, and electrochemical characteristics; they also have vast potential in multibit molecular information storage, sensors, nonlinear optical materials, nanomaterials, and single-molecule magnets.[2,3]

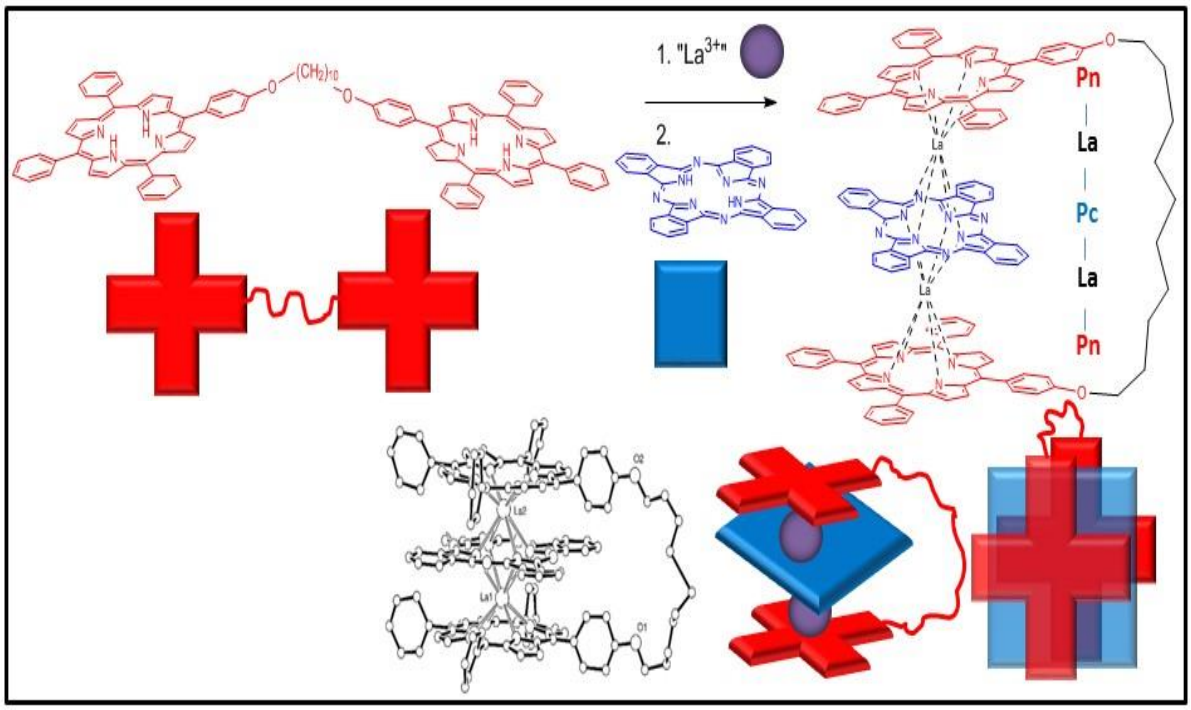

Scheme 2.1: Previous observation from our group.[1]

The first goal of this project was to extend this work, replacing the molecule of Pc with other porphyrinoid cores, such as octaethylporphyrin **2.1** and protoporphyrin (IX) **2.2**, resulting in the heteroleptic (Pn-La-OEP-La-Pn) **2.3** and (Pn-La-PPN-La-Pn) **2.4** triple-decker structures shown in Scheme 2.2.

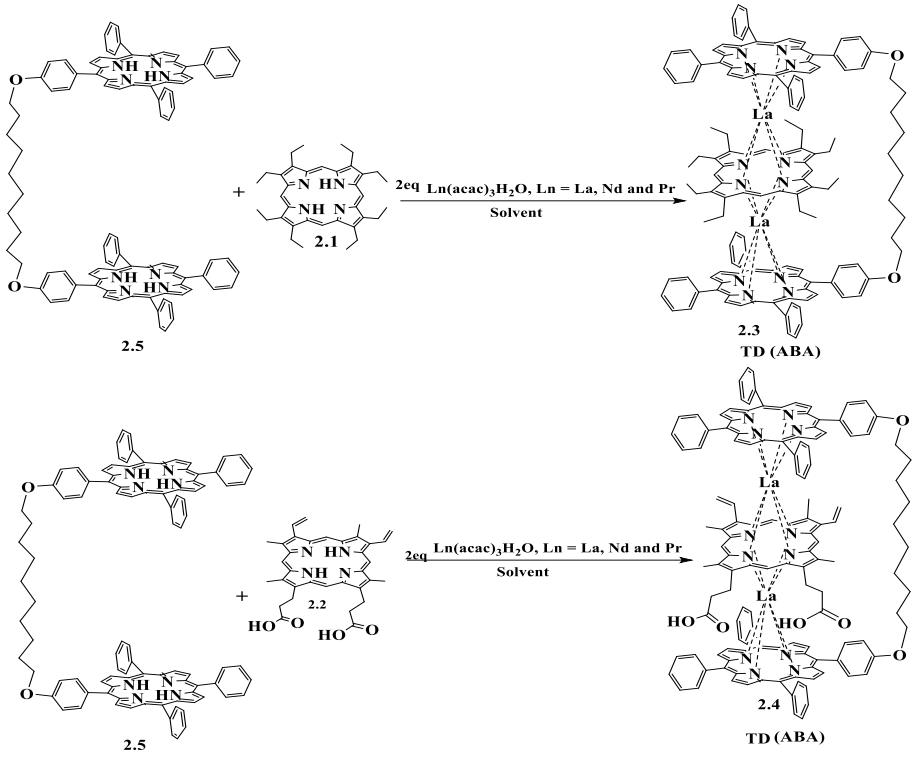

Scheme 2.2: Initially planned routes to linked porphyrin TDs.

If successful, the second goal of this project was to incorporate porphyrins in the bridge by reacting protoporphyrin and TPP-OH to produce porphyrin triad **2.13**, as shown in Scheme 2.3.

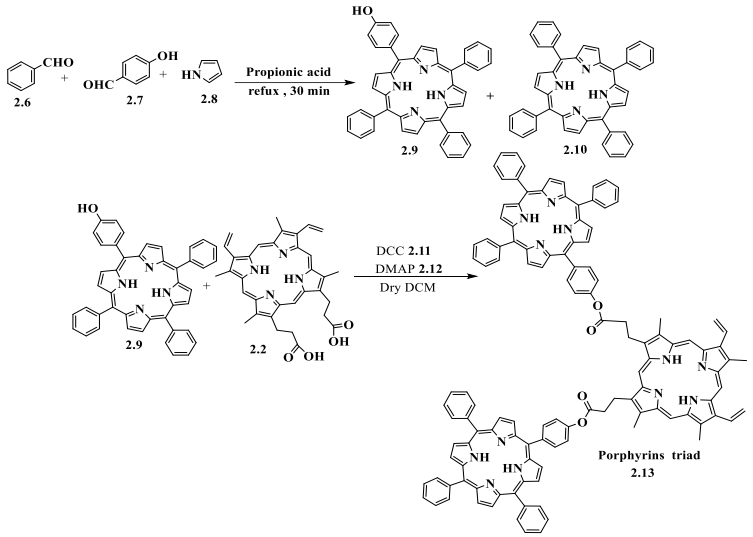

Scheme 2.3: Final planned routes to form porphyrin triad **2.13**.

The final stage, linking the porphyrin triad with 2 eq. of Ln and 1 eq. of another molecule of **2.1**, would yield the assemblies as shown in Scheme 2.4.

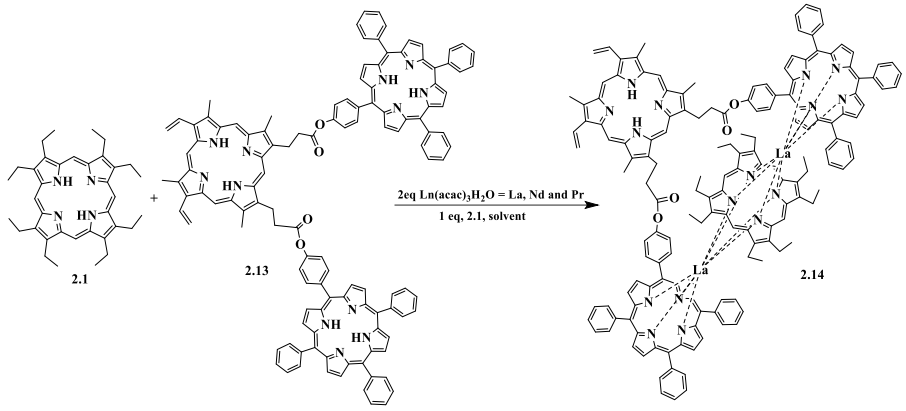

Scheme 2.4: Final planned route to form porphyrin triple-decker **2.14**.

2.2 Synthesis of *p*-hydroxyphenyl-10,15,20-triphenyl-porphyrin TPPOH:

The TPPOH was prepared by using a modified version of Adler's methodology,[4,5] by using (2:2) and (3:1) benzaldehyde **2.6** and 4-hydroxybenzaldehyde **2.7**, respectively. Propionic acid, benzaldehyde **2.6**, and 4-hydroxybenzaldehyde **2.7** were combined and heated to reflux. The mixture was further refluxed after adding freshly distilled pyrrole **2.8** dropwise.

Methanol was added once the mixture had cooled. The crude was placed in the refrigerator overnight to form a precipitate comprising mostly the desired TPPOH **2.9 (**5-p-hydroxyphenyl-10,15,20- triphenyl-porphyrin) and tetraphenyl porphyrin **2.10** as a side product (Scheme 2.5).

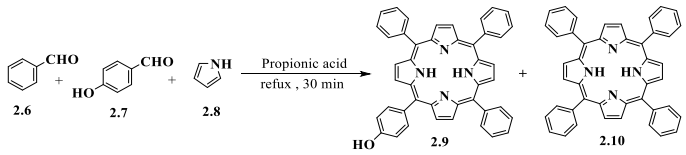

Scheme 2.5: Synthesis of TPP-OH **2.9**.

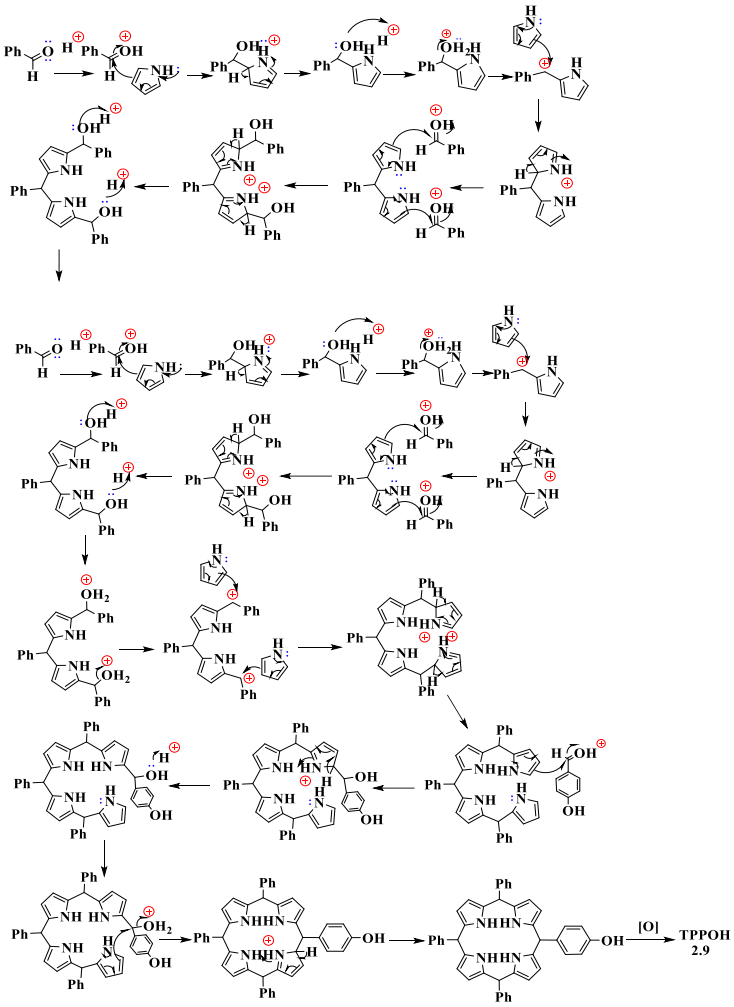

Scheme 2.6: Mechanism of TPP-OH formation.

We used the group's method to separate TPPOH **2.9**,[6] by using a silica gel column. The first purple fraction TPP **2.10** was collected by using DCM: Pet-ether (1:1). After no more purple solution eluted, the solvent system was changed to 100% DCM to recover all TPP-OH fractions. The yield was only 1.2–2%, indicating that further attempts to improve the yield of TPPOH were justified. The results are presented in Table 2.1.

Table 2.1: Attempts to improve the yield of TPPOH **2.9**:

En-try	2.6 Eq, (g)	2.7 Eq, (g)	2.8 Eq, (g)	Propionic-acid ml	Reflux-Time	Addition of 2.9	Yield % of 2.9
1.	2, (5.3)	2, (6.1)	4, (6.7)	200	1 hr	one time	1
2.	2, (5.3)	2, (6.1)	4, (6.7)	200	15 min	one time	trace (0.1)
3.	2, (10.6)	2, (12.2)	4, (13.4)	400	1	one time	no TPPOH iso-lated
4.	3, (7.96)	1, (3.05)	4, (6.94)	250	30 min	dropwise	1.6
5.	3, (3.97)	1, (1.52)	4, (3.14)	200	45 min	dropwise	4.05
6.	3, (7.96)	1, (3.05)	4, (6.94)	150	30 min	Dropwise 7 – 9 min	1.44
7.	3, (3.97)	1, (1.52)	4, (3.14)	200	1	one time	4.13
8.	3, (7.96)	1, (3.05)	4, (6.94)	200	1	Dropwise	1.2
9.	3, (17.5)	1, (7)	4, (14.95)	460	1hr 30 min	one time	5.1
10.	3, (15.92)	1 (6.1)	4, (13.42)	400	1	dropwise	4.24

2.2.1 Attempts to prepare and speed up the separation of TPPOH:

Table 2.1 shows 10 attempts to prepare TPPOH **2.9**, varying solvent amount and distilled pyrrole addition, and using (2:2) and (3:1) ratios for **2.6** and **2.7**, respectively. The experiment involved adding four equivalents of distilled pyrrole **2.8** in various ways, including dropwise and all-at-once, and refluxing all entries, with reaction times ranging from 15 to 90 min. In attempt (4), the reaction mixture was divided into two equal flasks to investigate the impact of the lack of propionic acid after the end of the reaction by examining the yield after precipitation. One was placed directly with methanol after cooling to precipitate. In the other, MeOH was added after evaporating half of the acid. We noticed that removing part of the acid after the end of the reaction did not increase the yield. Reaction 9 provided a high yield (5.1%) of TPPOH **2.9** when using the high quantity of reacting materials **2.6**, **2.7**, and **2.8** in 460 ml of propionic acid. The original method [6] was initially employed for a column chromatography, with a solid phase length of 6 cm and DCM: Pet-ether (1:1) solvent to collect side product TPP **2.10** and then 100% of DCM to recover the desired product **2.9**. The system is effective but takes 8 hrs

to isolate **2.9**, prompting numerous attempts using various solvent systems to reduce this time. A combination of dichloromethane/petroleum ether (3:7) and THF/petroleum ether (1:1) was used; however, it failed to produce a pure fraction and required two columns for the separation of TPPOH.[7] The secondary solvent system, using THF: Pet-ether (1:9 v/v) as an eluent, required an additional column to isolate TPPOH.[8]

The optimum solvent solution identified for isolating TPPOH **2.9** was (3:1) and (4:1) DCM: Pet-ether, with TPP **2.10** recovered as the first fraction. The second fraction created a 250 ml mixture of **2.10** and **2.9**. The polarity was increased to 100% for pure TPPOH, as shown in the TLC plate in Figure 2.1. This proved superior to the reported system,[6] as it took only 3 hrs, as opposed to 8 hrs.

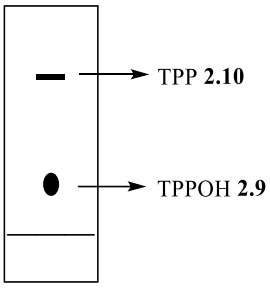

Figure 2.1: TLC shows the fractions of the TPPOH reaction in the (3:1) DCM:Pet-ether eluant.

We recommend a refluxing time of 30 min for normal quantities, 1 hr for double quantities, and 90 min for high scales. In terms of ratio, (3:1) produced a good amount of **2.9**, as shown above in Table 2.1. A 2:2 ratio of starting materials causes a low yield of TPPOH due to the potential for side products, as shown in Figure 2.2.

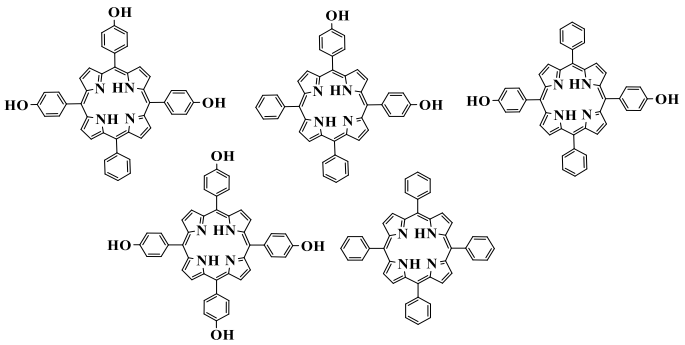

Figure 2.2: Possible side products from a **2:2** aldehyde ratio reaction.

As discussed above, the modifications to isolate the TPPOH have a big impact on time, effectiveness, and solvent consumption. To minimise solvent consumption and expedite TPPOH purification time, the solid phase's length is limited to 10 cm. The solvent system used to isolate **2.9** should have an (Rf) of 0.21–0.4. Distilled pyrrole can be added at once or drop by drop

without affecting the reaction. The monohydroxy porphyrin TPPOH **2.9** was obtained in 5.1% yield and was characterised by using ^{1}H NMR and UV-vis spectroscopy.

The ^{1}H NMR spectrum showed a signal from the OH group in the para position, which has a chemical shift of 5.18 ppm. The protons in the porphyrin ring a, b, c, d, and e were in the aromatic range and were more deshielded. Signals for e and c clearly indicate formation of the unsymmetrical TPPOH. The shielded amino protons of the macrocycle resonate at -2.77, as shown in Figure 2.3.

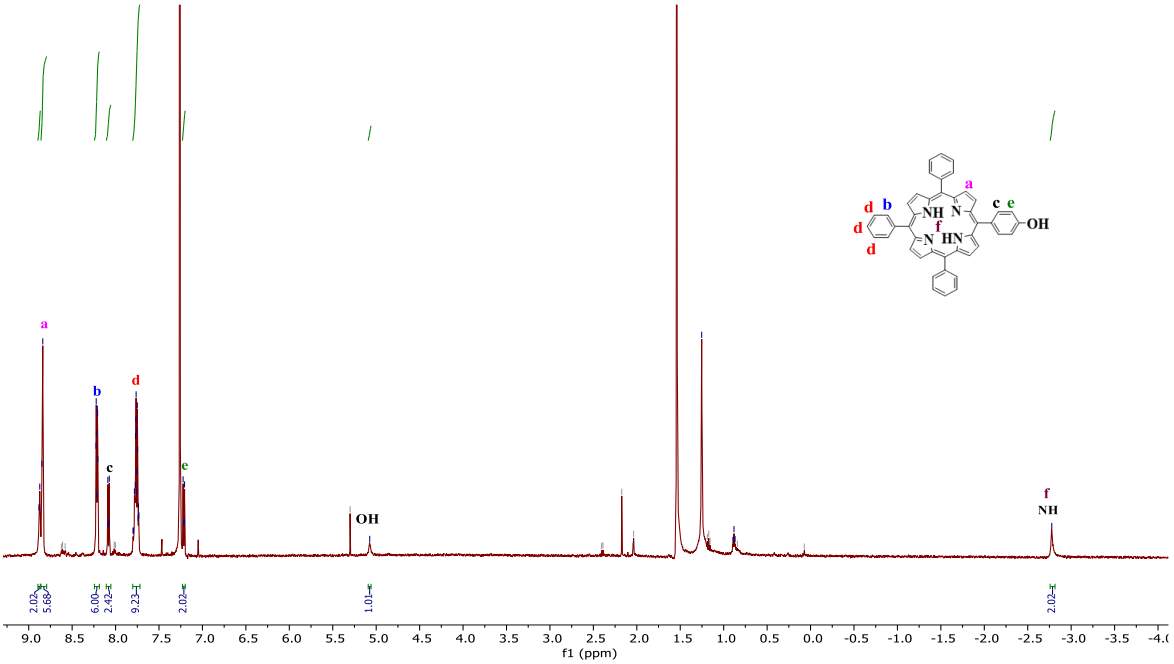

Figure 2.3: ^{1}H NMR spectrum of TPPOH **2.9**.

Porphyrins exhibit characteristic absorption spectra in the near-UV and visible regions, which is attributed to their π-conjugation system. This conjugation system considerably decreases the energy gap between the highest occupied molecule orbital (HOMO) and the lowest unoccupied molecule orbital (LUMO). As a result, some absorption bands [9,10,11,12] can be observed around 400 nm, which are referred to as (B) bands, and weaker absorption bands may be noticed in the range between 500 and 750 nm, which are referred as Q bands. The TPPOH **2.9** showed the two types of characteristic bands; the B band is at 418 nm, while the Q bands are 515, 550, 591, and 648 nm, as shown in Figure 2.4.

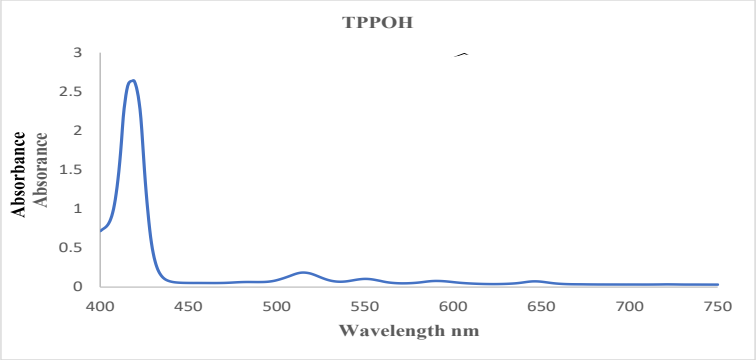

Figure 2.4: UV-vis spectrum of TPPOH **2.9** in DCM.

The second product that formed from the TPPOH **2.9** reaction as a side product was TPP **2.10** in 19% yield, and the ^{1}H NMR spectrum of TPP is shown in Figure 2.5. The **2.10** molecule is more symmetrical than **2.9**.

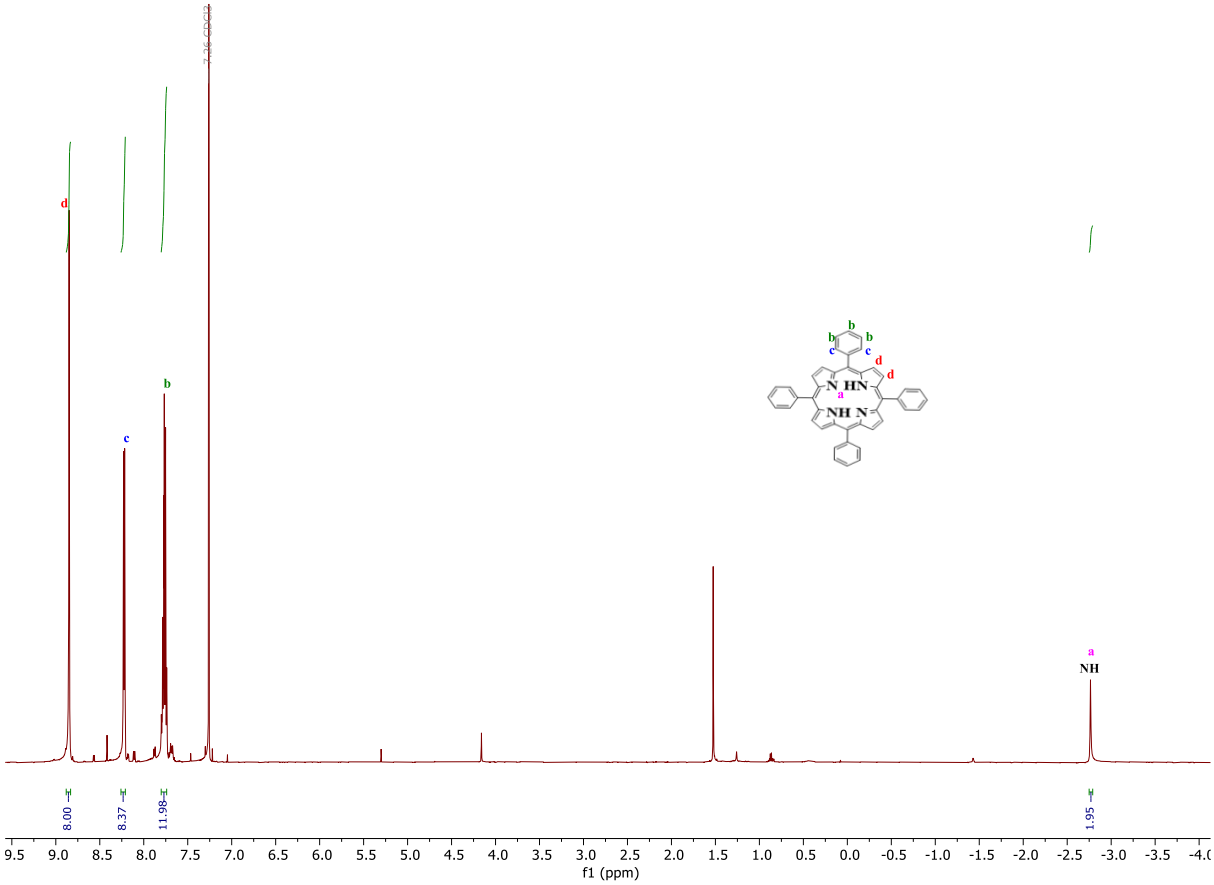

Figure 2.5: ^{1}H NMR spectrum of TPP **2.10**.

The UV-vis spectrum is almost identical to that of TPPOH: the B band is at 417 nm, while the Q bands are at 514, 549, 590, and 648 nm, as shown in Figure 2.6.[9,10,11,12]

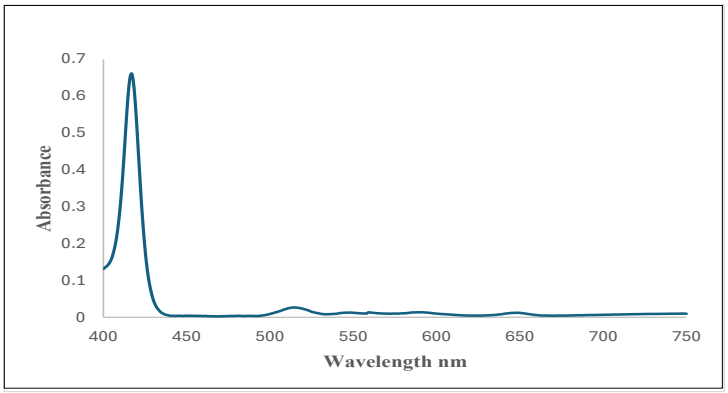

Figure 2.6: UV-vis spectrum of TPP **2.10** in DCM.

2.3 Alkylation of TPP-OH:

As shown in Scheme 2.7, there are two potential methods for preparing the required porphyrin-porphyrin dyad **2.5**. Pathway **a** was chosen for synthesising the porphyrin dyad, which was directly synthesised using a well-established alkylation method for creating multi-porphyrin arrays.[6,13,14] In method **b**, the product is synthesised sequentially by reacting one equivalent of TPP-OH **2.9** with an excess of dibromodecane to make a monosubstituted porphyrin **2.15**. This is then reacted with another equivalent of TPP-OH to generate the final product C_{10} dyad **2.5**.

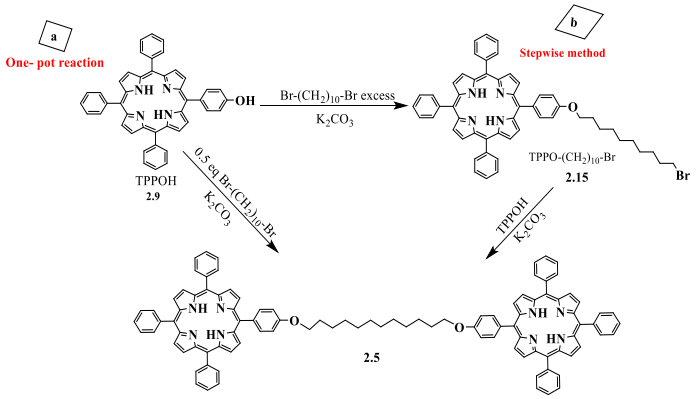

Scheme 2.7: Preparation of di-porphyrin **2.5** in two ways **a** and **b**.

Although the process of creating the dyad may seem straightforward, managing the unwanted by-products has proven to be a significant challenge. The selection of base, solvent, temperature**,** and reaction duration all influence the outcome of this reaction.

The dyad reaction gave a low yield and took a long time, which caused us to make many attempts to improve the yield. We have made many attempts to form a C_{10}-dyad by the one-pot reaction using different conditions, as shown in Table 2.2.

Table 2.2: Attempts to improve the yield of C_{10}-dyad **2.5**:

En-try	2.9, (g)	1,10 Dibromo-decane, (g)	Base/ (g)	Solvent	Temp. / Time	(g), Yield of 2.5
1.	(0.2)	(0.048)	K_2CO_3/ (0.4582)	Dry-acetone, (10) ml	At 70 °C for 48 hrs in a sealed tube	(0.051), ≈ (23%).
2.	(0.466)	(0.111)	K_2CO_3/ (1.23)	Dry-acetone, (8) ml	9 days at 70 °C, in a sealed tube	(0.22), ≈ (43%).
3.	(0.3)	(0.07)	K_2CO_3/ (0.85)	Dry-acetone, (8) ml	18 days at 70 °C, in a sealed tube	(0.13), ≈ (39%).
4.	(0.25)	(0.0595)	K_2CO_3 / (0.329)	Dry-acetone, (6) ml	12 days at 70 °C, in a sealed tube	(0.15), ≈ (54%).
5.	(0.1)	(0.024)	K_2CO_3/ (0.6)	DMA, (6) ml	3 days. reflux at 165 °C, Under N_2	(0.05), ≈ (45%).
6.	(0.27)	(0.06)	K_2CO_3, / (1.062)	Dry-acetone, (12) ml	At 70 °C, 18 days gave pure dyad, in a sealed tube	(0.17), ≈ (56%).
7.	(0.3)	(0.07)	K_2CO_3 / (1.12),18-crown-6 / (0.11).	Dry-acetone, (12) ml	2 weeks at 70 °C, in a sealed tube	(0.165), ≈ (49%).
8.	(0.22)	(0.052)	K_2CO_3 / (0.22)	Dry-acetone, (10) ml	10 days at 70 °C, in a sealed tube	(0.12), (49%).
9.	(0.235)	(0.056)	K_2CO_3 / (0.52) & 18-crown-6 / (0.1)	Dry-acetone, (8) ml	Week at 70 °C, catalyst cause to decrease the time of reaction, in a sealed tube	(0.19), ≈ (72%).
10.	(1)	(0.24)	K_2CO_3/ (0.44)	Dry-acetone, (12) ml	12 days at 70 °C, in a sealed tube	(0.984), ≈ (88%).
11.	(1.6)	(0.38)	K_2CO_3 / (0.52)	DMF, (23) ml	At 70 °C, for 2 hrs. and 2 hrs. at 90 °C, Under N_2	(1.15), ≈ (64%).
12.	(0.6)	(0.143)	K_2CO_3 / (0.66)	DMF, (17) ml	At 70 °C, for 2 hrs. and 3 hrs. at 90 °C, Under N_2	(0.3), ≈ (45%).

Twelve attempts were made to form the C_{10} dyad **2.5**, varying the conditions to improve the process. The first attempt yielded the lowest (23%), despite following the same conditions as previous work,[1,6] except that we added the reactants in a sealed tube. Some improvements were

noted in attempts (2), (3), (4), (6), and (8), as the use of a sealed tube addressed the issue of the evaporation of the solvent caused by the tiny quantity of acetone utilised (6–12 ml). A 56% yield of pure dyad was achieved after 18 days.

In an attempt (9), we achieved a significant improvement in yield. After 7 days, 72% of pure dyad was produced due to the use of 18-crown-6 as a catalyst, resulting in a shorter reaction time, while in attempt (7), we added the same catalyst after a week from starting the reaction and the reaction took around two weeks to complete.

Experiment (10) utilised a high-scale reaction involving 1,10 dibromodecane and excess K_2CO_3 in dry acetone for 12 days at 70 °C, resulting in a yield of 88% of the dyad. In (5), (11), and (12), we used DMA and DMF as solvents instead of dry-acetone due to their higher boiling point. In an attempt (5), the yield was 45% after 72 hrs. The reaction was analysed using TLC after 24 hrs, revealing the dyad as a distinct spot, weak elimination side product **2.16**, and clear monosubstituted porphyrin **2.15**. The reaction was stopped after 72 hrs due to the strong spot corresponding to elimination product **2.16**.

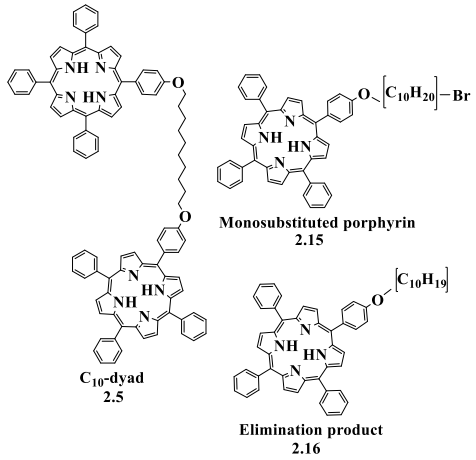

Figure 2.7 Porphyrin dyad **2.5** and expected side products **2.15** and **2.16**.

The time needed for a good yield was around three days. The optimisation of di-porphyrin preparation and isolation attempts using DMF as a solvent was conducted in attempts (11) and (12). In attempt (11), TPPOH **2.9** was reacted with 0.5 eq. of 1,10 dibromodecane and excess K_2CO_3 in DMF for 2 hrs at 70 °C and 2 hrs at 90 °C, yielding 64% of the desired product **2.5**. In attempt (12), we used a smaller scale and reacted TPPOH with 1,10 dibromodecane and excess base in DMF, taking 2 hrs at 70 °C and 3 hrs at 90 °C, yielding 45%. Reactions (11) and (12) were concluded when the colour changed from reddish brown to bright purple, indicating the end of the reactions, as shown in Figure 2.8.

Figure 2.8: Dyad C_{10} **2.5** reaction in DMF at the start and end of reaction in attempts (11) and (12).

In attempt (5), the solvent was evaporated, DCM added and washed. Column chromatography was used for purification, with a (3:1) ratio of DCM: Pet-ether. The first fraction was ($TPPOC_{10}H_{19}$) **2.16**, while the second fraction was dyad **2.5**. Increasing the polarity to 100% DCM enabled the recovery of unreacted TPPOH **2.9**, and the TLC of these attempts is illustrated in Figure 2.9.

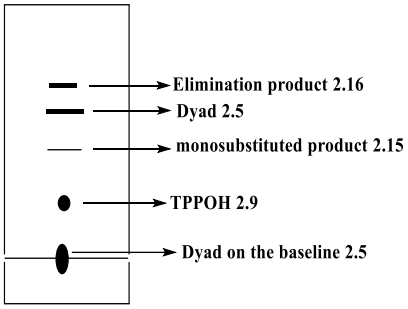

Figure 2.9: TLC showing fractions in attempt (5) during the reaction.

The dyad was found to stick on the baseline in attempts (5), (11), and (12); some quantity was recovered by using DCM: THF (9:1) and gradually increasing the polarity of the solvent system. The low solubility of the dyad **2.5** was unavoidable due to it crystallising in the column, although many types of solvents were used, even THF. The overall yield of target product **2.5** in attempts (5), (11), and (12) did not increase to more than 64% due to the formation of a by-product **2.16**. Eventually, we developed a purification protocol that avoided chromatography and used recrystallisation only.

Figure 2.10 shows the ^1H NMR spectrum of the C_{10} dyad. The triplet signal at 4.28 ppm is for protons that are near the oxygen atom from the aliphatic chain of the dyad. There is no triplet signal at 3.37 ppm (CH_2–Br), indicating that monosubstituted porphyrin **2.15** is absent. The

shielded four amino protons of the macrocycle have resonance at -2.77 ppm due to the ring current effect.[14]

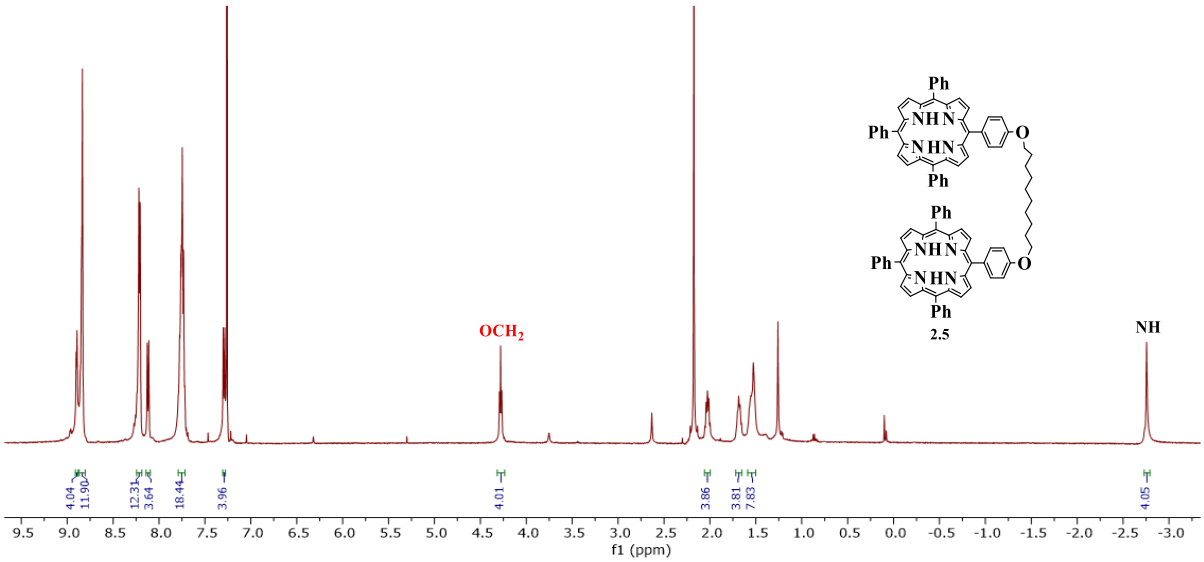

Figure 2.10: ^{1}H NMR spectrum for C_{10} dyad **2.5** in $CDCl_3$.

The C_{10} dyad UV-V spectrum has a B-band around 419 mm, while the Q-bands are 516, 551, 591, and 648 nm, as shown in Figure 2.11. We also checked MALDI-TOF-MS of pure **2.5**.

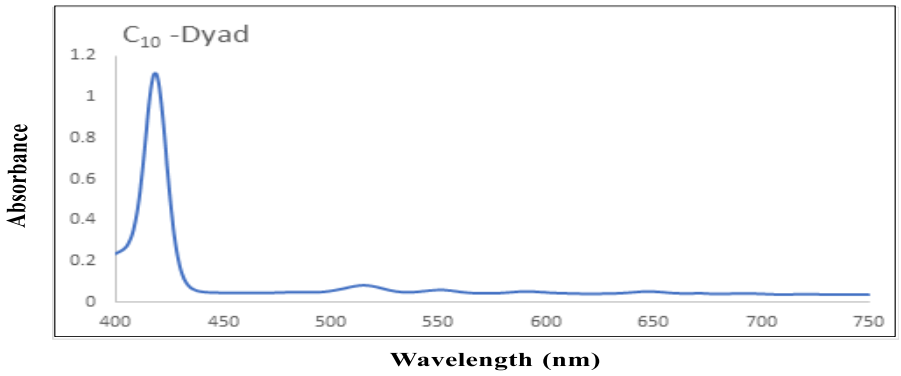

Figure 2.11: UV-vis spectrum of C_{10} dyad in DCM.

In summary, the optimal reaction conditions involved 12 days of refluxing the mixture in acetone, adding water, filtering the precipitate, and recrystallising to produce a purple solid product with 88% yield. We were also able to prepare the dyad by a two-step reaction. We formed **2.15** in a first stage by reacting one equivalent of TPPOH **2.9** with 1.2 eq. of 1,10 dibromodecane in dry-acetone in the presence of K_2CO_3 for 34 hrs.

Using column chromatography over silica gel with THF: Pet-ether (1:3 v/v) and then recrystallising from DCM/MeOH produced 42% of **2.15**. It was then possible to form the dyad (20%) by reacting TPP-OC_{10}Br with another equivalent of TPPOH and an excess of K_2CO_3 in dry-

acetone for 72 hrs. The UV-vis spectrum of **2.15** showed the expected similar peaks, with B band at 418 nm and Q bands at 516, 551, 593, and 651 nm, as shown in Figure 2.12.

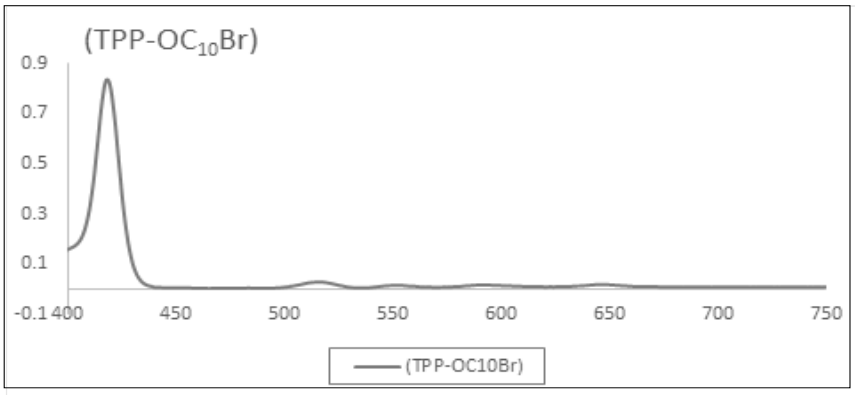

Figure 2.12: UV-vis spectrum of (TPP-OC_{10}Br) **2.15** in DCM.

The ^{1}H NMR spectrum of **2.15** showed two (2H) triplet signals at 4.25 ppm and at 3.44 ppm, indicating the monosubstituted porphyrin, as shown in Figure 2.13. Also, we checked MALDI-TOF-MS of pure **2.15**.

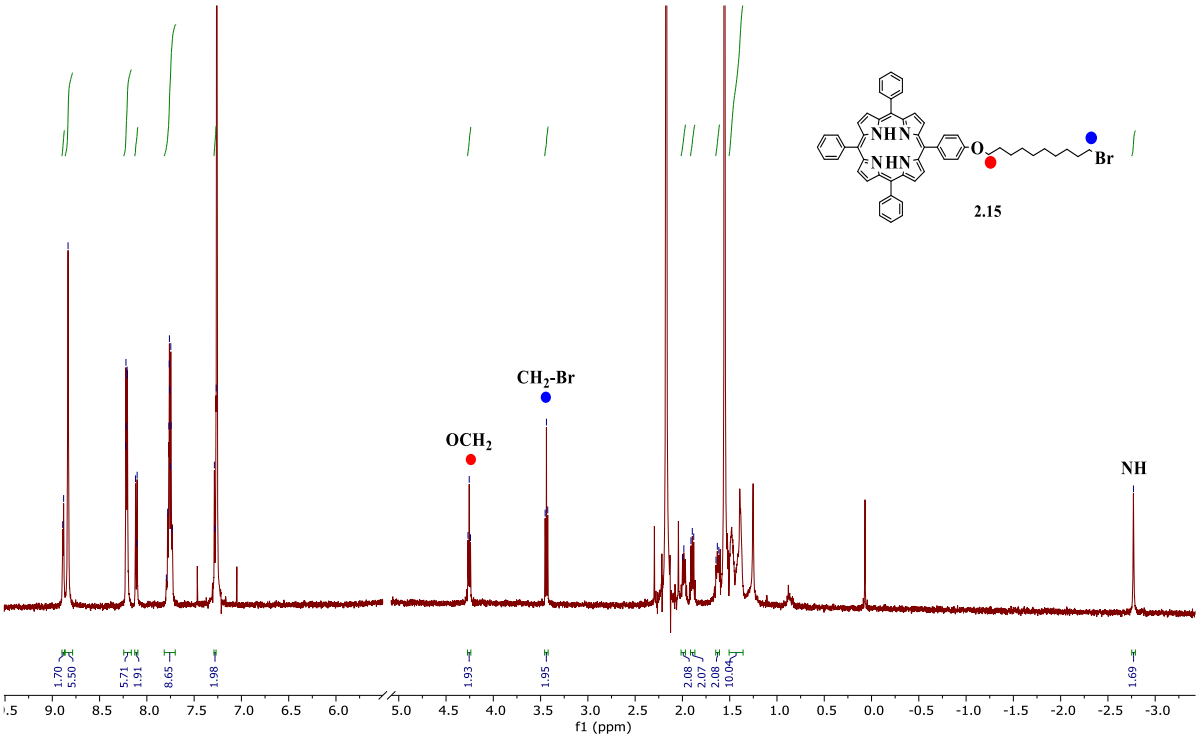

Figure 2.13: ^{1}H NMR spectrum of TPP-OC_{10}Br **2.15** in $CDCl_3$.

Based on the information shown in Table 2.3, we also made four efforts to synthesise the porphyrin C_{12}-dyad **2.17**.

Table 2.3: Attempts for the formation of C_{12}-dyad **2.17** in different conditions:

Entry.	2.9, g	1,12-dibromo-dodecane, (g)	Base / g	Solvent, ml	Temp. / & time of reaction	Weight g of 2.17, Yield
1.	(0.259)	(0.067)	K_2CO_3 / (0.398) and Potassium iodide / (0.137)	MEK, (10)	Under N_2 At 80 °C, 29 hrs	0.051, ≈ (17%),
2.	(0.260)	(0.068)	K_2CO_3 / (0.3994), Potassium iodide (0.14)	MEK, (10)	Under N_2 At 80 °C, 6 days	(0.154), ≈ (52%)
3	(0.94)	(0.245)	K_2CO_3 / (1.44) and Potassium iodide / (0.5)	MEK, (25)	Under N_2 At 80 °C, 2 days and 19 hrs	(0.754), ≈ (70%)
4	(0.94)	(0.025)	K_2CO_3 / (0.137)	Dry-acetone (8) in a sealed tube	At 70 °C, 8 days	(0.501), ≈ (47%)

The process of creating C_{12} Dyad is straightforward, but managing unwanted by-products was also challenging.[6,13,14] Use of TPPOH and 1,12-dibromododecane in MEK solvent under N_2, K_2CO_3, and potassium iodide, resulting in a desired product of C_{12}-dyad at a 17–70% yield in the three first attempts and took around 29–144 hrs. The elimination side product **2.18** consistently occurred for reactions (1), (2), and (3). Utilising a catalyst to speed up the reaction rate led to a 70% yield of the desired product **2.17**. Longer reaction durations of around 144 hrs resulted in an increase in the yield of the elimination product **2.18**.

In an attempt (4), dry acetone was used at 70 °C with K_2CO_3, and the desired product yield was 47% in 8 days. KI was not used for the reaction. The ^{1}H NMR spectrum of C_{12}-dyad is shown in Figure 2.14. The 4H triplet signal at 4.26 ppm are the protons that are near the oxygen atom from the aliphatic chain of **2.17**. There is no triplet signal at 3.37 ppm (CH_2–Br), indicating that monosubstituted porphyrin **2.19** is absent. The shielded (4H- amino protons) of the macrocycle have resonance at −2.76 ppm due to the ring current effect.[14]

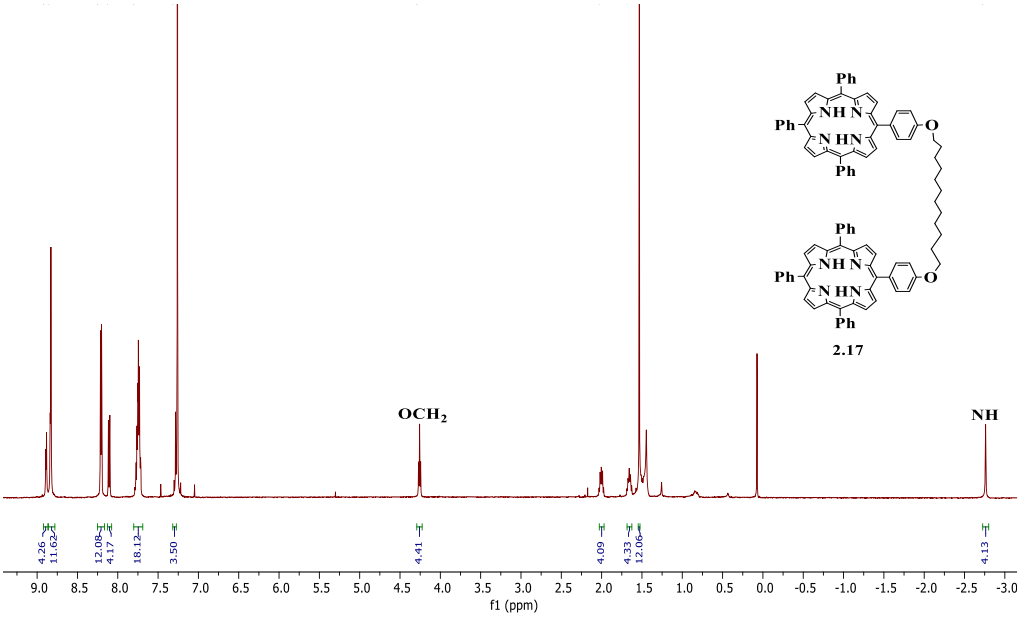

Figure 2.14: ^{1}H NMR spectrum of C_{12}-dyad **2.17** in $CDCl_3$.

2.4 Synthesis of metal-free phthalocyanine:

Metal-free phthalocyanine **2.21** is crucial for lanthanide triple-decker synthesis and is easily synthesised. After reviewing the literature, the general method mentioned by Galanin and Shaposhnikov was chosen due to its high yield, as shown in Scheme 2.8.[15,16]

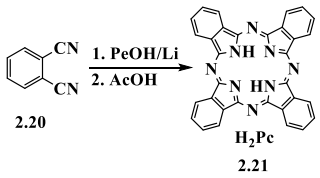

Scheme 2.8: Synthesis of metal-free phthalocyanine **2.21**.

We succeeded in preparing the metal-free phthalocyanine **2.21** by dissolving phthalonitrile **2.20** in 1-pentanol, adding excess lithium metal, and refluxing for another hour. Acetic acid was added to quench the reaction, removing excess metal. Methanol was added to precipitate the desired Pc as a dark blue solid with a 49% yield.

Figure 2.15 demonstrates the formation of metal-free phthalocyanine as shown by UV-vis spectra; the H_2Pc has a B band and two Q bands: 377, 654, and 690 nm. Due to the Pc's **2.21** very limited solubility in organic solvents, it was not possible to achieve ^{1}H NMR spectra and additional characterisation.

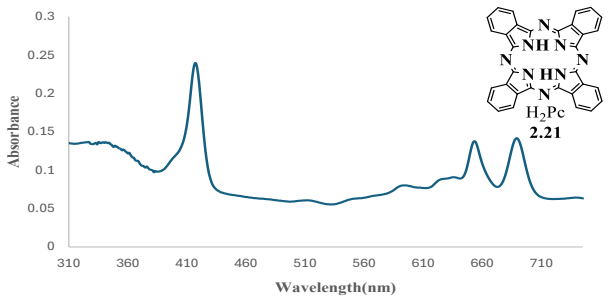

Figure 2.15: UV-vis spectrum of metal-free phthalocyanine **2.21** in THF.

2.5 Formation of triple decker by using unsubstituted phthalocyanine:

Cammidge's group has recently successfully prepared tripledeckers by linking porphyrin dyads with Pc. The best length to employ was found to be n-decane.[1,6] Previous studies have successfully created the heteroleptic triple-decker porphyrin to phthalocyanine, utilising both multi-step and single-step synthetic approaches.[17,18,19]

The multi-step process was chosen in prior investigations due to its ability to provide a better product yield, as stated by the Cammidge group.[1,6] The bridged porphyrins prefer to choose the porphyrin-phthalocyanine-porphyrin triple-decker arrangement (ABA) **2.22**, as shown in Scheme 2.9.

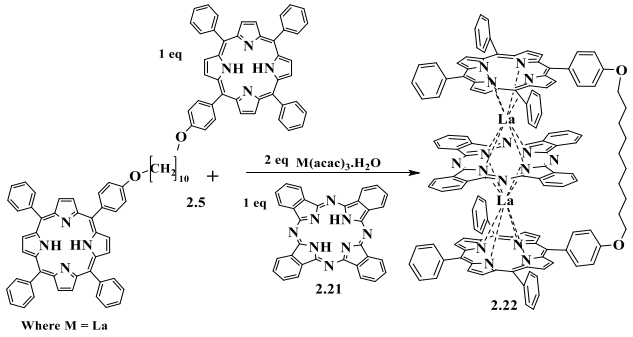

Scheme 2.9: Procedure of Cammidge group for formation of bridged TD **2.22**.

Following the method of Lucas,[1,6] the first attempt to synthesise compound **2.22** first used a metalation stage, which involved refluxing lanthanum (III) acetylacetonate hydrate with C_{10}-dyad **2.5** in octanol under nitrogen for 16 hrs. Pc **2.21** was added and the reaction was prolonged for 18 hrs.

We checked this reaction by MALDI-TOF-MS, as shown in Figure 2.16, and it shows many peaks of side products 651 La-Pc **2.23**, 738 unknown, 1163 La-Pc_2 **2.24**, 1186 unknown, 1811 m/z unknown, and triple-decker **2.22** at 2182 m/z. The solvent was distilled off, and the product was obtained by column chromatography, using a DCM: Pet-ether eluent, as a dark brown solid with a meagre yield of around 3%, as shown in Table 2.4.

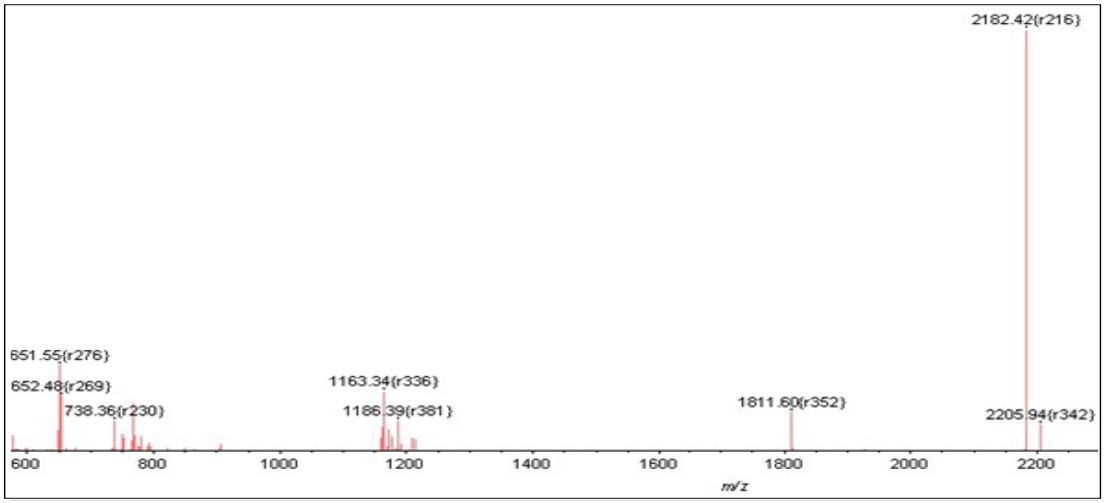

Figure 2.16: MALDI-TOF MS result for reaction in attempt (1) following previous work.

We made many attempts to improve the yield of the triple decker by using different methods, solvents, reaction times, and equivalences of reactants. We used sealed tubes and normal conditions under N_2 or Ar. Because of the challenges associated with octanol removal, experiments were also attempted using pentanol as a solvent.

Table 2.4: Attempts for the formation of triple-decker Pc with La **2.22**.

Entry	2.5, g	Eq of La/(acac)$_3$, g	2.21, Eq, g	Solvent ml	Temp.	Time, hrs	Method	2.22, g, (%)
1	0.02	2, (0.0124)	1, (0.01)	3, Octanol	At 195 °C under N_2	34	2-steps under N_2	0.001/ ≈ (3%)
2	0.02	2, (0.0124)	1, 0.007	3, Pentanol	At 165 °C, 20 hrs and 6 hrs at 170 °C	26	One pot, in a sealed tube	Trace 0.0023/ ≈ (8%)
3	0.02	2, (0.0124)	1, (0.007)	3, Pentanol	At 165-170 °C	21	1-Step, in a sealed tube	0.002/ ≈ (6%)
4	0.12	2.2, (0.08)	1.1, (0.05)	6, Pentanol	At 170 °C	27	Step-wise, in a sealed tube	very Trace
5	0.054	2, (0.036)	1, (0.02)	12, Pentanol	At 140 °C	24	Step-wise, Under N_2	Trace
6	0.05	3.5, (0.055)	1.5 / (0.3)	15, Pentanol 6 drops DBU	At 140 °C	34	One pot reaction and	trace

							degassed by bub-bling Ar.	
7	0.053	2, (0.0357)	1, (0.02)	4, Pentanol	At 165 °C	34	In a sealed tube	Trace amount
8	0.1	2, (0.0623)	1, (0.036)	15, Octanol	at 200 °C for 32 hrs metalation-stage. At 200 °C-re-fluxed, after add-ing Pc for18 hrs	50	2-step Under N_2	Decom-posed
9	0.123	2, (0.083)	1, (0.045)	15, Octanol	at 200 °C	82	2-step Under N_2	(0.1)/ ≈ (50%)

The second attempt produced a triple decker by reacting **2.5**, **2.21**, and $La(acac)_3$ in pentanol at 165 °C for 20 hrs. The presence of TD **2.22** was noticed, and raising the temperature to 170 °C for 6 hrs strengthened the spot. TD was produced with around 8% yield in this attempt. The third attempt involved a one-pot reaction, with a temperature range of 165–170 °C for 21 hrs, resulting in only 6% of **2.22**. Attempts 4, 5, 6, and 7 were less successful, producing only trace amounts of the desired product **2.22**.

In attempt 6, Ar was bubbled through the reaction following recommendations of Birin al.,[20] but likewise produced only very low yields and many by-products, as shown in Figure 2.17, which were 1159 $LaPc_2$ **2.24**, 1281 unknown, 1394 C_{10}-Dyad **2.5**, 1536 La-dyad **2.25**, and La-Pc-TD 2186 m/z.

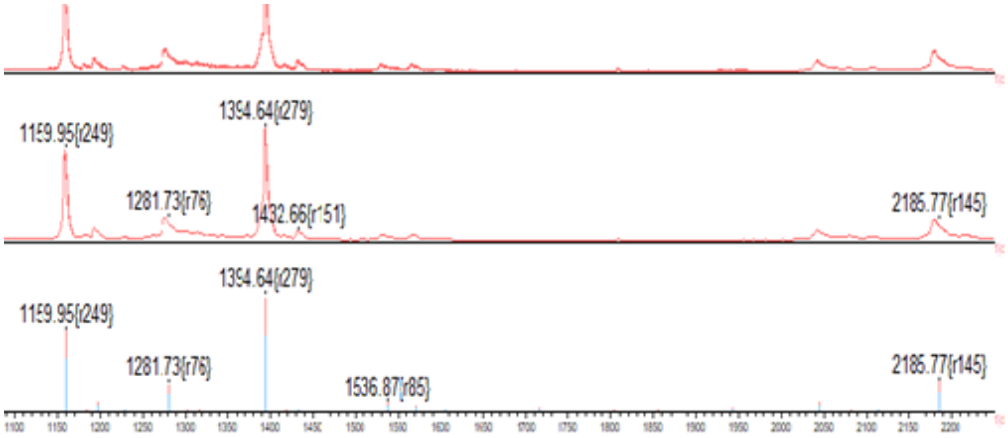

Figure 2.17: MALDI-TOF MS result for attempt (6) to form **2.22**.

In the 8th attempt, we used a long time for the metalation step for dyad **2.5** and La metal in a stepwise reaction of around 32 hrs, then added Pc, and we found only the starting materials

demonstrated in TLC. We confirmed this situation by MALDI-TOF MS, as shown in Figure 2.18.

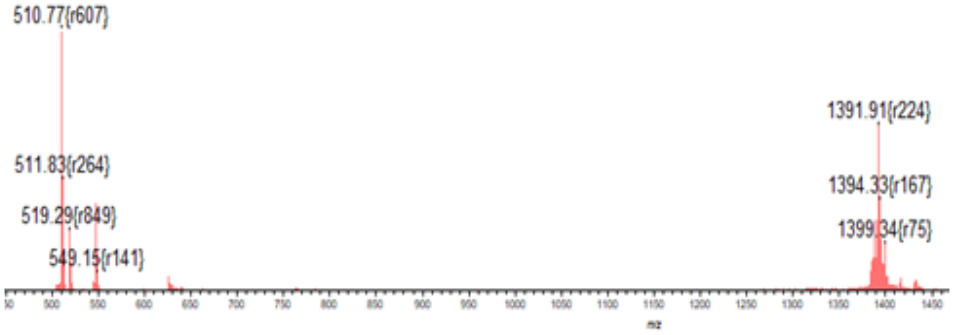

Figure 2.18: MALDI-TOF MS result after 52 hrs in attempt 8.

However, the 9th attempt proved more successful because, in this attempt, we achieved a 50% yield of **2.22**. We followed Lucas,[1,6] except for the time of reaction. We increased the reaction time from 34 hrs to 3 days and 10 hrs.[20] In this attempt, the MALDI-TOF-MS also showed many side products: 1164 **2.24**, 1532 **2.25**, 1730 unknown, 1928 unknown, and La-TD **2.22,** as shown in Figure 2.19.

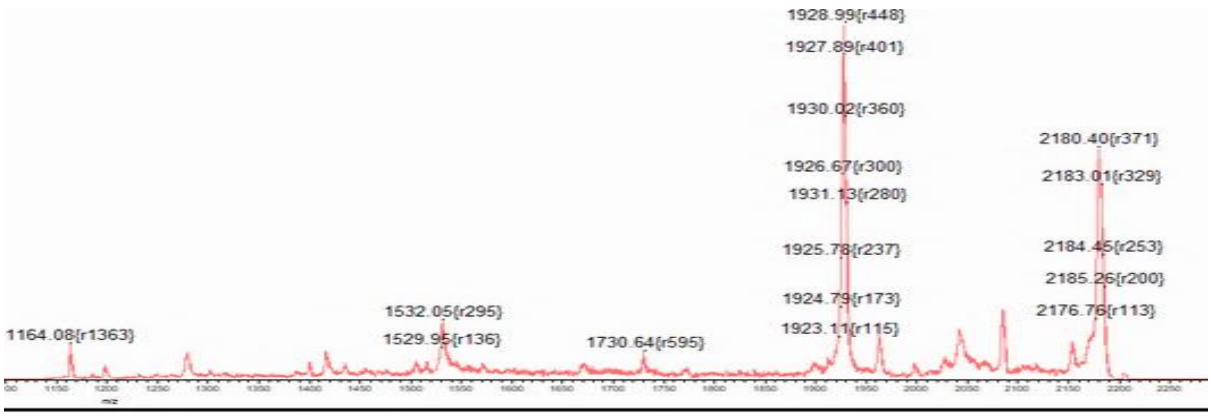

Figure 2.19: MALDI-TOF MS result after 3 days and 10 hrs in attempt (9).

An earlier investigation by the Cammidge group[1,6] provided a description of the ^{1}H NMR spectra of **2.22**. As shown in Figure 2.20, the typical signal at -2.7 ppm has been seen to be absent, which suggests that there is no metal-free porphyrin. A single triplet for the alkoxide peak (-O-CH_2) at around 4.6 ppm indicates that both ends of the aliphatic chain are placed in an identical environment (symmetrical molecule).

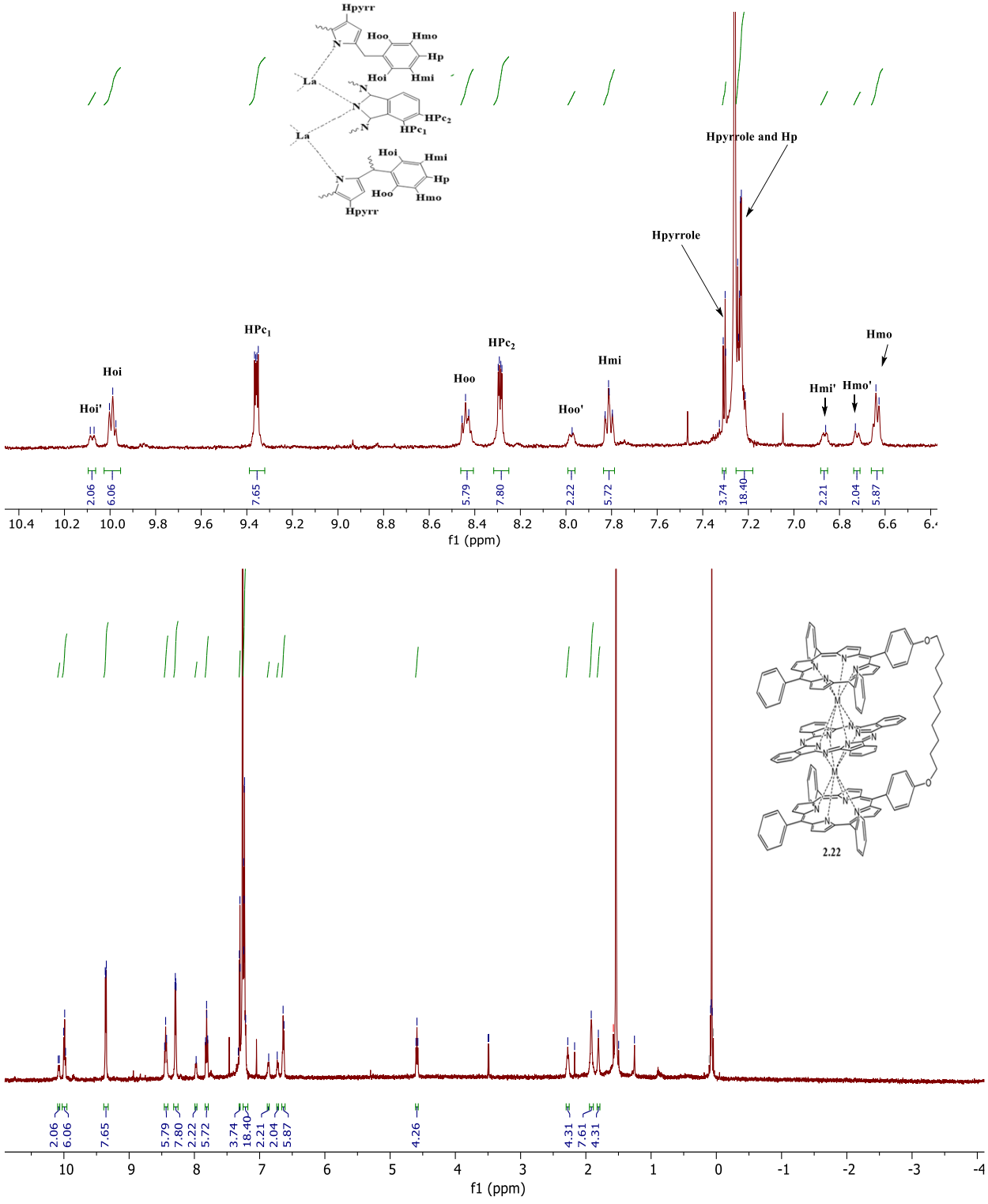

Figure 2.20: Analysis of ^{1}H NMR spectrum of the lanthanum triple-decker **2.22** complex in $CDCl_3$.

The TD UV-vis spectrum is shown in Figure 2.21 and exhibits a broad absorption at 360 nm, characteristic of a sandwich-like complex, a strong absorption at 423 nm in the porphyrin zone, and bands at 486, 549, and 603 nm.[1,6] The results agreed with the expected spectra of structures

of this type of triple-decker **2.22**, where the Pc is between two porphyrin units ([Por]La [Pc]La [Por]).

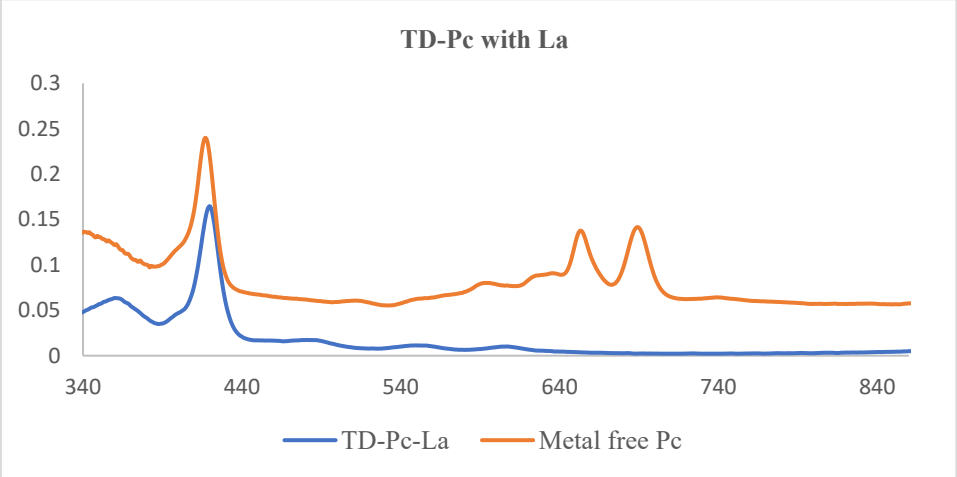

Figure 2.21: UV-vis spectra of TD **2.22** and metal-free Pc **2.21**.

2.6 Metalation studies on porphyrins and C_{10}-dyad with lanthanide metals, La and Gd:

2.6.1 Dyad- metalation: Time-dependent study of absorption spectra:

This section attempts to determine the exact time the metal binds with di-porphyrins. Owing to the extensive π-conjugated structure, porphyrins and metalloporphyrin exhibit intense absorption features in the near-UV and visible regions. These bands are sensitive to various factors, including the ligand structure and the type of metal centre.[21,22] To monitor the effect of adding metal to ligand at different time intervals, we added $La(acac)_3.H_2O$ (0.099 g, 0.31672 mmol) to a refluxing solution of the C_{10}-dyad **2.5** (0.06g, 0.0428 mmol) in octanol, and the absorption spectra were collected labelled as (zero, 1, 12) hrs respectively, as shown in Figure 2.23 .

In the next phase of the experiment, $La(acac)_3.H_2O$ was added to the mixture on the following day (after overnight) and refluxed for the next 12 hrs (total 24 hrs). We found that the reaction sample after 24 hrs had a cloudy appearance compared with the dyad **2.5** sample in the same solvents (octanol and dry DCM), as shown in Figure 2.22.

We collected the next set of spectra labelled as 24 hrs for (La-dyad) **2.25**, as shown in Figure 2.23. It is to be noted that the total number of bands remains the same as dyad **2.5**, indicating the presence of free ligand cores. Therefore, we added Gd- salt to the mixture at different time intervals, as shown in Figure 2.24. Interestingly, the addition of the second metal (Gd) led to a reduction from four to three bands at 521, 559, and 601nm, as shown in Figure 2.24, indicating the inclusion bonding between Gd and the C_{10}-dyad **2.5**.

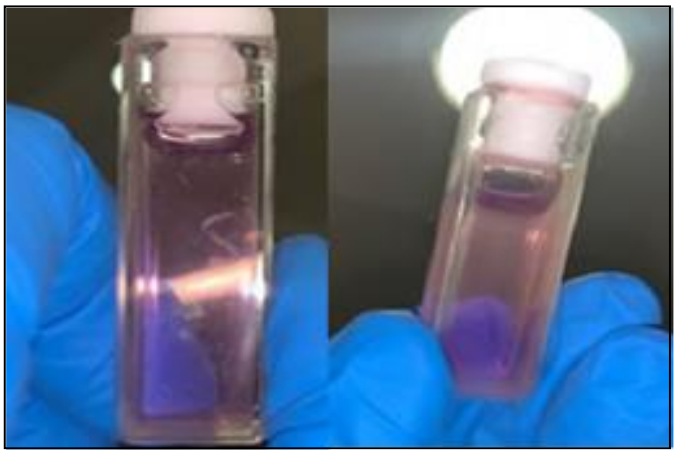

Figure 2.22: Samples of reaction on the right side have a cloudy sample (reaction sample) while the left side was a pure dyad **2.5**.

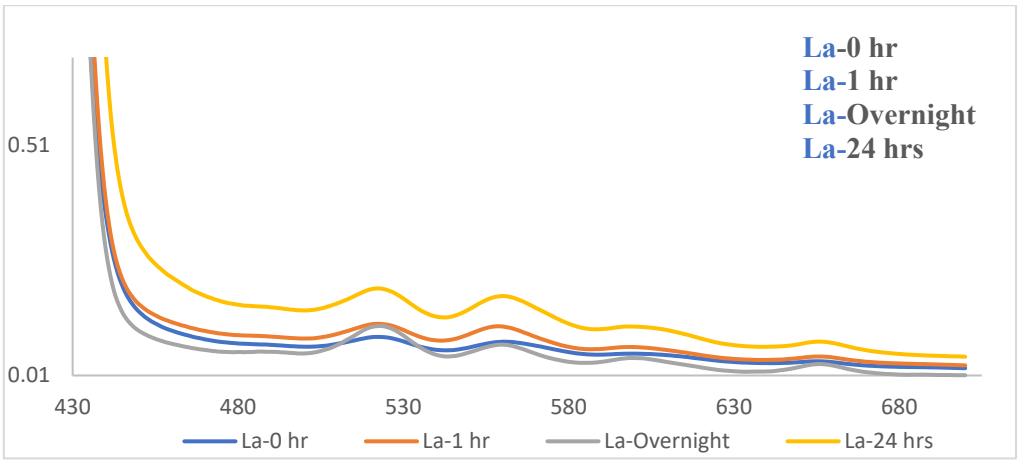

Figure 2.23: Samples of reaction La-Dyad **2.36** in mixed solvents, octanol and dry DCM.

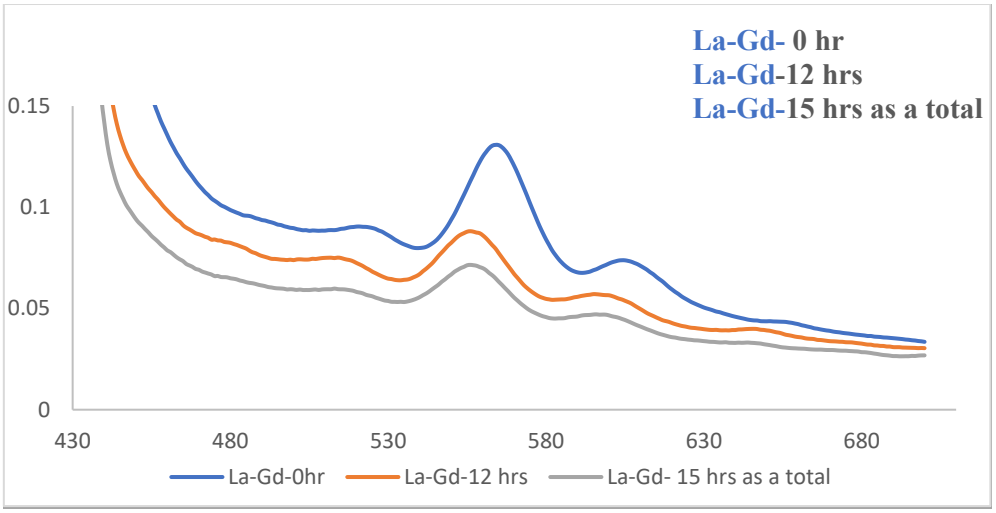

Figure 2.24: Samples of reaction La-Gd-Dyad in mixed octanol and dry DCM.

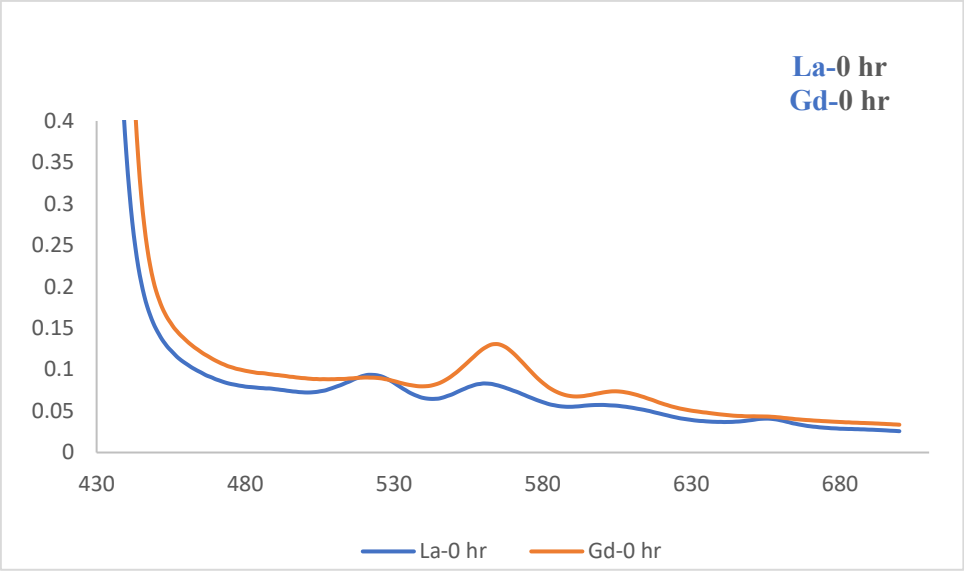

Figure 2.25: Samples of reaction Ln-Dyad in mixed solvents octanol and dry DCM at zero hr.

There are a number of credible explanations for these observations. Alhunayhin and Soobrattee [23,8] did not monitor metalation via UV-vis spectroscopy as there was hydrolysis during the sample preparation process for UV-vis. In other words, metalated products have low stability. Additionally, we suggest that the metalation product may not be visible in the UV-vis spectra due to its low solubility, resulting in a cloudy sample, as shown in Figure 2.22.

We suspected that the insoluble product is the bridged Por-La-Por double decker (**2.25**). Finally, adding different types of lanthanide metal may produce soluble metal derivates, resulting in the appearance of the peak for the Gd-dyad (likely **2.26**) in both UV spectra and MALDI-TOF MS, as shown in Figures 2.24 & 2.25. It was not isolated and only proven by MALDI-TOF-MS, as shown in Figure 2.26.

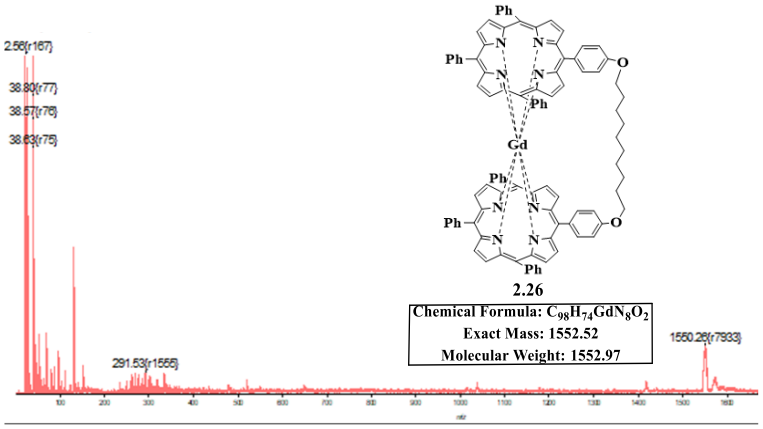

Figure 2.26: MALDI-TOF MS analysis of the final sample of Ln-Dyad reaction and displays the expected compound Gd-dyad in MALDI-TOF MS.

2.7 Synthesis of lanthanum porphyrin C_{10}-dyad 2.25:

We attempted to prepare La-Dyad **2.25** to achieve characterisation. In the first attempt, the reaction was performed on a good scale by reacting 1 eq. of porphyrin dyad with 1.1 eq. of lanthanum acetylacetonate hydrate in the presence of DBU, heating in the pentanol at 180 ℃ in a sealed tube. In this reaction, we checked TLC after 12 hrs, 2, 3, and 5 days total reaction time. Three spots stuck to baseline, mostly La-Dyad **2.25** plus unknowns at 733 and 762 m/z, as shown in Figure 2.27.

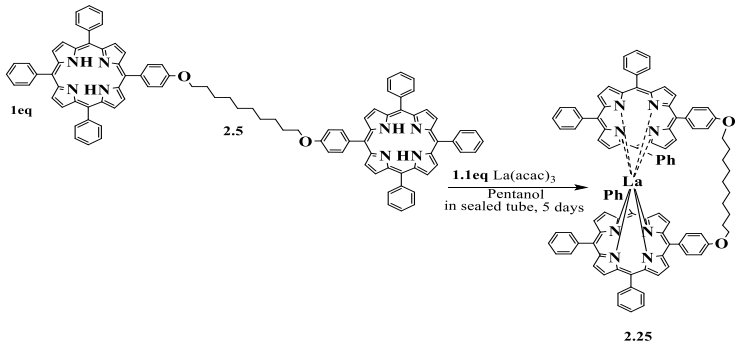

Scheme 2.10: Procedure of formation of La-Dyad **2.25**.

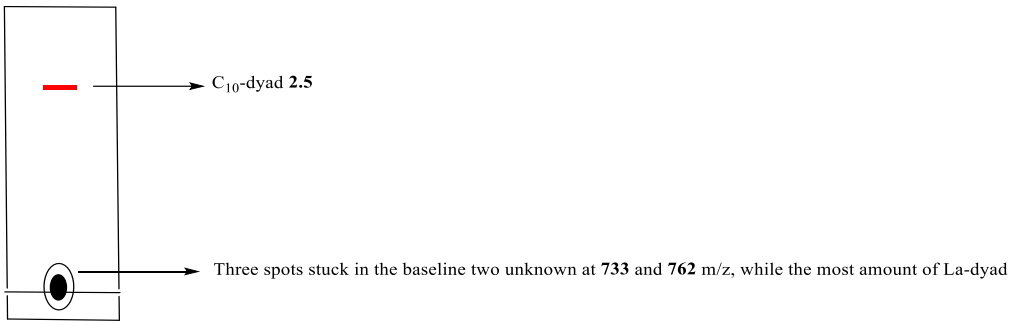

Figure 2.27: TLC during the reaction after 12 hrs, in 1:6 THF: Pet-ether.

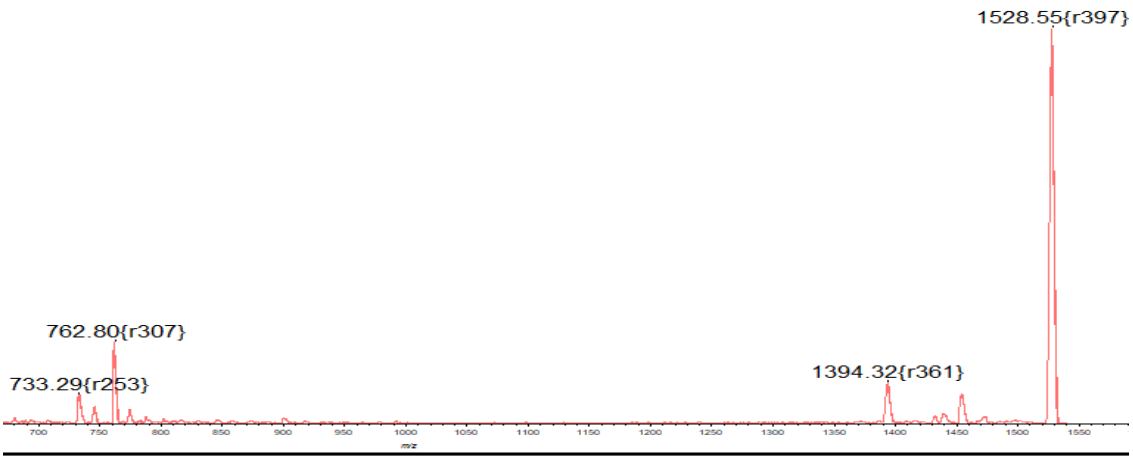

Figure 2.28: MALDI-TOF MS of di-porphyrin + La reaction after 12 hrs.

The solvent was distilled off, and the solid residue was found to not dissolve well in any solvents, even THF. This observation is consistent with the UV-vis study but made the product impossible to purify by column chromatography. MALDI-TOF-MS was checked after the reaction, and the expected peak at 1534.46 m/z was observed, as shown in Figure 2.29. We were not able to obtain satisfactory ^{1}H NMR spectroscopic data, even after addition of hydrazine,[24] due to the low solubility. Many attempts have been made to recrystallise the desired product **2.25** to create an XRD structure. We used DCM: MeOH, DCM: Ethanol, Iso-propanol, Chloroform: MeOH, DCM, and Hexane. In all recrystallisation attempts, we dissolved the solid **2.25** in solvents in a water bath and heated it, but all the attempts failed.

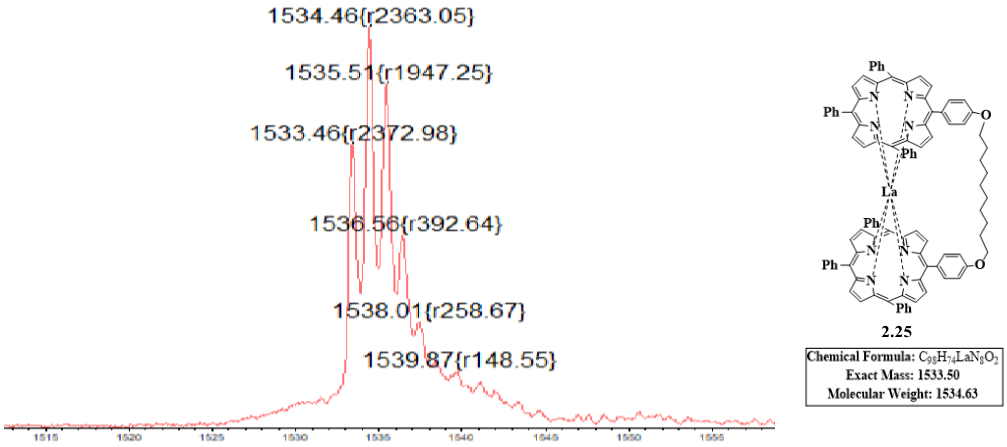

Figure 2.29: MALDI-TOF MS of La-dimer porphyrin **2.25**.

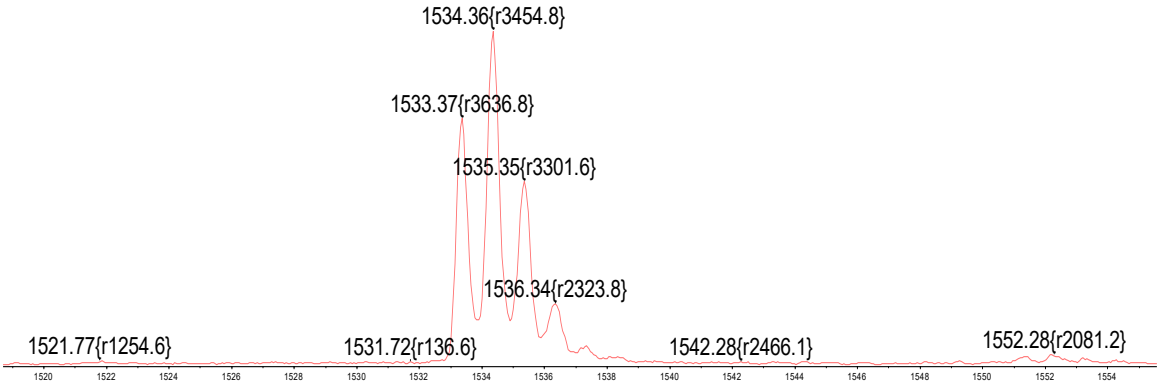

Figure 2.30: Negative-reflectron mode MALDI-TOF MS for a new product **2.25**.

2.8 Selective synthesis of bridged porphyrin-Pc triple deckers with lanthanum metal:

When synthesising heteroleptic triple deckers, many factors must be considered, including whether single- or multi-step techniques are used. For example, a simple, flexible chain

connecting porphyrins facilitates the assembly of the (ABA) TD when simple Pc is employed as the third macrocycle. Scheme 2.11 shows our target structure of a bridged Ln-triple-decker **2.3** with OEP **2.1** replacing Pc.

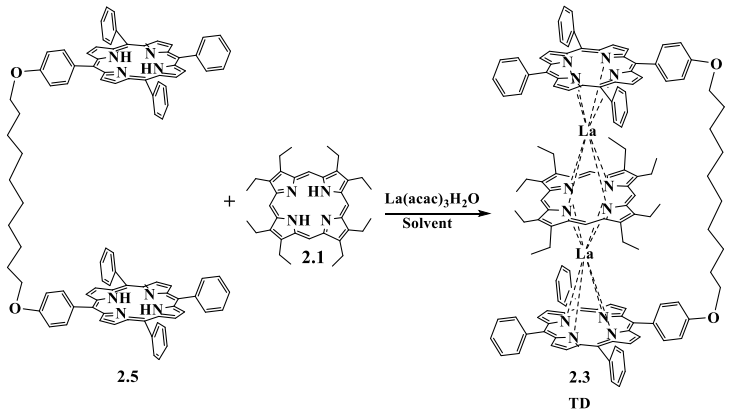

Scheme 2.11: Synthesis of La-OEP-C_{10}-dyad triple-decker **2.3**.

Exchanging Pc for OEP proved to be much less straightforward than expected, and many attempts to produce the desired TD were made using different techniques, solvents, temperatures, and timings, as set out in Table 2.5, and considerable variation in the outcomes was observed.

Table 2.5: Attempts for the formation of closed La-porphyrin TD with C_{10}-dyad **2.3**:

Entry	Eq. 2.5 (g)	Eq. 2.1 (g)	Eq. La-metal, g	Solvent(ml)	Temp. °C	Time, hrs	Reaction
1.	1, (0.1)	1, (0.04)	2, $La(acac)_3$, (0.0623)	Pentanol, 4	165	46	Stepwise
2.	1, (0.06)	1, (0.023)	6, Latrifluoro-methanesulfonate (III), (0.151).	Pentanol, 6, DBU.	139-165	33	Stepwise
3.	1, (0.1)	1, (0.04)	2, $La(acac)_3$, (0.062)	Pentanol, 8	170	108	One-pot
4.	1, (0.044)	1, (0.017)	2, $La(acac)_3$, (0.0273)	Pentanol, 3, DBU	165	40	One-pot
5.	1, (0.07)	1, (0.03)	2, $La(acac)_3$, (0.05).	Pentanol, 3	165	72	One-pot
6.	1, (0.0636)	1, (0.024)	2, $La(acac)_3$, (0.0396).	Pentanol, 12, under N_2	140	24	One-pot
7.	1, (0.1)	1.1, (0.04)	2, $La(acac)_3$, (0.0675).	Pentanol, 6	165	24	One-pot
8.	1, (0.042)	1, (0.02)	2, $La(acac)_3$, (0.0261).	Pentanol, 4	165	120	One-pot

9.	1, (0.1)	0.9, (0.034)	2, $La(acac)_3$, (0.0674).	Pentanol, 6	180	161	One-pot
10.	1, (0.0437)	1, (0.017)	2, $La(acac)_3$, (0.027)	Octanol, 10, under N_2	200	34	Stepwise
11.	1, (0.1)	1, (0.038)	4, $La(acac)_3$, (0.1246)	Octanol, 10, under N_2	200	72	One-pot
12.	1, (0.01)	1, (0.0038) and 1, **2.21** (0.0037)	3.9, $La(acac)_3$, (0.013)	Octanol, 5, under N_2	200	144	One-pot
13.	1, (0.1)	1, (0.038)	2, $La(acac)_3$, (0.0623)	Hexanol, in a sealed tube	175	34	One-pot
14.	1, (0.1)	1, (0.038)	2, $La(acac)_3$, (0.081)	Octanol, 5, and drops of DBU in a sealed tube	195	34	One-pot

In the first attempt, we reacted 1 eq. of **2.5** and 2 eq. of $La(acac)_3 \cdot H_2O$ in pentanol at 165 °C in a sealed tube for 13 hrs. After that, **2.1** was added to the reaction mixture and the system was heated for 33 hrs. A drawback of this stepwise reaction is the generation of side products such as La-Dy **2.25** and La_2-OEP_3 **2.27**, which caused no formation of the desired porphyrin triple-decker. In the second attempt, we reacted 1 eq. of **2.5** and 6 eq. of La trifluoromethanesulfonate (III) in pentanol with of DBU in a sealed tube for 3 hrs at 139 °C. After that, we added 1 eq. of OEP **2.1** and increased the temperature to 165 °C for 30 hrs. We checked TLC and found two unknown spots plus a La-Dyad **2.25** spot. In Figure 2.31, MALDI-TOF-MS showed the peak of La-dyad **2.25** at 1539 plus an unknown at 770 m/z. TD was not achieved in this attempt, and we suggested that the low temperatures and metalation step were unproductive.

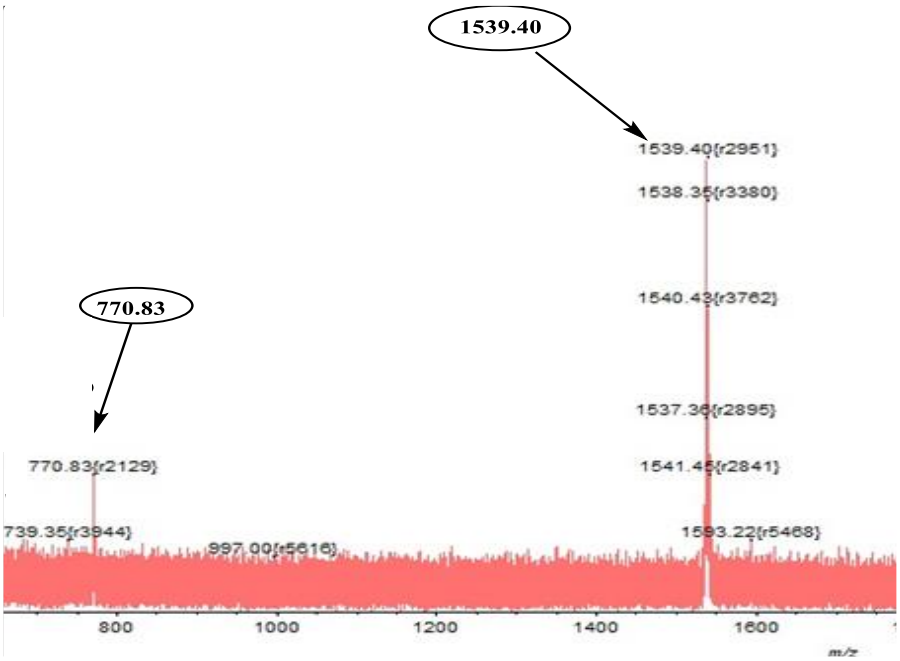

Figure 2.31: MALDI-TOF-MS showing the unknown product and La-dyad peak at 1539.40 m/z.

The one-pot reaction in the third attempt, which included the reflux of **2.5**, 2 equivalents of $La(acac)_3.H_2O$ and one equivalent of OEP **2.1** in pentanol at 170 °C in a sealed tube for 4.5 days, was unsuccessful. The fourth attempt, using **2.5** and 2 eq. of $La(acac)_3 \cdot H_2O$, one equivalent of **2.1**, and several drops of DBU in pentanol in a sealed tube at 165 °C for 1.5 days also failed to produce the desired product. In this attempt, by-products were again identified, including La-dyad at 1530 m/z **2.25** and an unknown product at 770 m/z, in addition to unreacted starting material OEP **2.1**.

Although TD started to form during the initial 17 hrs of the 5th attempt, using 1 eq. of **2.1** and **2.5** with 2 eq. of $La(acac)_3$ in pentanol, the method did not produce a good yield of the triple decker. Likewise, neither did the 6th nor 7th attempt. However, the 8th attempt was more promising. This technique used 1 eq. of **2.1** and **2.5** with 2 eq. of $La(acac)_3$ in pentanol at 165 °C for 5 days in a sealed tube and produced a low yield, so we tried to improve this by increasing the time to 120 hrs. La-TD **2.3** formed, as shown in Figure 2.32.

Figure 2.32: MALDI-TOF-MS of promising reaction indicating triple decker **2.3**.

We used a size exclusion column (THF the first time and DCM on the second attempt) to separate TD **2.3**, but all these attempts failed to give pure products. In the 8th attempt, recrystallisation using (1:1) DCM: MeOH, in Figure 2.33, MALDI-TOF-MS showed the peak of La_2-OEP_3 **2.27** at 1876 plus an unknown at 671 m/z.

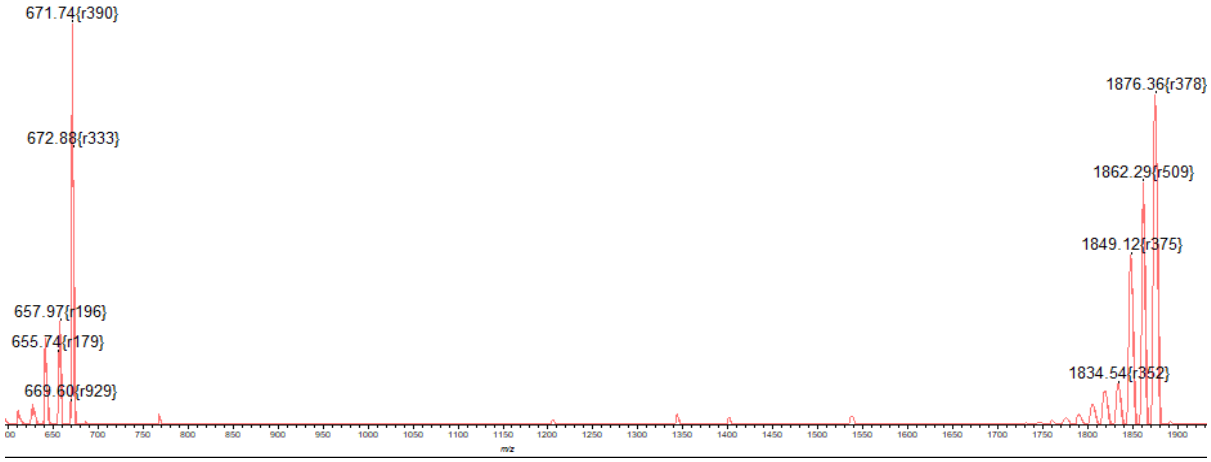

Figure 2.33: MALDI-TOF-MS shows the side products unknown at 671 m/z and **2.27**.

Efforts were made to purify TD **2.3** without column chromatography, but a tiny amount of side product, La_2-OEP_3 **2.27**, remained and couldn't be removed. Further, all recrystallisation attempts were unsuccessful, and column chromatography was required. Our 9th attempt initially appeared successful, as when we reacted 1 eq. of **2.5**, 2 eq. of $La(acac)_3$, and 0.9 eq. of **2.1** in pentanol at 180 ℃ in a sealed tube, the TLC showed the spot of TD after 17 hrs. After 120 hrs, TLC showed a very dark reddish-brown spot of **2.3**, plus **2.27** in burgundy colour, and a dark olive-green spot close to the baseline likely to be double-decker **2.25**. After one further day, the spot of La-TD was very faint, while **2.27** and dyad-La **2.25** were in good quantity. By 6 days and 17 hrs, the **2.3** had wholly decomposed. The 10th attempt, following previous Cammidge work, produced only a trace amount of the desired product TD **2.3**. Still, the side products **2.27**

and **2.25** and some unreacted starting materials **2.1** were present. Neither the 11th nor 12th attempts produced any positive results. In the former case, since a temperature of 200 °C was used for 3–6 days, this may have decomposed the TD product. In the latter case, only the starting materials were found, as shown in Figure 2.34.

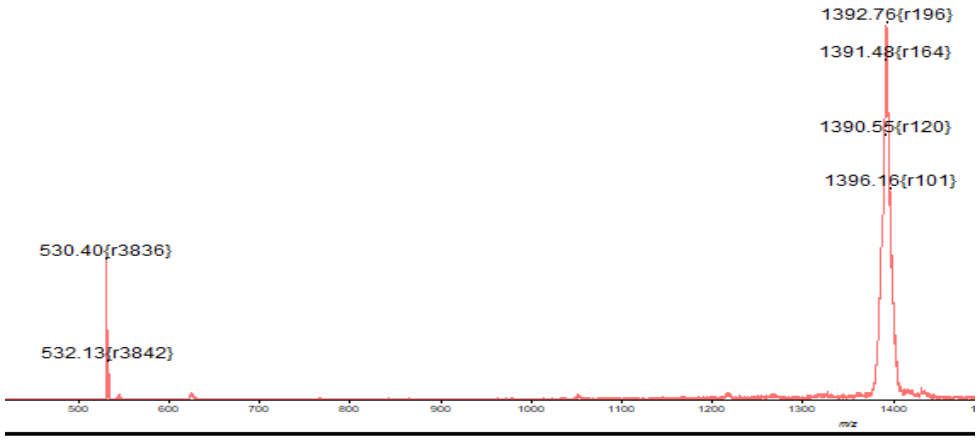

Figure 2.34: MALDI-TOF-MS of the 12th attempt showing unreacted starting materials **2.1** and **2.5**.

We added Pc **2.21** in the 12th reaction, but there was no TD formation, leading to the abandonment of the reaction. The 13th and 14th attempts also failed to give significant quantities of TD. In summary, first, high-boiling-point solvents such as octanol and hexanol were unsuitable for TD porphyrins. Second, DBU may be best avoided in the La-Por-TD **2.3** reaction as it causes the formation of La-dyad **2.25** as a significant product. Third, the metalation stage in the stepwise reaction must be 16 hrs and no more because we found 24–34 hrs led to a decomposition reaction.

Finally, we found the best equivalents of reactants was (1:0.9:2) (dyad: OEP: $La(acac)_3.H_2O$ respectively), and the time to obtain porphyrins TD in a good yield was five days at 180 °C, while leaving the reaction for longer caused decomposition of La-TD.

2.9 Attempts to improve the yield of lanthanum porphyrins triple decker:

2.9.1 Attempt to produce La-Por-TD by using Na metal:

We dissolved 0.0012 grams of Na metal in pentanol before adding all reactants[25] from 1 eq. of **2.5**, 2 eq. of $La(acac)_3.H_2O$, and 1 eq. of **2.1** in the solvent. After heating at 180 °C in a sealed tube, with regular TLC checks, it was left overnight, as shown in Scheme 2.12.

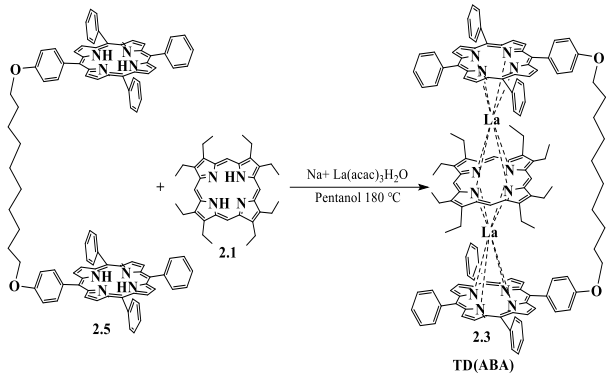

Scheme 2.12: Synthesis of the La-porphyrins TD **2.3** by using Na metal.

After 48 hrs, TLC was used to check the reaction, revealing two starting materials, OEP **2.1** and C_{10}-Dyad **2.5,** and three new spots. After 96 hrs, TLC analysis showed that the desired triple decker **2.3** was not achieved; only a very faint spot of **2.5** and four spots of by-products were observed. The MALDI-TOF-MS and TLC were checked after four days, and we found unreacted starting material C_{10}-dyad **2.5**. In Figure 2.35, the peak of La-dyad **2.25** was at 1529 and La_2-OEP_3 **2.27** at 1873 m/z, plus an unknown at 764 m/z. A very faint, unknown new spot was at 2067 m/z, as shown in Figure 2.35.

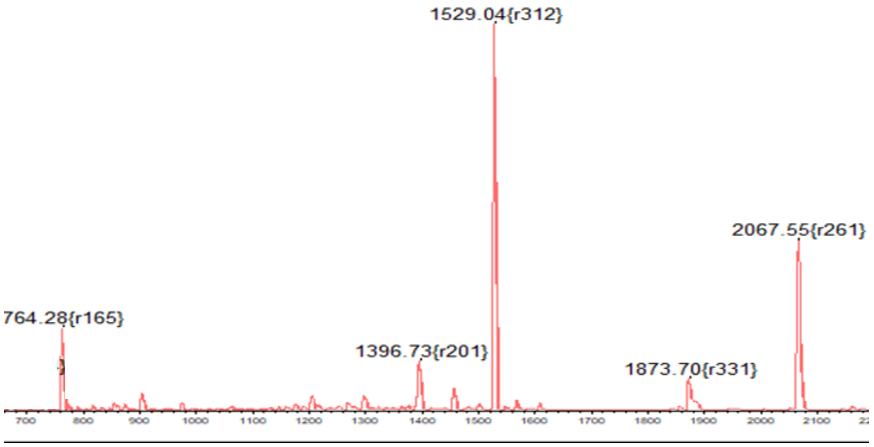

Figure 2.35: MALDI-TOF-MS shows lanthanum triple-decker reaction with sodium pentoxide/pentanol.

2.9.2 Formation of bridged La-TD using the dry La(acac)3:

In this experiment,[26] we aimed to minimise the moisture by subjecting $La(acac)_3$ to a drying process under vacuum conditions at 80 °C for 8 days. We reacted dyad-C_{10} **2.5** with two equivalents of dried lanthanum$(acac)_3$ in pentanol at 165 °C in a sealed tube for 3 hrs. 1 eq. of OEP **2.1** was added. After 17 hrs, a strong spot with a burgundy colour was observed corresponding to La_2-OEP_3 **2.27**, while unreacted spots **2.5** and **2.1** were also found. We left the reaction for 4 hrs; a faint spot of TD **2.3** was observed and most of the dyad spot had gone.

We stopped the reaction after 45 hrs as a total reaction time, and the solvent was evaporated. A product corresponding to the desired TD **2.3** was isolated in a trace amount. We concluded that two attempts to improve the yield by reducing the moisture in the reactions of porphyrins triple-decker **2.3** did not yield any positive results. We concluded this for both the above attempts: the first attempt, using sodium metal, gave another new product but in a small yield that was difficult to purify, while the second attempt gave TD in a very low yield.

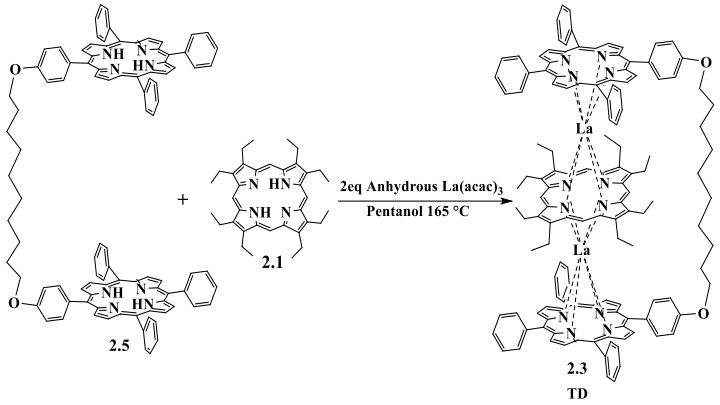

Scheme 2.13: Synthesis of the La-porphyrins La-Por-TD **2.3** by using dry metal salt.

2.9.3 Checking the stability of homoleptic porphyrin triple-decker La_2-OEP_3 and potential production of La-TD 2.3:

This attempt investigated the stability of the side-product La_2OEP_3 **2.27**, formed at the beginning of TD **2.3** reactions. TLC indicated its formation, which showed that it decreased when the reaction continued for a longer time, with the appearance of new spots in which the desired product was observed. As shown in Scheme 2.14, we reacted **2.1** with $La(acac)_3$ in TCB under N_2 reflux.[27,28]

It took only an hour before it was possible to observe that the colour had changed from burgundy to dark brown. After a further 19 hrs, the TLC revealed two spots. The first spot was burgundy in colour. It was identified as La_2-OEP_3 **2.27** since unreacted OEP **2.1** is dark pink. The TLC result remained unchanged after a further 3 hrs. On prolonged reflux, however, new spots (TLC) and products (MALDI-MS) started to appear, notably at 531 **2.1**, 1202 m/z La-OEP_2 **2.28,** and La_2OEP_3 **2.27** at 1874 m/z as significant peaks. There was also an unknown peak at 1440 and 669 m/z, as shown in Figure 2.36.

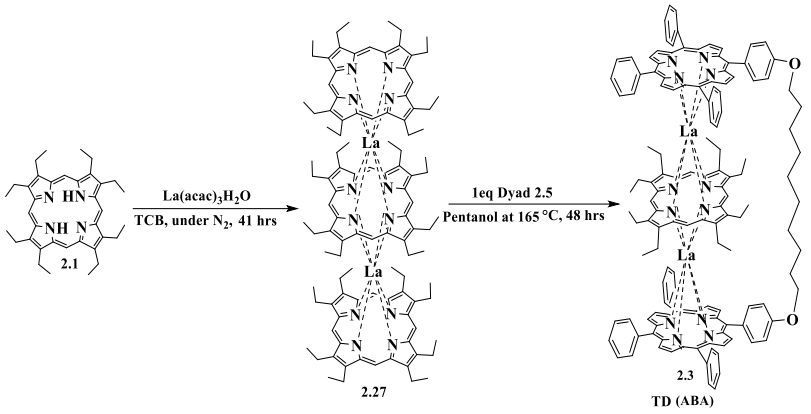

Scheme 2.14: Synthesis of OEP triple-decker with La and its further reaction with porphyrin dyad.

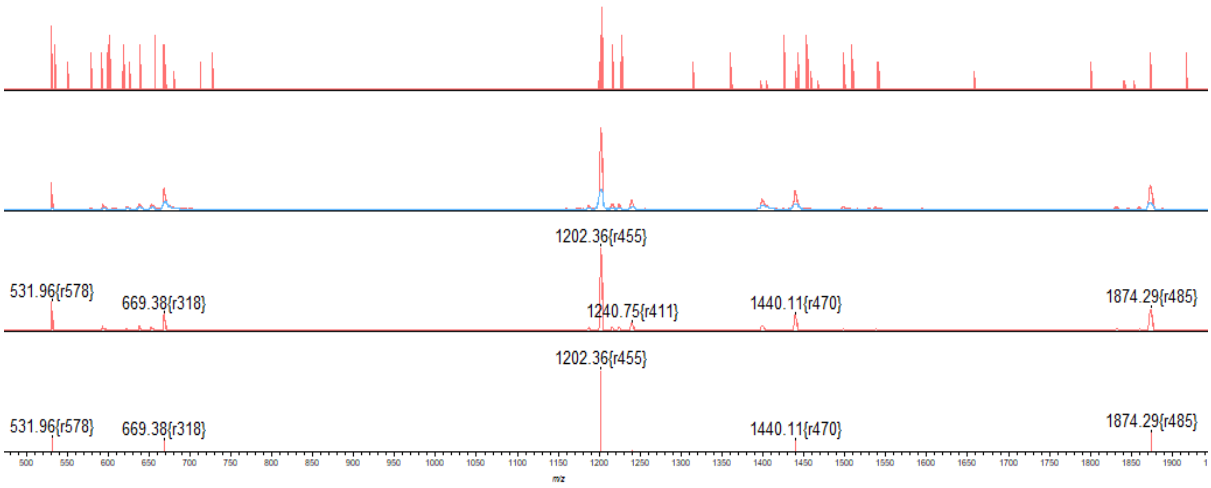

Figure 2.36: The synthesis of TD using a checked stability of **2.27** reaction after 24 hrs.

After the reaction was stopped after one day and 17 hrs (41 hrs), TLC showed a fourth unreacted spot of **2.1**, **2.27** as a strong, burgundy-coloured spot. The third and fourth spots indicated the presence of side products La-OEP_2 **2.28**, and unknown at 669, 1440 m/z, but these were very faint spots. Once the reaction had been stopped and cooled, MeOH was added, and the mixture was left overnight, and the resulting precipitate was filtered off.

It turned out to be primarily unreacted **2.1** and side products, while the solution was a mixture of **2.27** and **2.1**, making it necessary to isolate the homoleptic triple decker using column chromatography. The desired compound, **2.27**, was found in the last fraction. It was possible to recrystallise this using DCM: MeOH. The crystal was dark black at a yield of 5%, and TLC showed one spot of **2.27**, which has a dark burgundy colour, as expected for this TD of **2.27**.

The ^{1}H NMR spectrum in toluene is shown in Figure 2.37. The external -CH_3 groups appear at around 1.15 ppm as a triplet peak, while another triplet signal at 2.74 ppm is seen for internal CH_3. The external diastereotopic protons for 2-CH appear at 3.49 ppm and 3.92 ppm and both are doublet quartet signals. The internal CH_2 is a quartet at 4.25 ppm. The internal meso-protons

are at 8.40 ppm are a singlet signal, and the external meso-protons at 8.49 ppm are also a singlet signal.[29]

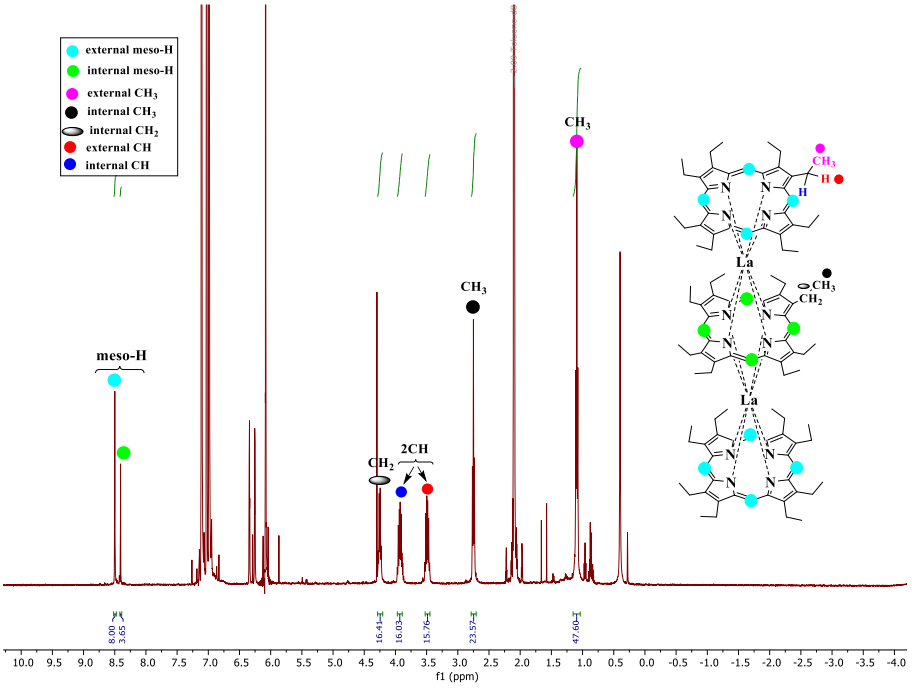

Figure 2.37: ^{1}H NMR spectrum of (La_2-OEP_3) **2.27** in toluene-d_8.

MALDI-TOF-MS was checked after isolation of **2.27**, and the expected peak at 1874.87 m/z was observed, as shown in Figure 2.38.

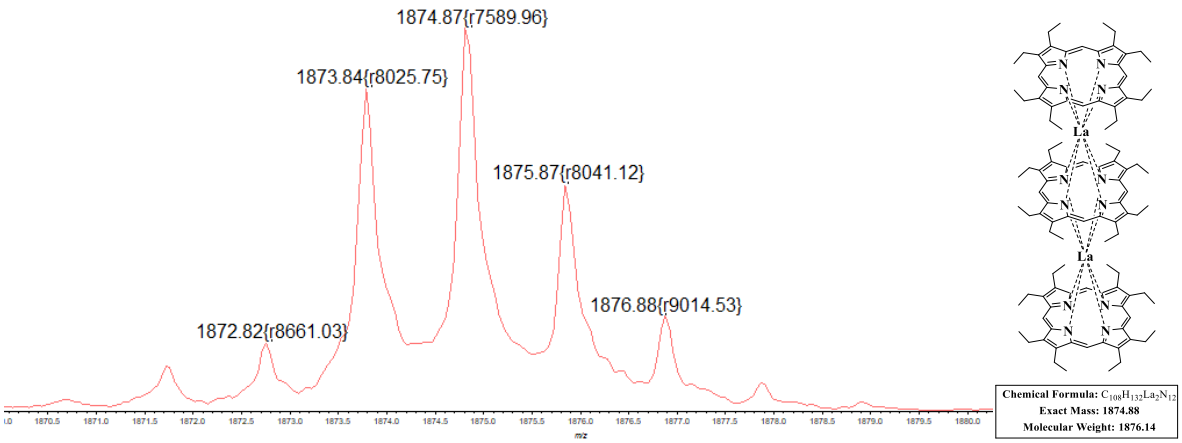

Figure 2.38: MALDI-TOF-MS of (La_2OEP_3), exact mass and molecule weight **2.27**.

La_2OEP_3 was reacted with 1 eq. of **2.5** in pentanol at 165 °C in a sealed tube. After 48 hrs, TLC showed a faint spot of OEP **2.1**, C_{10}-dyad **2.5**, La-TD **2.3,** and the baseline spot was dark purple. This gave a clear indication that the TD formation is an equilibrating process at this temperature(Figure 2.39).

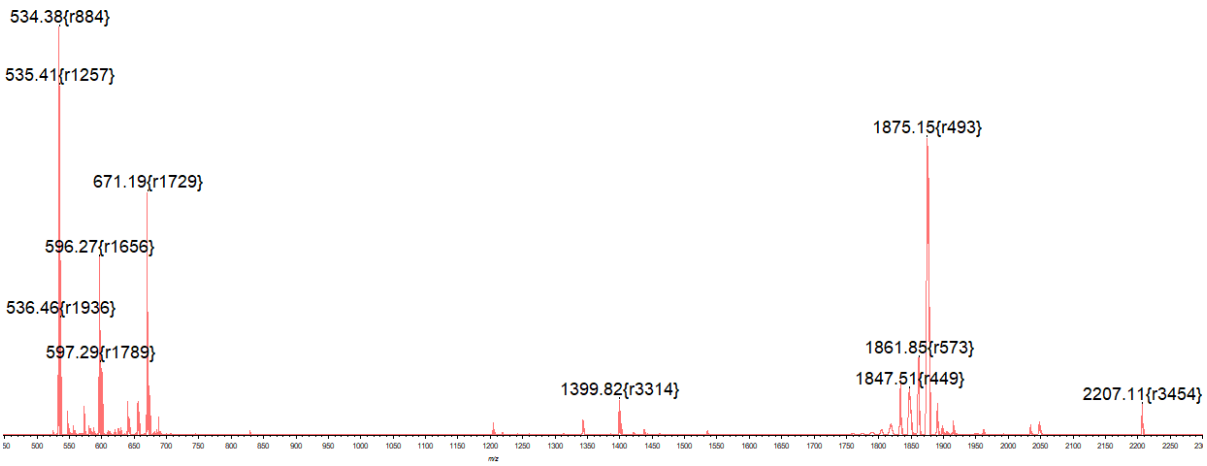

Figure 2.39: The synthesis of TD using **2.27** after 48 hrs.

A further TLC after 18 more hrs, however, indicated that the desired product **2.3** had disappeared while the spot of **2.5** had returned as a major component. We conclude that the goal of creating the desired product La-TD **2.3** with a good yield was not achieved. However, a small amount of TD formed after 48 hrs, but it was decomposed after 66 hrs, being the total time in this reaction.

2.10 The modification of the synthesis of lanthanum triple decker from the original method:

2.10.1 Optimisation of the reaction conditions for the formation of TD 2.3: TD synthesis was optimised with varying stoichiometry and reaction time (Table 2.6).

Table 2.6: Attempts for the synthesis of La-TD **2.3**.

Entry	Eq, g, 2.5	Eq, g, 2.1	$La(acac)_3$	Temp, °C	Time, days	Yield (%) of La-TD and La_2-OEP_3 2.27 respectively
1.	1, (0.1)	0.9, (0.0343)	2, (0.0622)	180	4	7 and 11
2.	1, (0.1395)	1.1, (0.059)	2.2, (0.0471)	165	5	5 and 29
3.	1, (0.1)	1, (0.038)	2, (0.0622)	180	5	6 and 12
4.	1, (0.1)	0.9, (0.0343)	2, (0.0622)	165	7	8 and 11
5.	1, (0.114)	0.9, (0.0378)	2, (0.0743)	180	5	12 and 7
6.	1, (0.1)	1.3, (0.0496)	2, (0674)	165	7	2 and 9

In the 1st attempt, we reacted **2.5** with two equivalents of $La(acac)_3$ and 0.9 eq. of OEP **2.1** in pentanol at 180 °C for 4 days in a sealed tube. After 4 days, the TLC showed a strong spot of TD **2.3**, a spot of the side product **2.27**, and an OEP spot. This attempt gave 7% of **2.3** (MALDI-MS) and the side product of **2.27** in 11%. On the 2nd attempt, we applied the conditions developed by the Cammidge group, except that the reaction time was increased from 24 hrs to 5 days. We heated 1 eq. of **2.5** and 1.1 eq. of **2.1** in pentanol overnight at 165 °C. After that, we added 2.2 eq. of $La(acac)_3$ to the mixture and refluxed it for 5 days. This reaction showed no real improvement and gave the desired TD (5%) and side product **2.27** (29%). The 5th attempt, giving the highest yield (12%), used 1 eq. of C_{10}-dyad **2.5**, 0.9 eq. of OEP **2.1**, and 2 eq. of $La(acac)_3$ in pentanol at 180 °C for 5 days. We conclude that the equivalence of reactants should be (1:0.9:2), **2.5**, **2.1,** and $Ln(acac)_3$, respectively, in pentanol. The formation of La-Por-TD requires considerable time, not less than 5 days and not more than 7 days, at 180 or 165°C, respectively.

Microwave irradiation[30] was also briefly investigated as an alternative. While this proved efficient for synthesis of OEP TD **2.27** (18% after 4 hrs), reactions only gave trace quantities of the desired TD.

2.10.2 Optimisation of the purification procedure for the formation of TD:

TD **2.3** proved very hard to isolate in pure form by chromatography. Many different systems were tried, but they mostly gave **2.3** contaminated with small quantities of OEP and/or unknown impurities. We eventually isolated pure product TD **2.3** as a reddish-brown solid using the solvent system (3.3:100) EtOAc/Hexane. The first fraction was side product **2.27**.

The second fraction was unreacted OEP **2.1**, while the third fraction was the reddish-brown desired product. The final fraction was La-dyad **2.25**, which is olive green in colour. TLC for this separation stage of La-TD is shown in Figure 2.40.

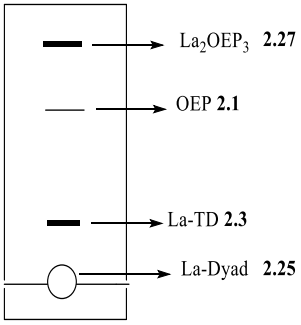

Figure 2.40: TLC shows four main spots in La-TD **2.3** using ethyl acetate: hexane or pet-ether (3.3:100) as an eluent.

The MALDI-TOF MS reveals a peak at 2204.48 m/z, which aligns with the anticipated desired product of a triple-decker structure **2.3** (ABA), as shown in Figure 2.41.

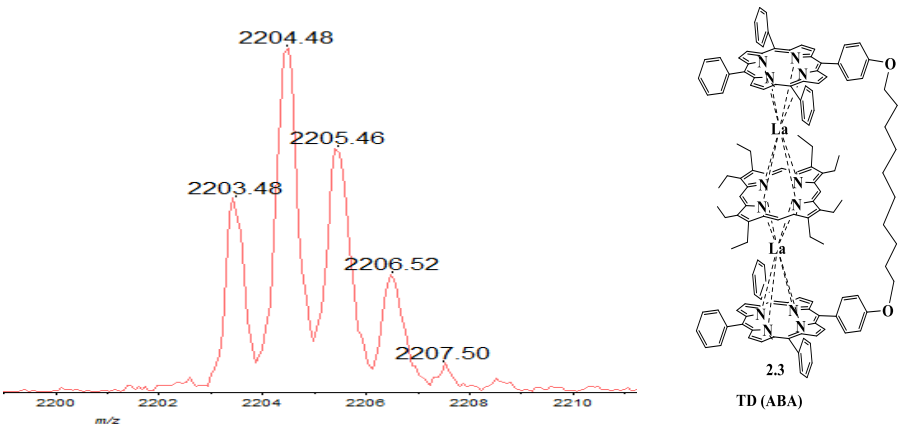

Figure 2.41: MALDI-TOF-MS confirms the formation of La-TD **2.3**.

^{1}H NMR and 2D spectra were obtained in $CDCl_3$ (Figures 2.42 and 2.44). However, we found the La-triple-decker spectrum to be complex and very different from the previous spectra obtained for ABA triple deckers incorporating Pc.[1,6] It was immediately clear that our formulation of structure **2.3** could not be correct and that a different TD structure was formed in these reactions. Spectra for the previous triple deckers in our group[1,6] clearly showed their symmetrical arrangement (ABA) in which the alkoxide peaks (-O-CH_2) at around 4.6 ppm appear as one triplet, which means that both ends of the aliphatic chain are in an identical environment (symmetrical molecule). In our TD (**2.29**), we found that two complex signals for alkoxide peaks (O-CH_2) were present in the spectrum, as shown in Figure 2.42.

The first (O-CH_2) (a′) appears as two broad signals at ~ 4.27–4.33 ppm; this indicates that the two protons are in different environments and rotation is restricted. The other alkoxide peak (O-CH_2) (a) showed as a simple triplet signal at 4.65 ppm with J = 6.2 Hz. These two signals of alkoxide protons have different environments that confirm that TD **2.29** has an asymmetric structure. Further evidence is provided by the appearance of the ethyl chains on the OEP. The 16 H for CH_2 groups in OEP ring **2.1** have two signals (2 x CH). Again, if the isolated molecule had the OEP sandwiched between the TPP units, we would expect a single signal. We conclude that the OEP is on the exterior of the triple-decker structure. The eight internal protons (assumed) for (CH) appear as a broad signal at δ 3.57 ppm, while the other eight external protons for (CH) appear as a well-resolved dq signal at δ 3.27 ppm with J = 15.6 and 7.8 Hz.

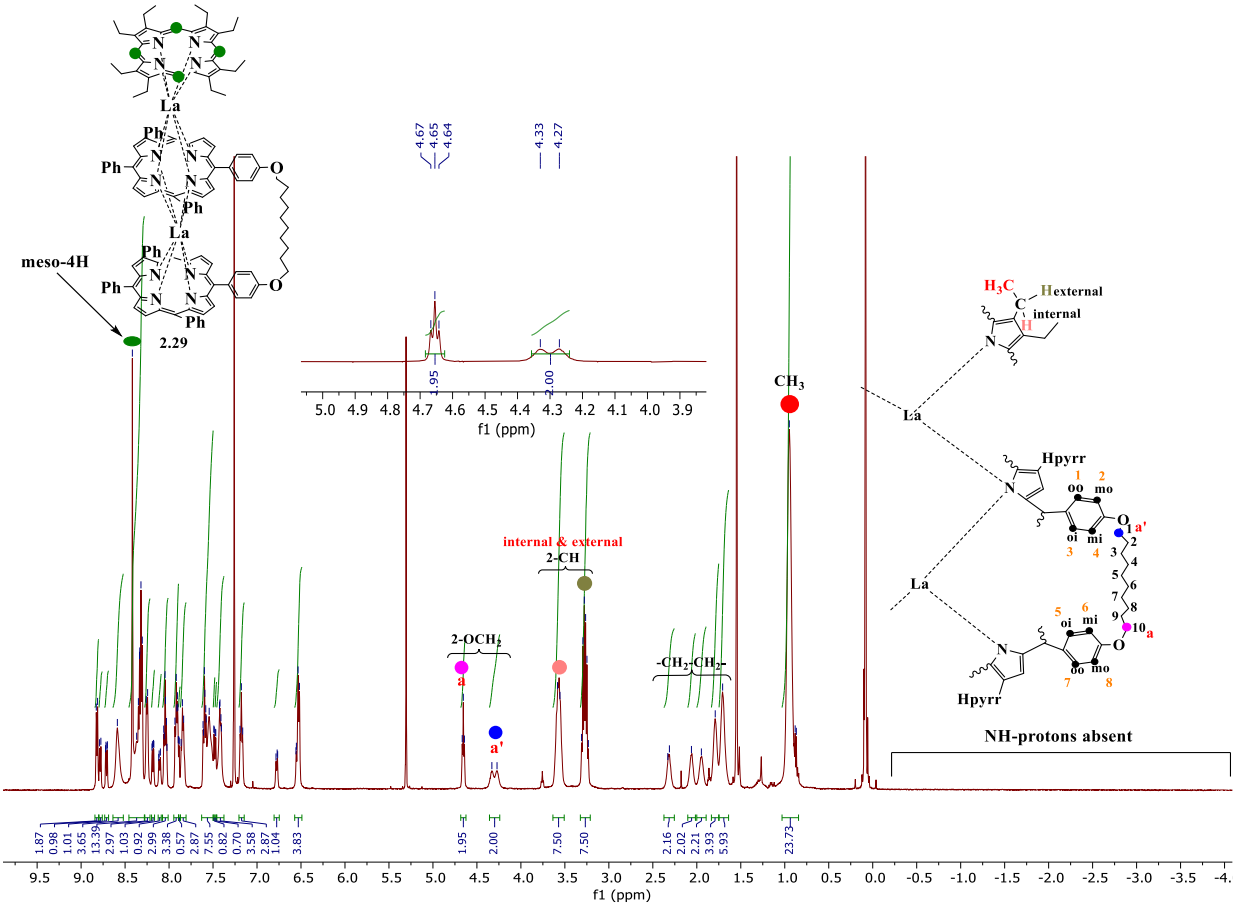

Figure 2.42: ^{1}H NMR spectrum of La-TD in $CDCl_3$ provides evidence of the asymmetrical character of the molecular environment, which confirms the production of **2.29**.

An expansion of the aromatic range is shown in Figure 2.43. There are well-resolved signals and some that are broad, probably due to restricted rotation, but all signals are accounted for in relation to the proposed AAB structure of **2.29**.

Like in other known examples, protons on the ortho and meta positions of the meso-phenyls are in different environments depending on whether they are oriented towards the outside of the molecules on the inside of the outer porphyrin, or on the inner porphyrin oriented towards either the TPP or OEP. The *meso*-H in the OEP ring appears as a sharp singlet signal at 8.41 ppm, integrating to 4H. The signals can be correlated using 2D COSY NMR spectroscopy, and this is shown in Figure 2.44.

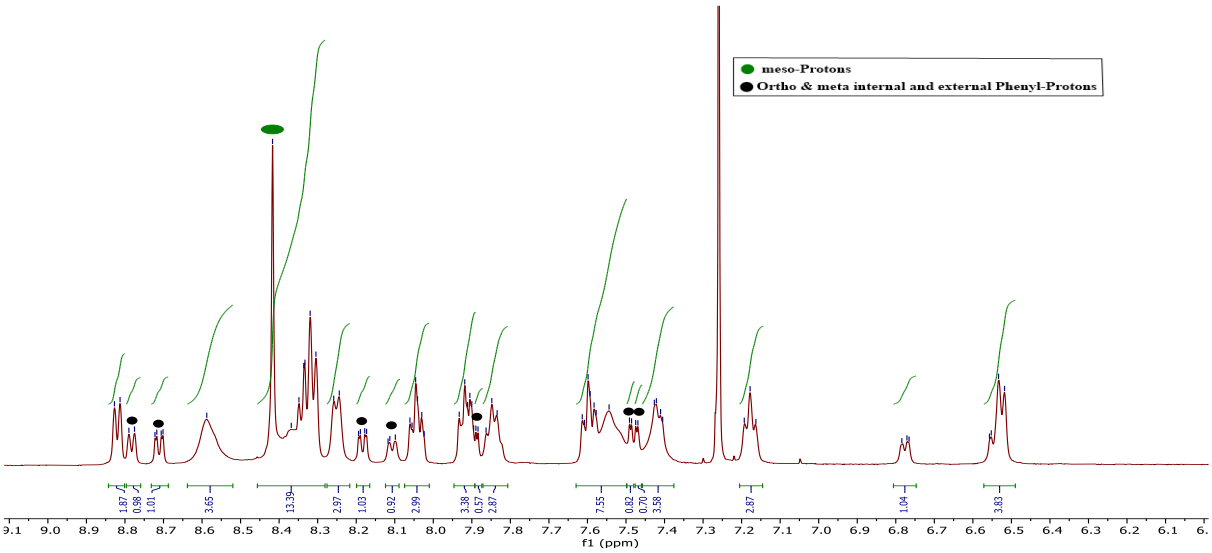

Figure 2.43: ^{1}H NMR spectrum for **2.29** in $CDCl_3$.

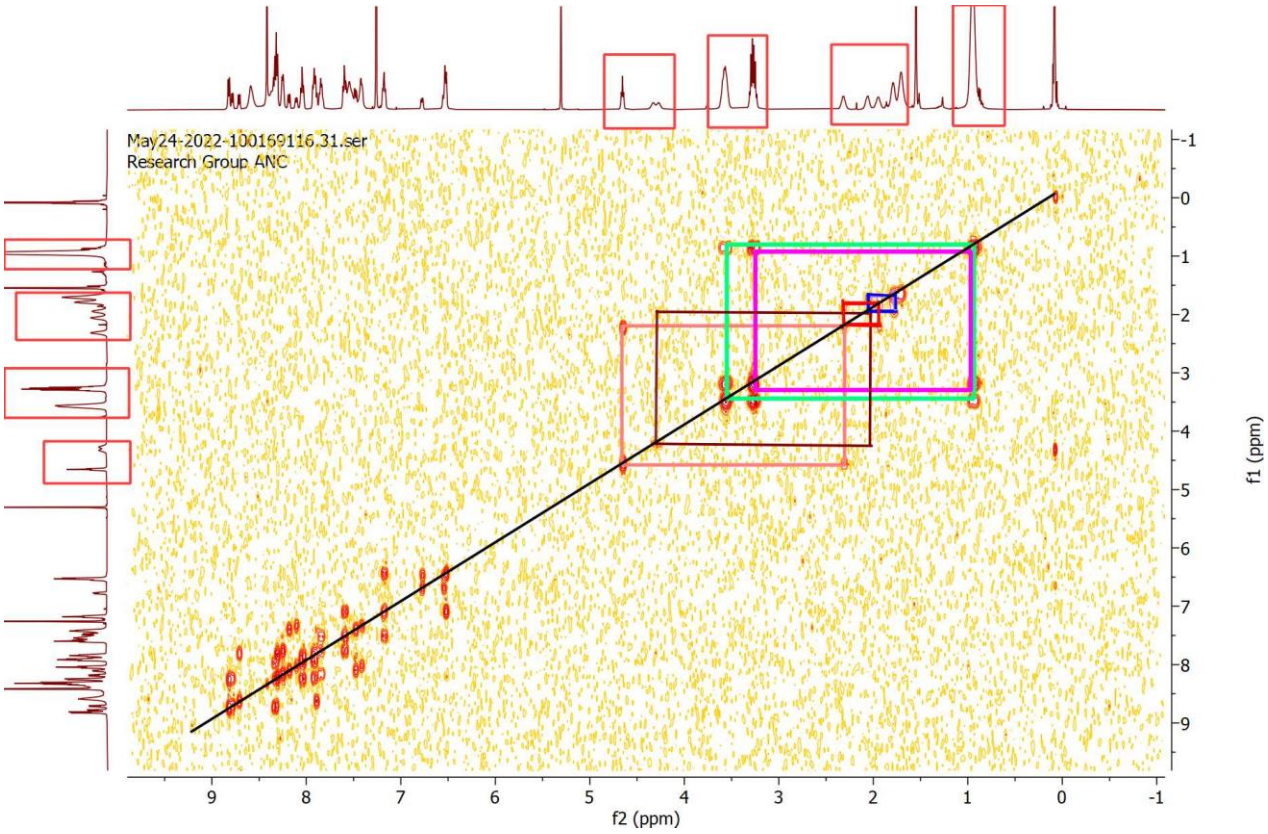

Figure 2.44: COSY experiment showing cross peaks in compound **2.29**.

Subsequently, we managed to crystallise the new La-triple-decker product **2.29**, confirming its structure, by using many attempts with different solvent systems, such as DCM Ethanol, DCM, Chloroform, and Isopropanol. We found that an excellent solvent system was (1:1) DCM: MeOH by slow evaporation. Also, we recrystallised the side product of **2.27** using EtOAc/Hexane or DCM: Pet-ether or hexane (1:1). The preliminary conclusion from this unexpected result is that there is a steric hindrance of the porphyrin cores because there are substituents in the

beta-positions (ethyl groups), CH_2CH_3. The OEP core cannot easily be accommodated inside the TD, which prevents symmetrical TD formation that has an ABA arrangement. We managed to grow a crystal that confirmed the (BAA) structure of La-TD **2.29** from DCM: MeOH, as shown in Figure 2.45, but we found a disorder in the chain and ethyl group when the crystal structure was solved by our collaborator, Dr David Hughes. Figure 2.45 shows the structure, and it is interesting to note that each ring is distorted from planarity, and this puckering is most pronounced in the top (bridged) porphyrin.

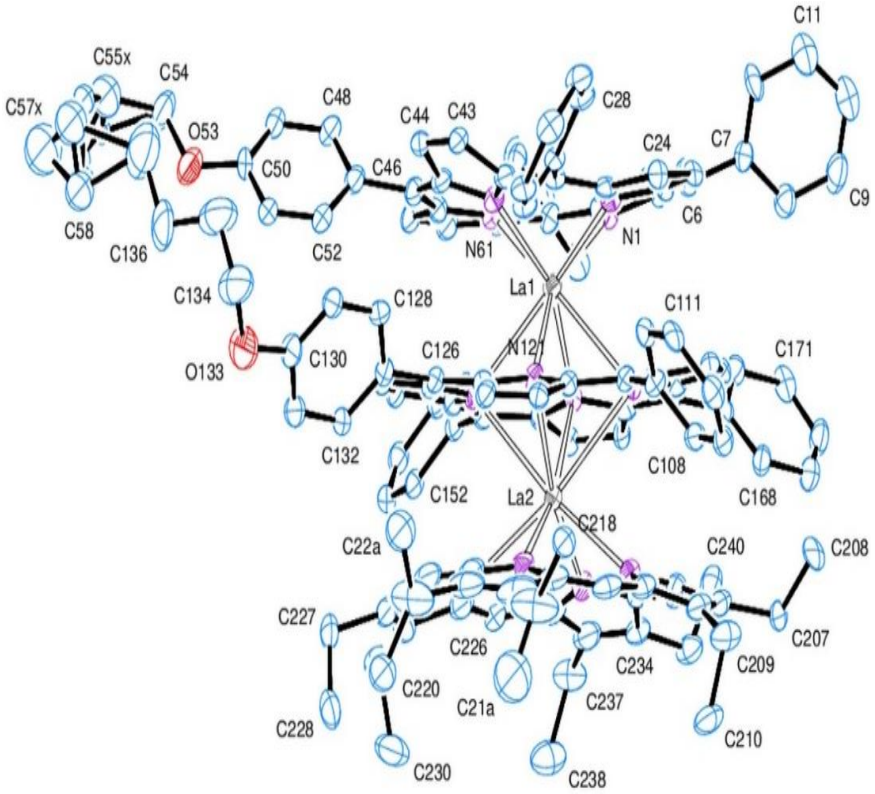

Figure 2.45: The XRD structure of TD **2.29**.

The UV-vis spectrum of TD **2.29** is shown in Figure 2.46 and has unique absorbance peaks that are different from the starting materials C_{10}-dyad **2.5** and OEP **2.1** and indicate pi-overlap in the TD structure.[31,32]

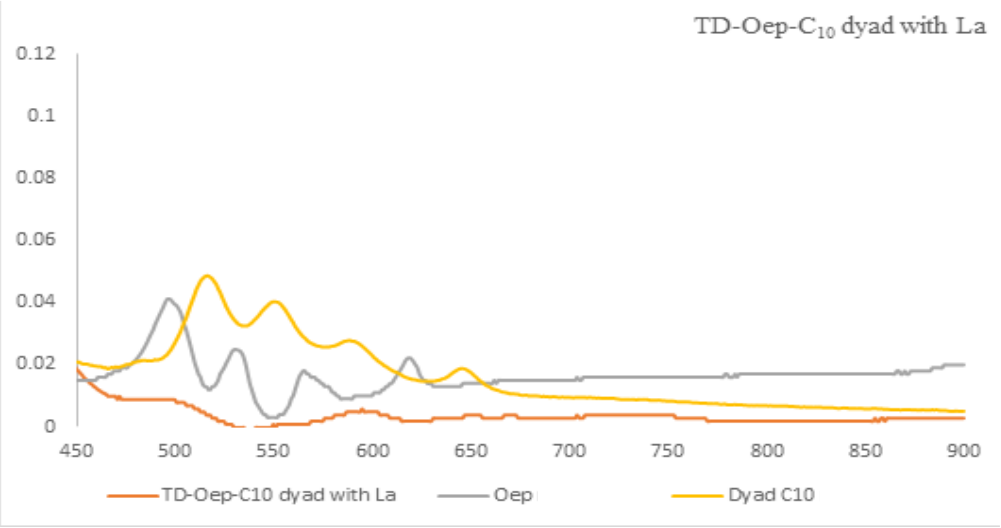

Figure 2.46: UV-vis absorption shows that the new compound TD(La) **2.29** differs from the starting materials **2.1** and **2.5**, indicating an overlap between components.

2.10.3 Synthesis of lanthanum triple decker with C_{12} porphyrin dyad:

We decided to examine the impact of chain length on forming La-triple-decker structures using metal-free OEP **2.1**, using a longer bridging chain. We used the C_{12}-porphyrin dyad **2.17**, which was synthesised from 1,12-dibromoundecane in the same optimised conditions as porphyrin dyad **2.5**. In this case, we reacted 1 eq. of C_{12}-porphyrin dyad **2.17** with 2 eq. of lanthanum acetylacetonate and 0.9 eq. of **2.1** in a one-pot reaction and refluxed in pentanol for 4 days to produce TD **2.30**, as shown in Scheme 2.15.

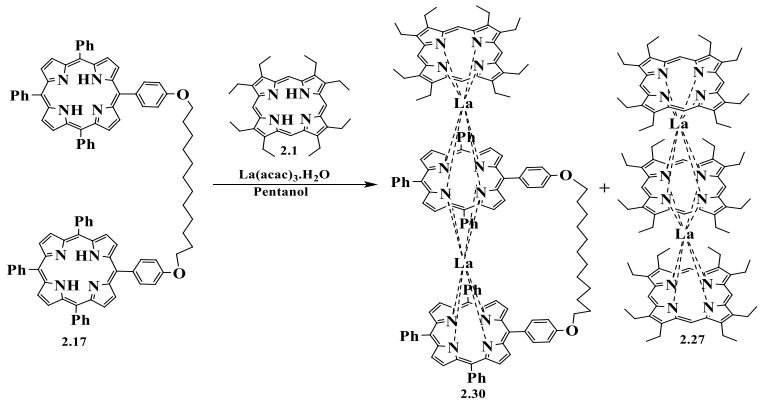

Scheme 2.15: Synthesis of La-TD **2.30** using the original process (Por-core ratio, temperature).

A TLC and MALDI-TOF-MS for this reaction showed that the desired triple-decker **2.30** at 2230 m/z was achieved while the starting materials were absent. Three unknown side products were present at 638, 668**,** and at 1857 m/z, while the homoleptic OEP triple-decker **2.27** was also a side product spot in the TLC (Figures 2.47 & 2.48).

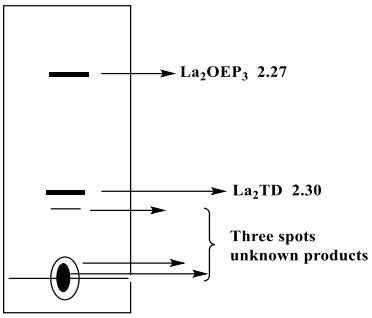

Figure 2.47: TLC showing four spots in La-TD using ethyl acetate: Hexane or pet-ether (3.3:100) as eluent.

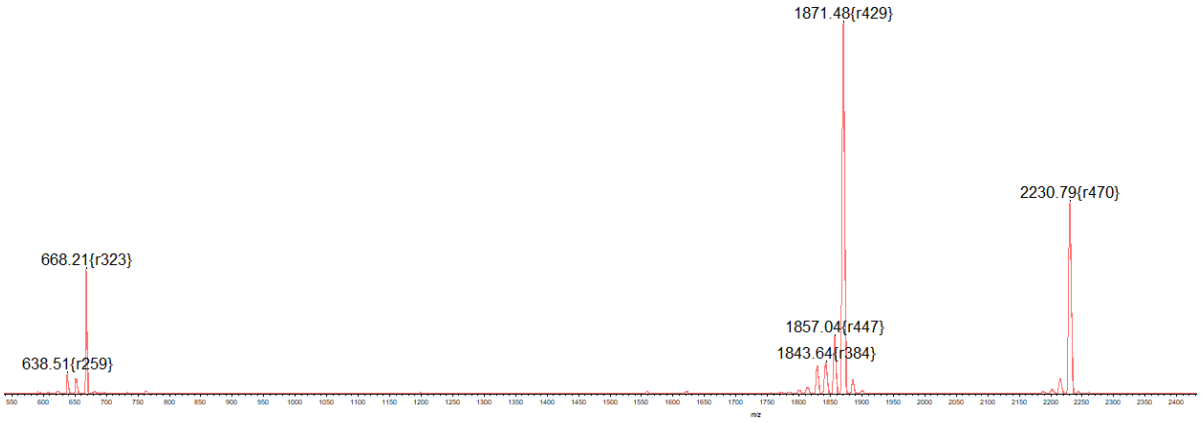

Figure 2.48: MALDI-TOF-MS of the reaction mixture of La-TD **2.30**.

We used ethyl acetate: Hexane or pet-ether (3.3:100) as eluent to isolate the desired product, and recrystallisation from DCM: MeOH gave pure La-TD **2.30** as a reddish-brown solid in 17% yield alongside La_2OEP_3 (8%) in a dark burgundy solid.

The ^1H NMR spectra of La-C_{10}-dyad-TD **2.29** and La-C_{12}-dyad-TD **2.30** are almost identical, confirming the (BAA) arrangement of macrocycles. When run in CD_2Cl_2, the peaks for the 2 x CH of the ethyl CH_2 groups are seen as a very broad signal in both samples of **2.29** and **2.30** (Figure 2.49). Therefore, we conclude that chloroform is the best solvent for analysing a sample of the La-OEP-TD compared to DCM. The MALDI-TOF MS reveals a peak at 2232.58 m/z for **2.30** TD, as shown in Figure 2.50.

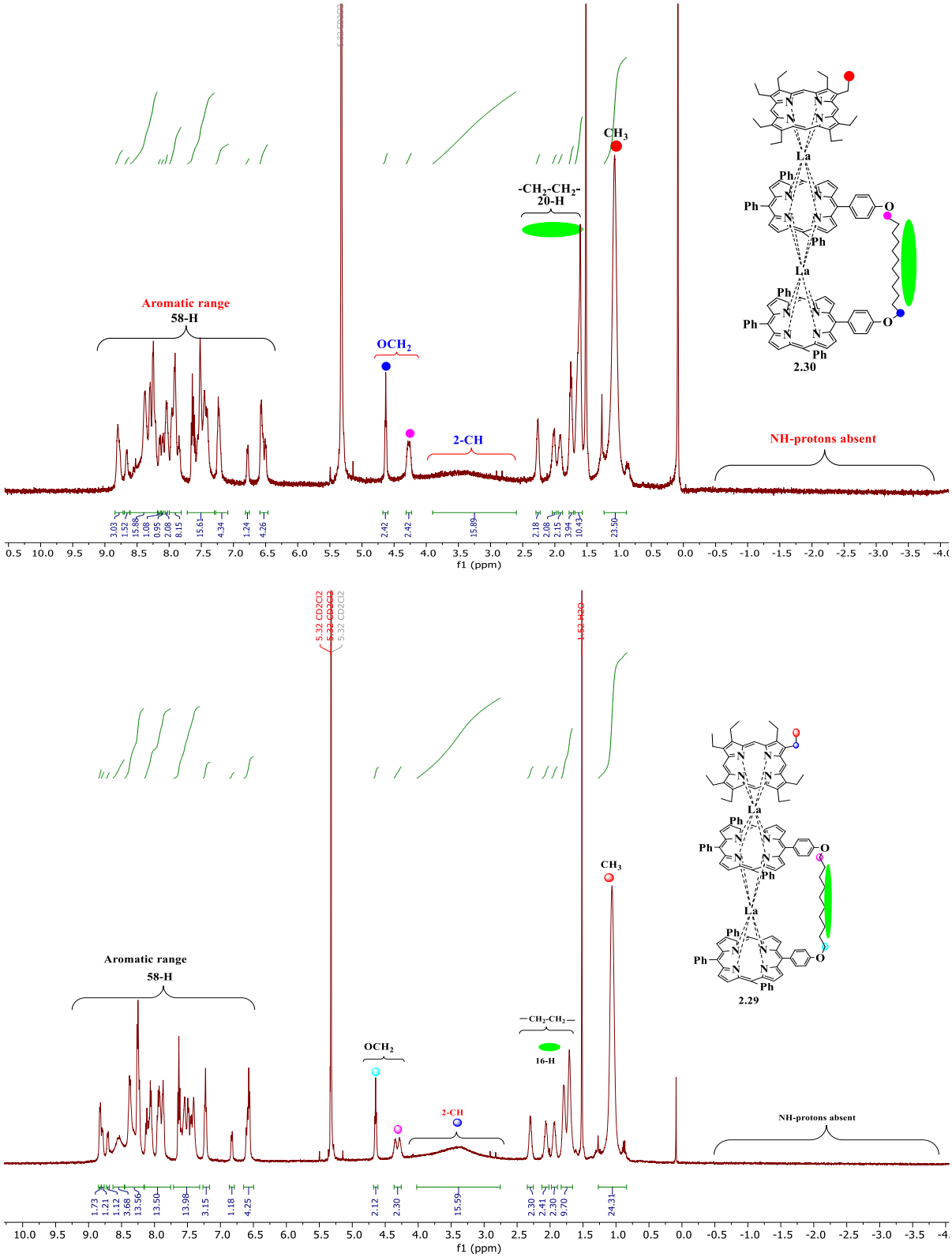

Figure 2.49: ^{1}H NMR spectrums of La-TD **2.30** and La-TD **2.29** in CD_2Cl_2.

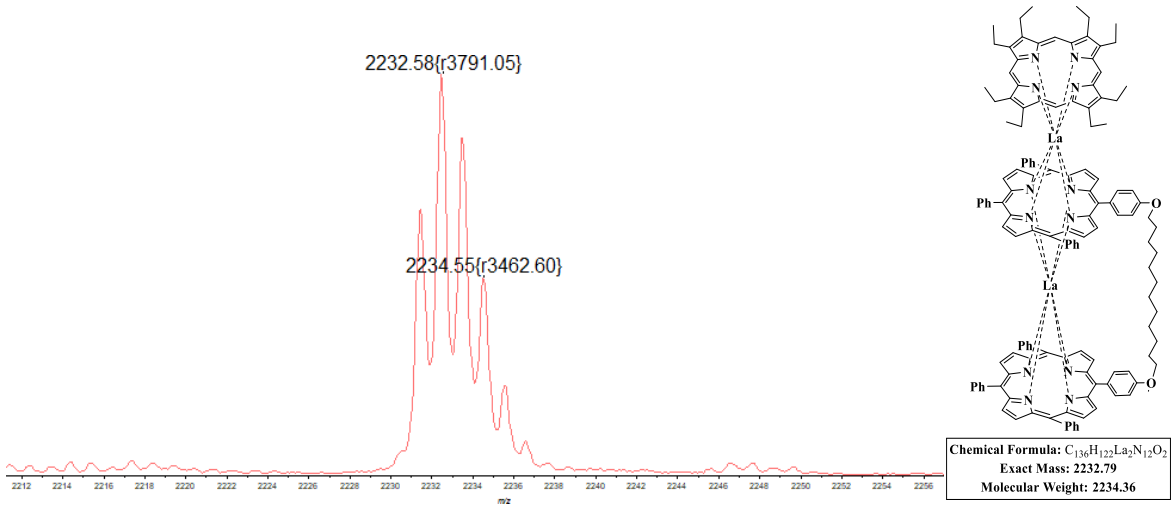

Figure 2.50: MALDI-TOF-MS confirms the formation of La-TD **2.30**.

2.11 Synthesis of the BAA TDs with different lanthanide metals:

2.11.1 Triple decker with neodymium:

We created the Nd-Por-C_{10} dyad triple decker using the previously applied conditions to produce La-TD **2.29**. In this attempt, we reacted 1 eq. of **2.5**, 0.9 eq. of **2.1** and 2 eq. $Nd(acac)_3H_2O$ in pentanol in a sealed tube at 180 °C, as shown in Scheme 2.16.

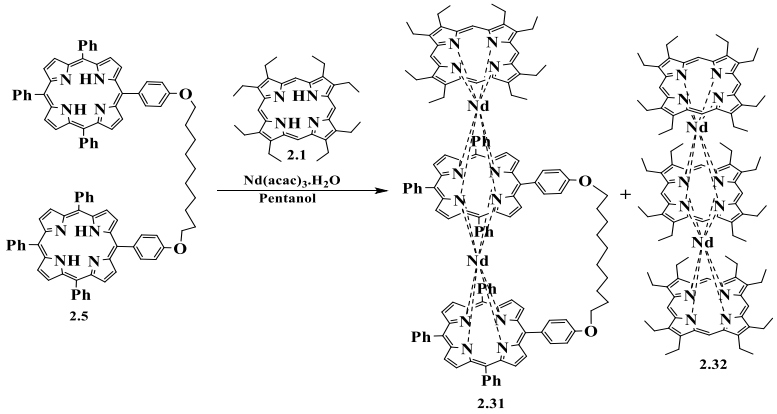

Scheme 2.16: Synthesis of Nd-TD **2.31**.

The reaction was completed after 5 days, and, after workup, the product was purified by chromatography using ethyl acetate: hexane or pet-ether (3.3:100) as eluent to purify the desired product and recrystallisation from DCM: MeOH to give a pure Nd-TD **2.31** as a reddish-brown solid in a 7% yield, and Nd_2OEP_3 **2.32** (10%) as a burgundy solid. Both were recrystallised from ethyl acetate: Hexane or DCM: MeOH.

While the starting materials were not present in TLC, we found additional unknown side products in the crude mixture, including unknown products 629, 671, and 1835.60 m/z, while the homoleptic Nd-TD **2.32**, was a first spot in the TLC at 1878.24 m/z, as shown in Figure 2.51.

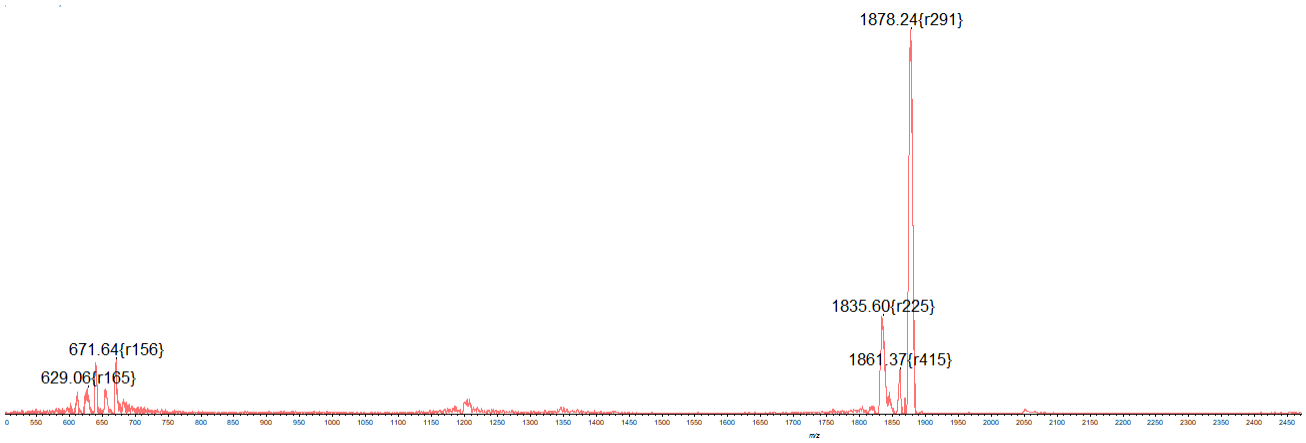

Figure 2.51: MALDI-TOF-MS of side products in Nd-TD **2.32** reaction.

The ^{1}H NMR spectra for Nd-triple-decker **2.31** were obtained in CD_2Cl_2, as shown in Figure 2.52. The magnetic properties of neodymium metals in compound **2.31** broaden the signals and add to the complexity of the spectra. Nevertheless, the ^{1}H NMR spectrum is consistent with the proposed BAA structure **2.31**. 2D NMR analysis was attempted (Figures 2.53 & 2.54) and allows identification of the CH_2 adjacent to CH_3 in the OEP ring that has two types of protons: external and internal (2-CH) protons, which were at ≈ 2.66 ppm for the external and ≈ 3.23 ppm for the internal protons, respectively. They appeared as broad singlet signals. The CH_3 ≈ 1.21–1.11 ppm.

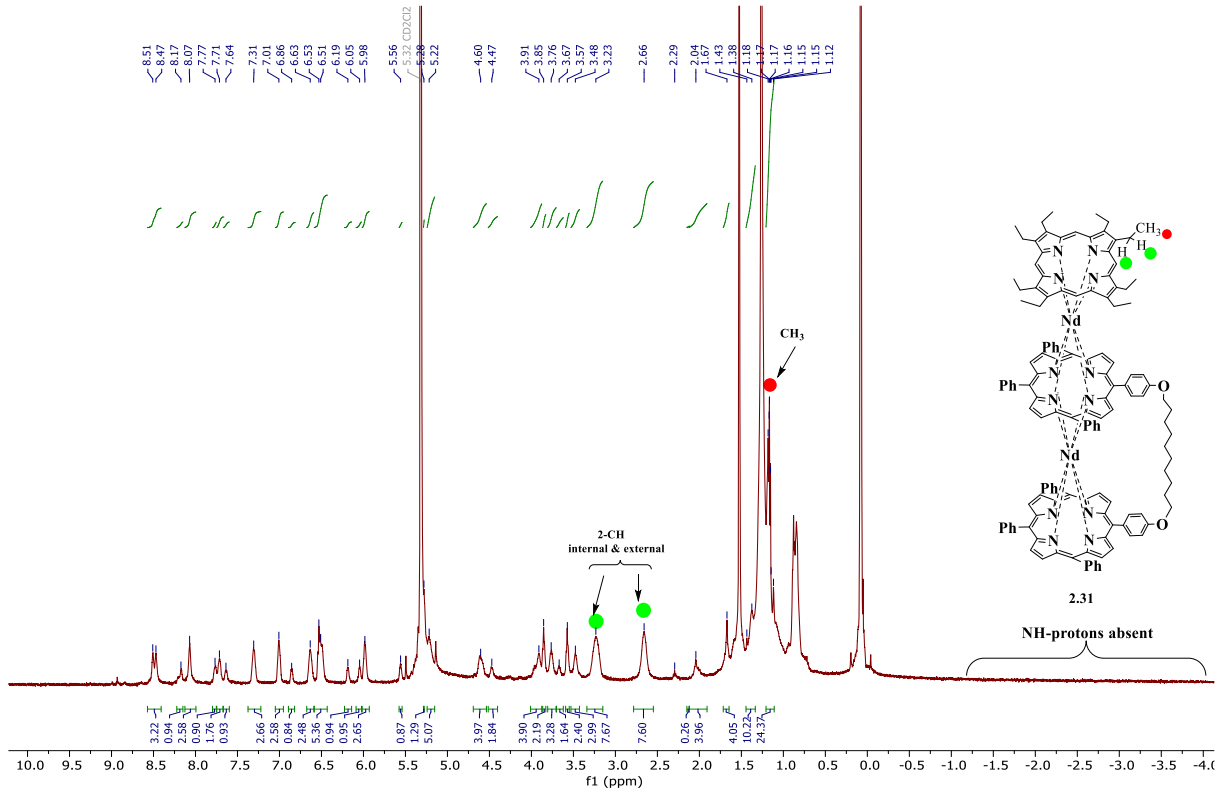

Figure 2.52: ^{1}H NMR of Nd-TD **2.31** in CD_2Cl_2

A more detailed 2D NMR analysis was attempted, allowing the identification of OEP **2.1** peaks and, tentatively, some other signals. The 2D NMR analysis of TD **2.31** supports the identification of the coupling of (2-CH) internal and external protons with CH_3 in OEP ring **2.1** in **2.31** molecules.

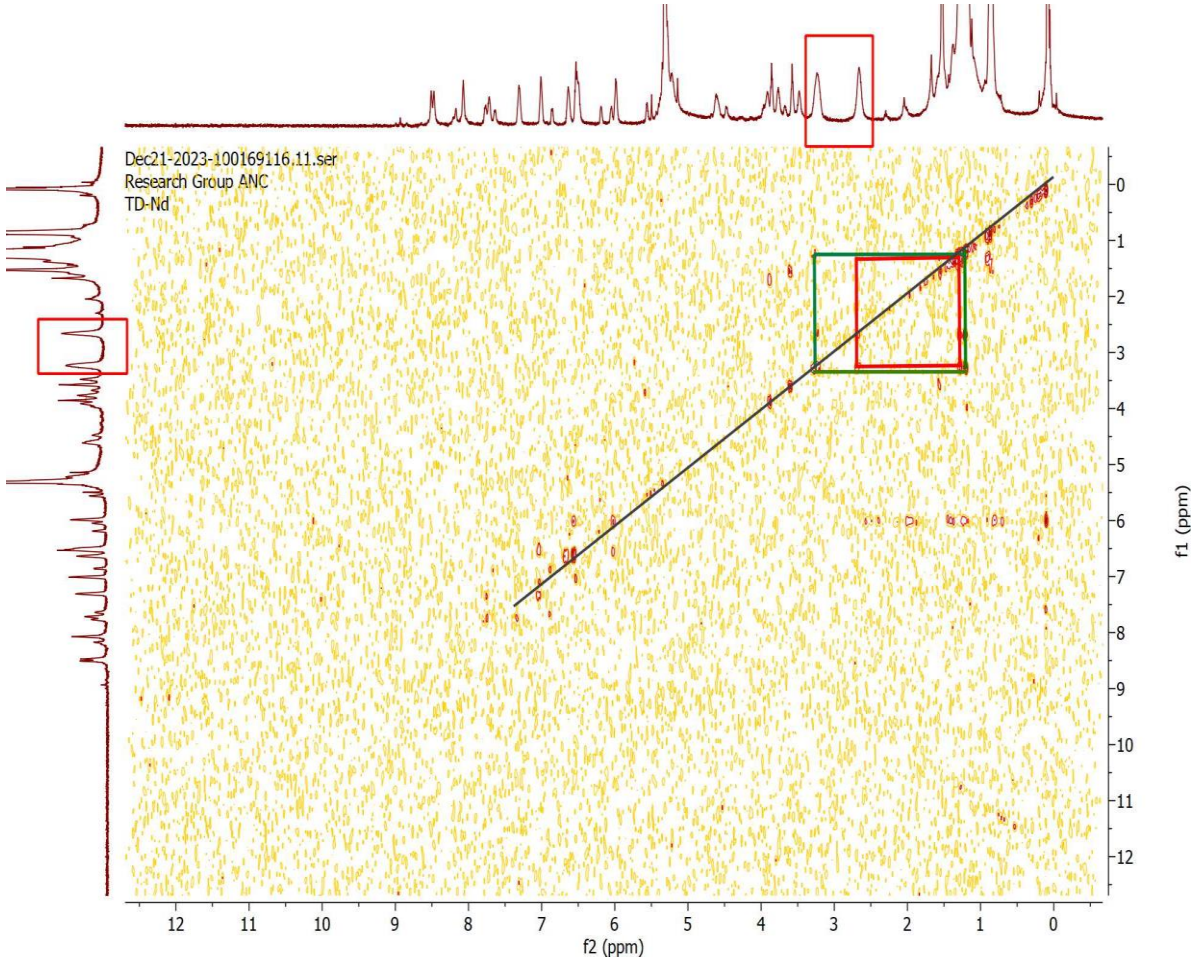

Figure 2.53: COSY experiment showing a cross peak in compound **2.31** in CD_2Cl_2.

MALDI-TOF-Ms of TD **2.31** showed a peak cluster at 2212.13 m/z (Figure 2.54). Subsequently, we attempted crystallisation using many different solvent systems, such as DCM: Ethanol, DCM, Chloroform, Isopropanol, and DCM: MeOH, but all attempts failed due to the small crystal size or disorder.

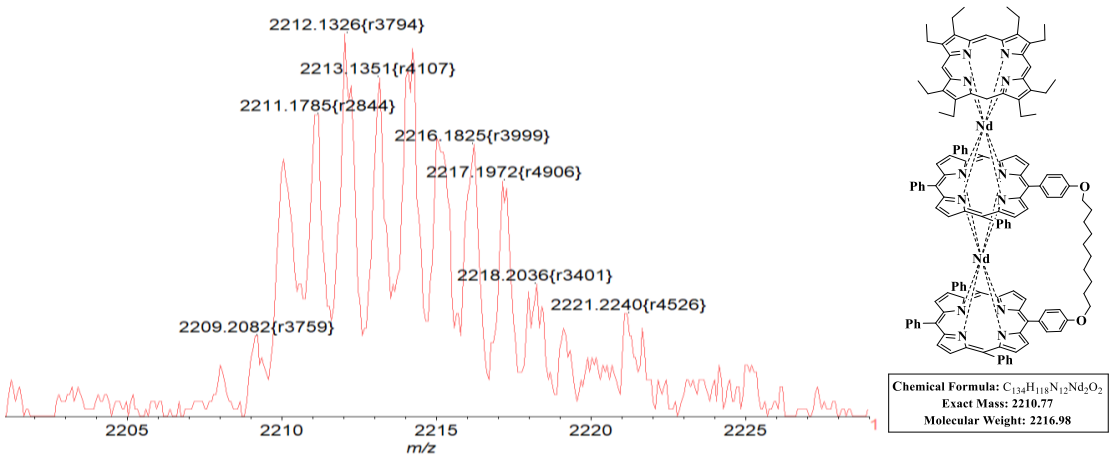

Figure 2.54: MALDI-TOF-MS of Nd-TD **2.31**.

The indication of TD formation can be detected by UV-vis and is shown in Figure 2.55; TD **2.31** exhibits an essentially identical spectrum to the corresponding La derivative.[31,32]

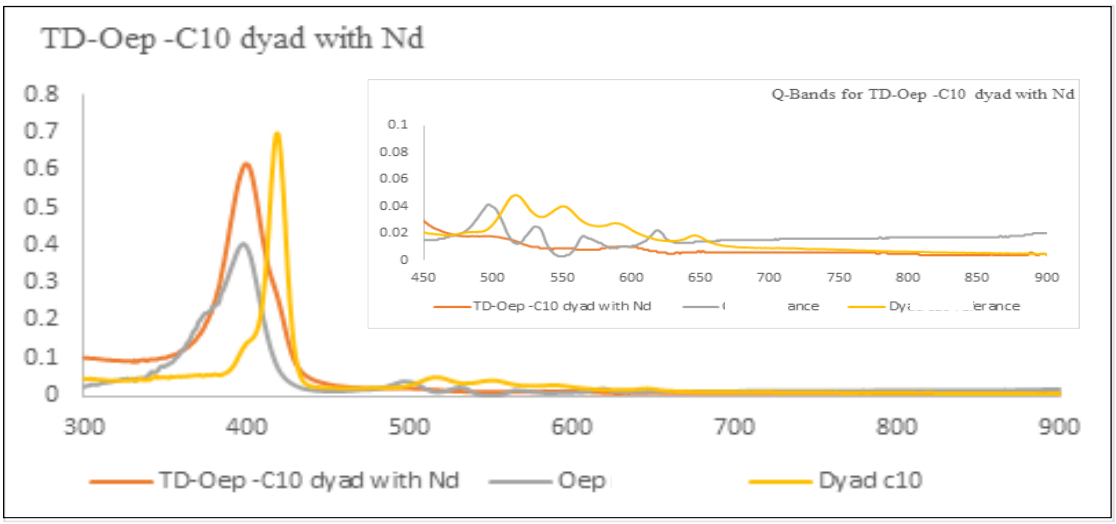

Figure 2.55: UV-Vis absorption of Nd-TD **2.31**, **2.5** and **2.1** in DCM.

The homoleptic compound OEP-Nd-TD **2.32** was also isolated and recrystallised from ethyl acetate: Hexane/pet-ether or DCM: MeOH. MALDI-TOF-MS (Figure 2.56) showed a cluster at 1879.59 m/z.

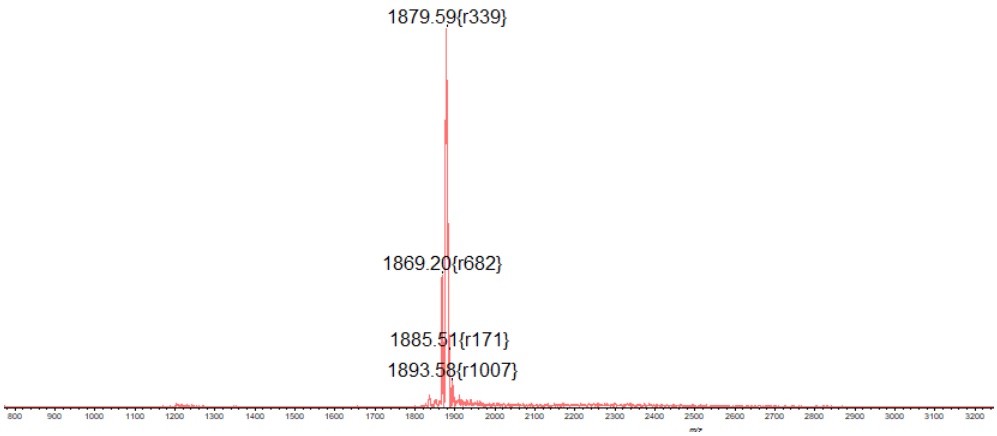

Figure 2.56: MALDI-TOF MS for Nd_2-OEP_3 **2.32**.

The ^{1}H NMR spectrum was run in toluene-d_8 for homoleptic TD **2.32** and is shown in Figure 2.57.[29]

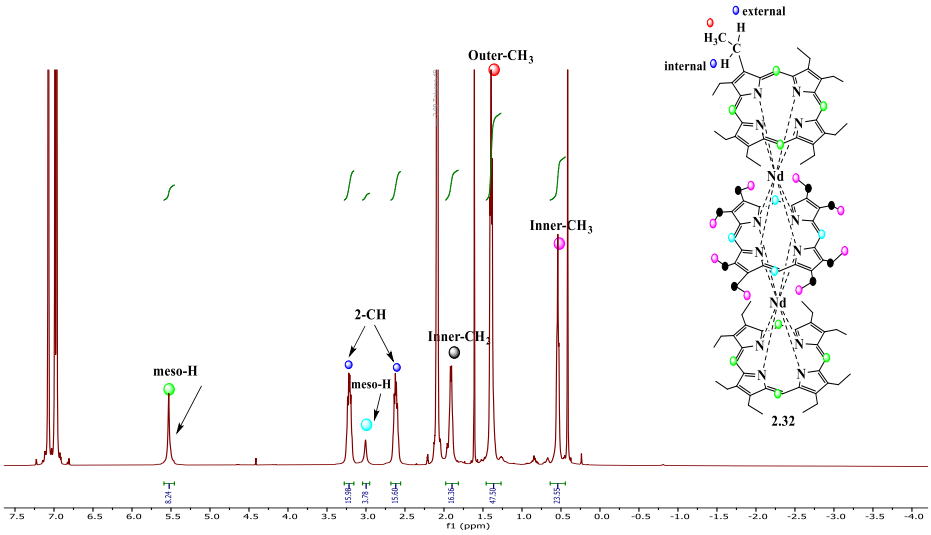

Figure 2.57: ^{1}H NMR of Nd-TD **2.32** in toluene-d_8.

2.11.2 Triple decker with praseodymium:

Pr-triple decker **2.33** was synthesised using the same conditions as for La-Por-TD by reacting 1 eq. of **2.5**, 0.9 eq. of **2.1** and 2 eq. of $Pr(acac)_3H_2O$ in pentanol at 180 °C for 5 days, as shown in Scheme 2.17.

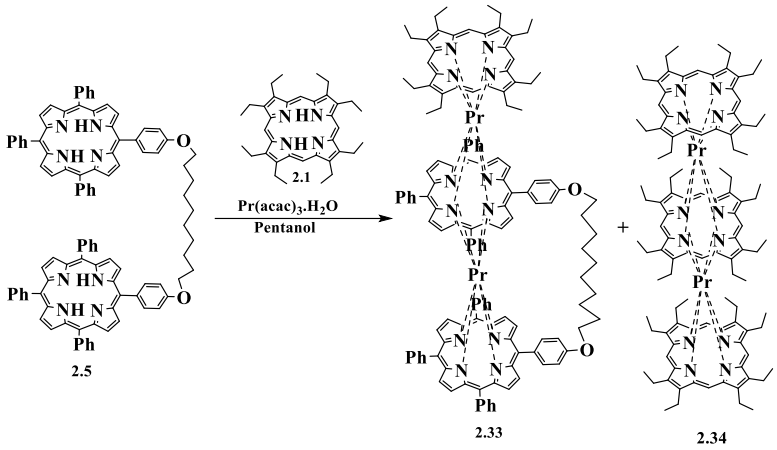

Scheme 2.17: Procedure to produce the Pr-TD **2.33**.

Analysis of the TLC spots by MALDI-TOF-MS revealed an unknown impurity at 673.18, and the homoleptic Pr-TD **2.34** at 1879.31 m/z plus a peak for unreacted starting material OEP **2.1** at 534.34 m/z, as shown in Figure 2.58.

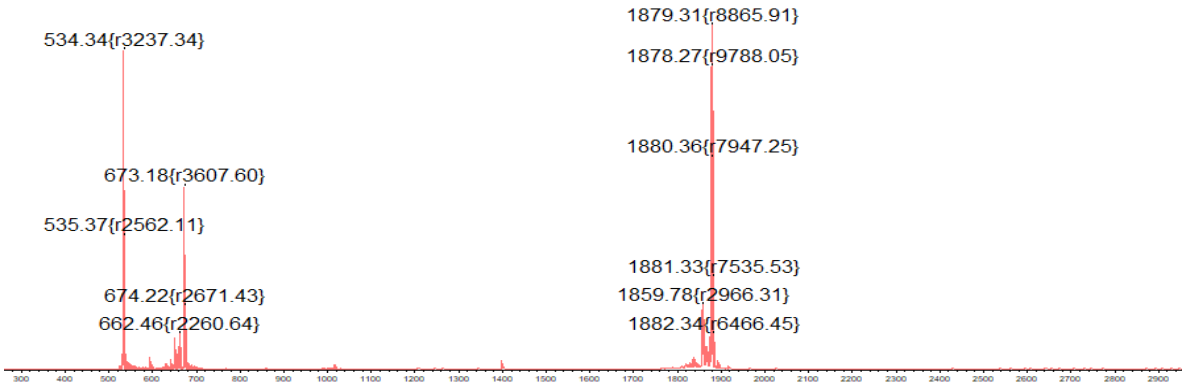

Figure 2.58: MALDI-TOF-MS of side product mixture from the Pr-TD **2.33** reaction.

Separation was achieved by column chromatography using a solvent system (3.3:100) EtOAc/Hexane mixture. The first fraction, Pr_2OEP_3 **2.34** (11%), appeared as a dark burgundy material; the second fraction was unreacted OEP, while the third fraction was the desired product, Pr-TD **2.33** (8%). ^{1}H NMR and 2D spectra are shown in Figures 2.59 & 2.60. The magnetic properties of praseodymium metals in compound **2.33** broaden the signals and add complexity to the spectra. Spectra taken at elevated temperatures in TCE showed little improvement, as shown in Figure 2.61.

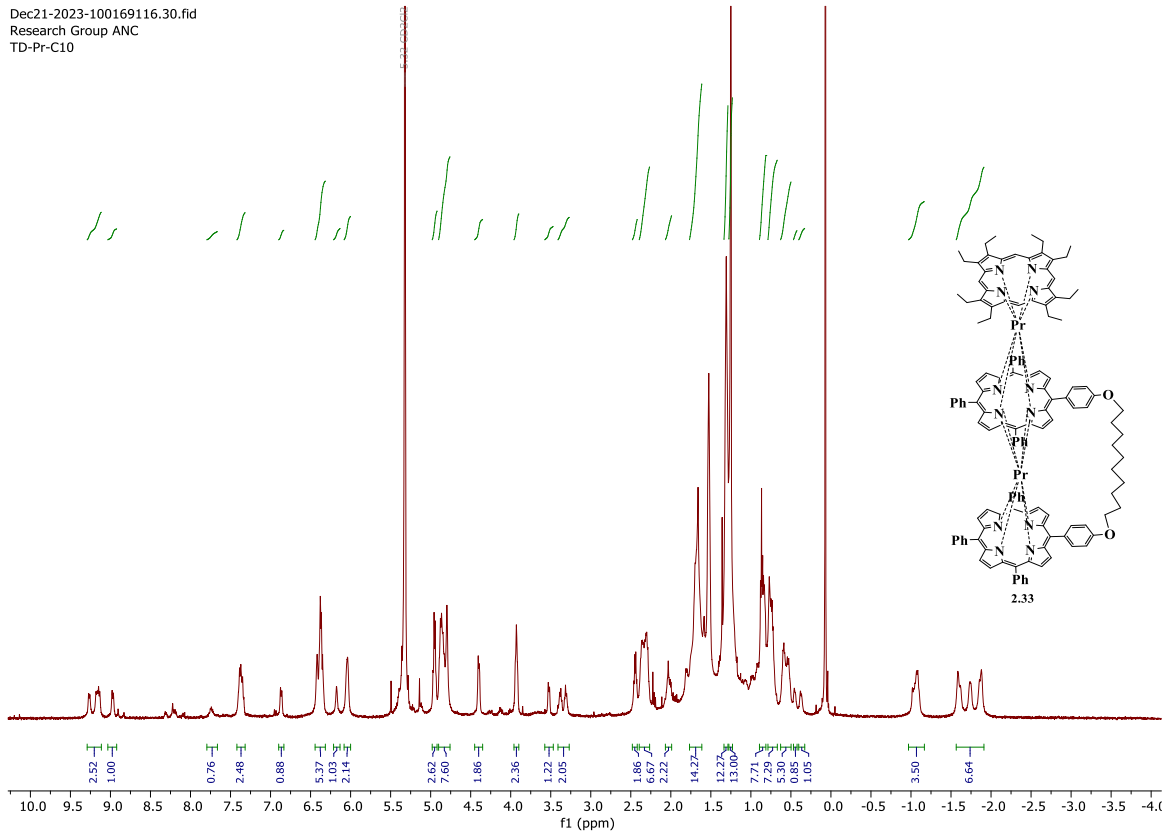

Figure 2.59: ^{1}H NMR of Pr-TD **2.33** in CD_2Cl_2.

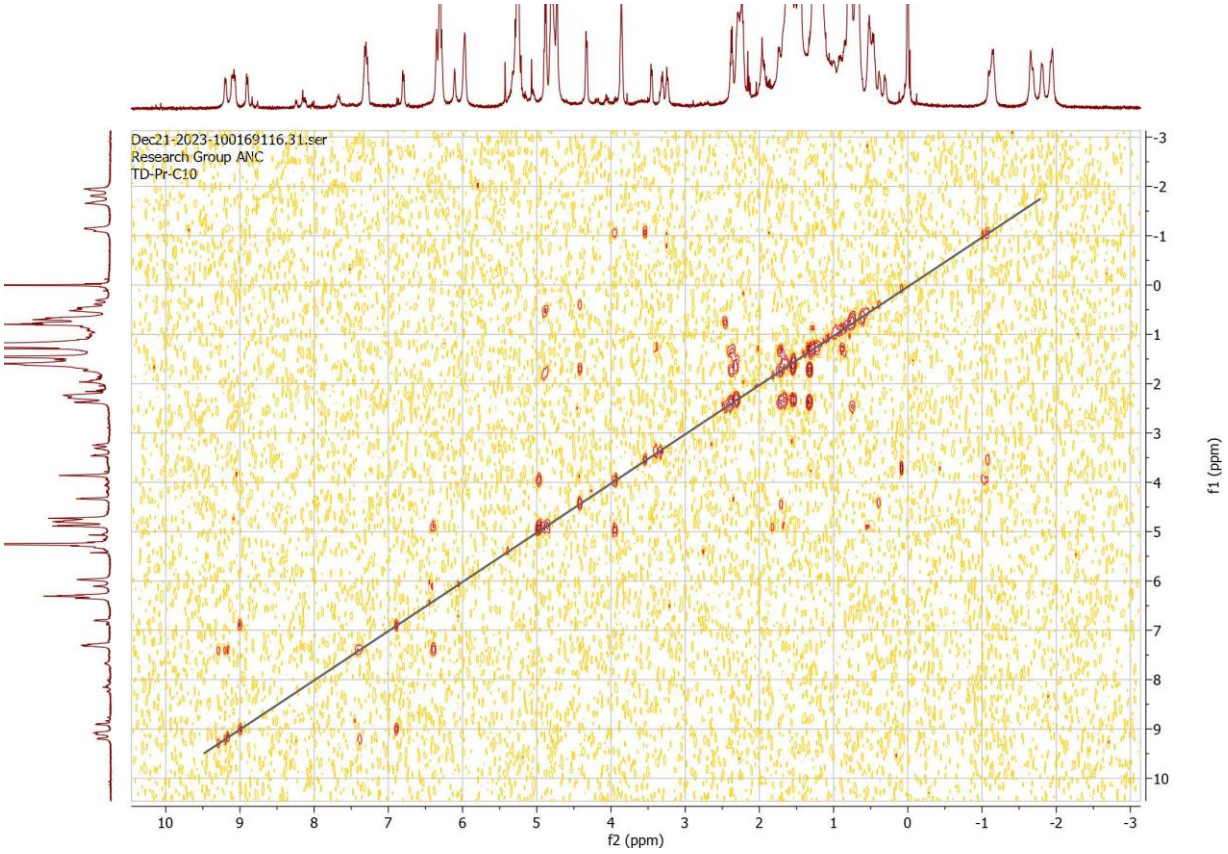

Figure 2.60: COSY experiment showing a cross peak in compound **2.33** in CD_2Cl_2.

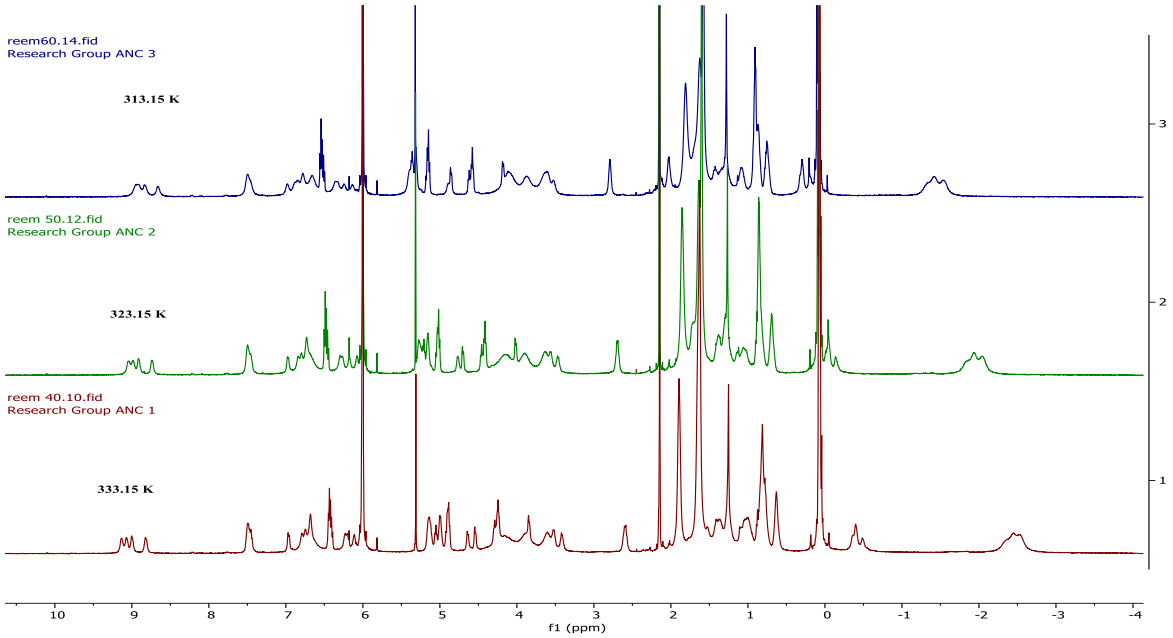

Figure 2.61: ^{1}H NMR spectra of Pr-TD **2.33** inTCE-d_2 using different temperatures of 40, 50 and 60 °C.

MALDI-TOF-MS confirmed the formation of Pr-C_{10} dyad triple decker as expected at 2208.0012 m/z, as shown in Figure 2.62.

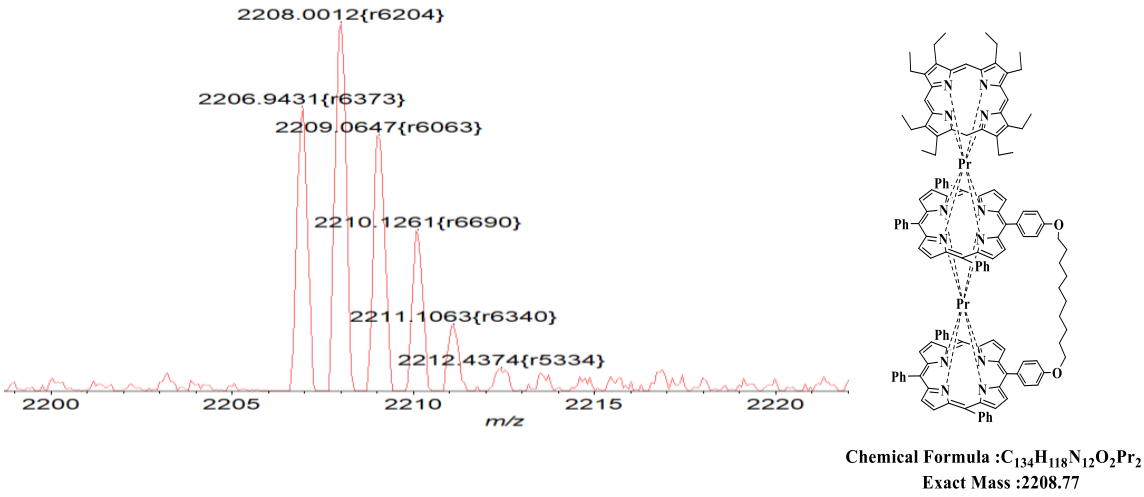

Figure 2.62: MALDI-TOF-MS of Pr-TD **2.33**.

We managed to grow a crystal that confirmed the (BAA) structure of Pr-TD **2.33** from DCM: MeOH: Isopropanol, as shown in Figure 2.63. The data confirm the BAA arrangement, but there is a lot of disorder in the chain and the OEP, preventing further detailed analysis of the structure.

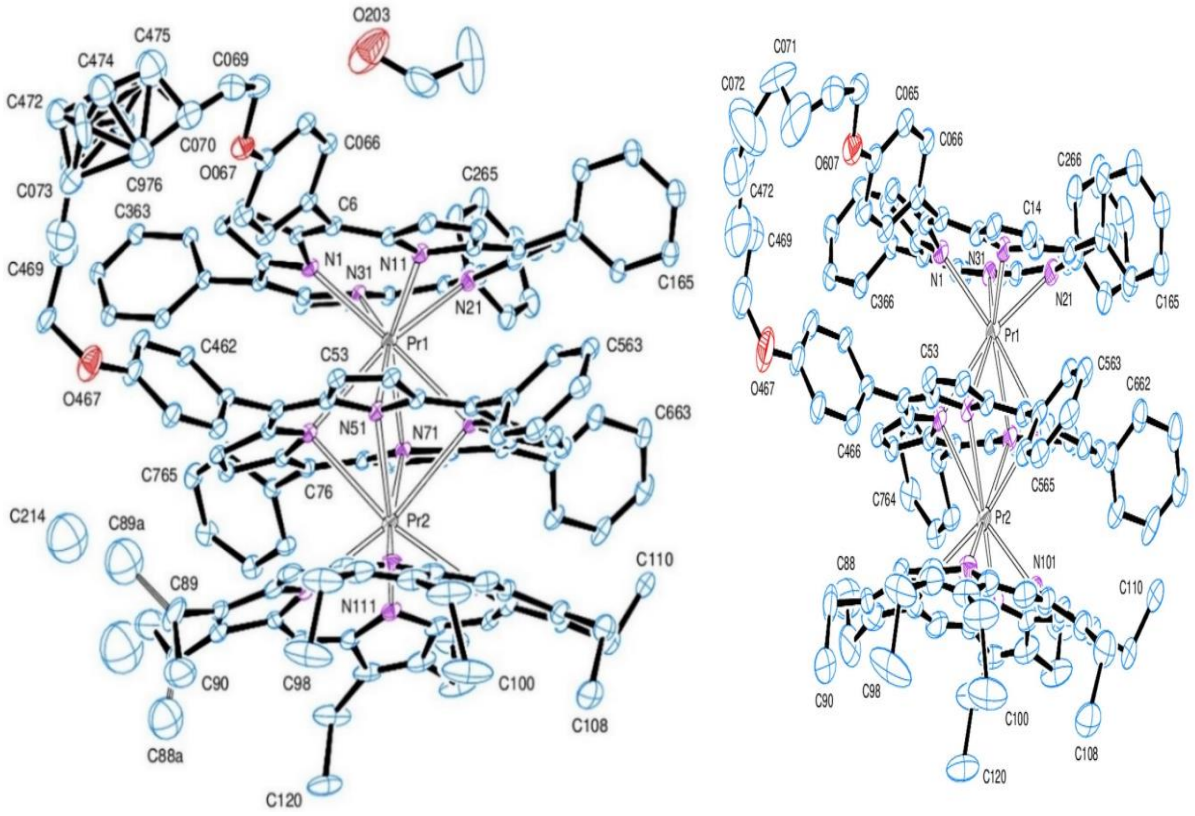

Figure 2.63: XRD structure for Pr-C_{10}dyad triple decker **2.33**

The indication of TD formation can be detected by UV-vis, and as shown in Figure 2.64, TD **2.33** exhibits an essentially identical spectrum to the corresponding La derivative.[31,32]

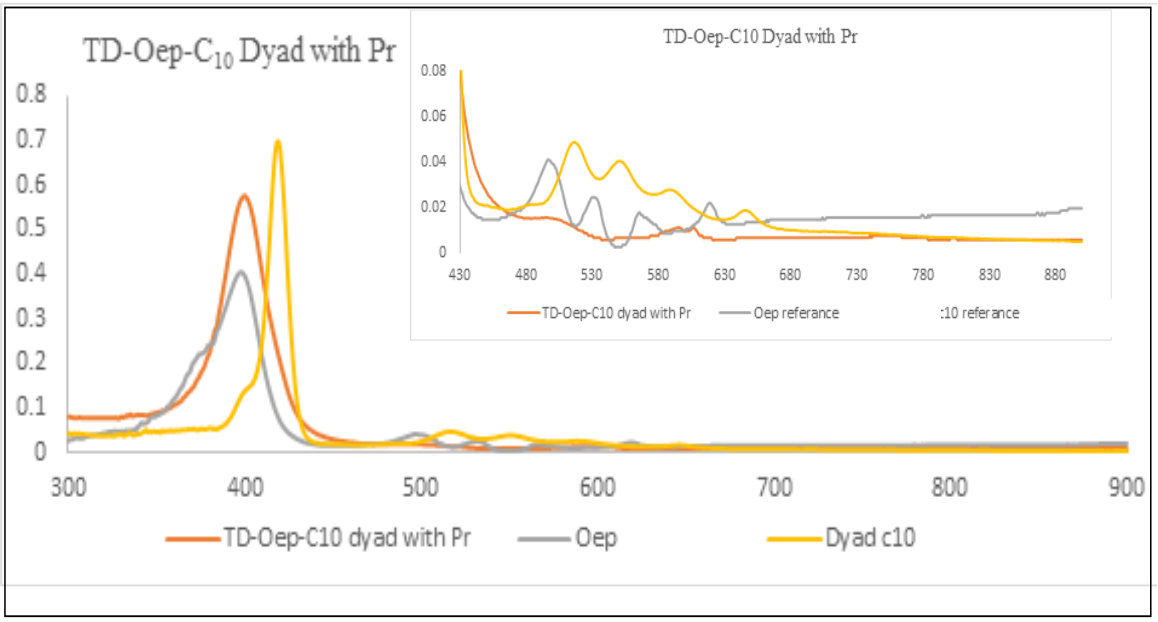

Figure 2.64: UV-vis absorption spectrum for TD **2.33**, **2.5** and **2.1** in DCM.

2.11.3 Synthesis of praseodymium-C_{12} porphyrin dyad triple decker 2.35:

TD **2.35** was prepared following identical conditions to that for the C_{10} derivative (Scheme 2.18). The desired product was obtained in 13% yield alongside the homoleptic Pr_2-OEP_3 **2.34** (9%). It was immediately apparent from the characterisation data that the longer chain dyad also produced the BAA arrangement.

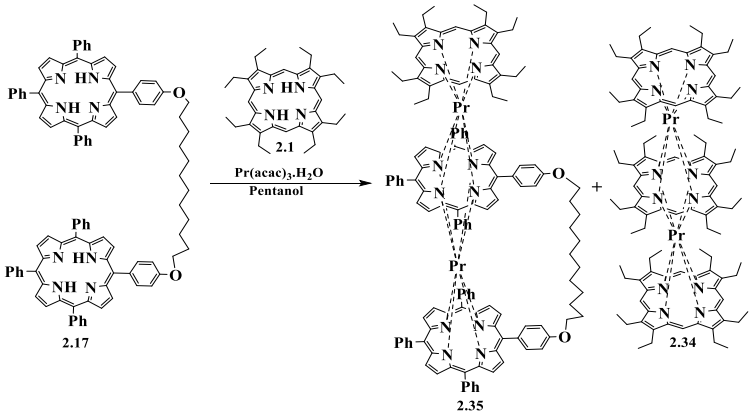

Scheme 2.18: Synthesis of Pr-TD **2.35**.

^{1}HNMR spectroscopy was carried out (Figure 2.65). Although similar to the C_{10} derivative (confirming the BAA structure), as we mentioned earlier, the magnetic properties of praseodymium metals in compound **2.35** broaden the signals and add to the complexity of the spectra, with several signals appearing upfield of 0 ppm.

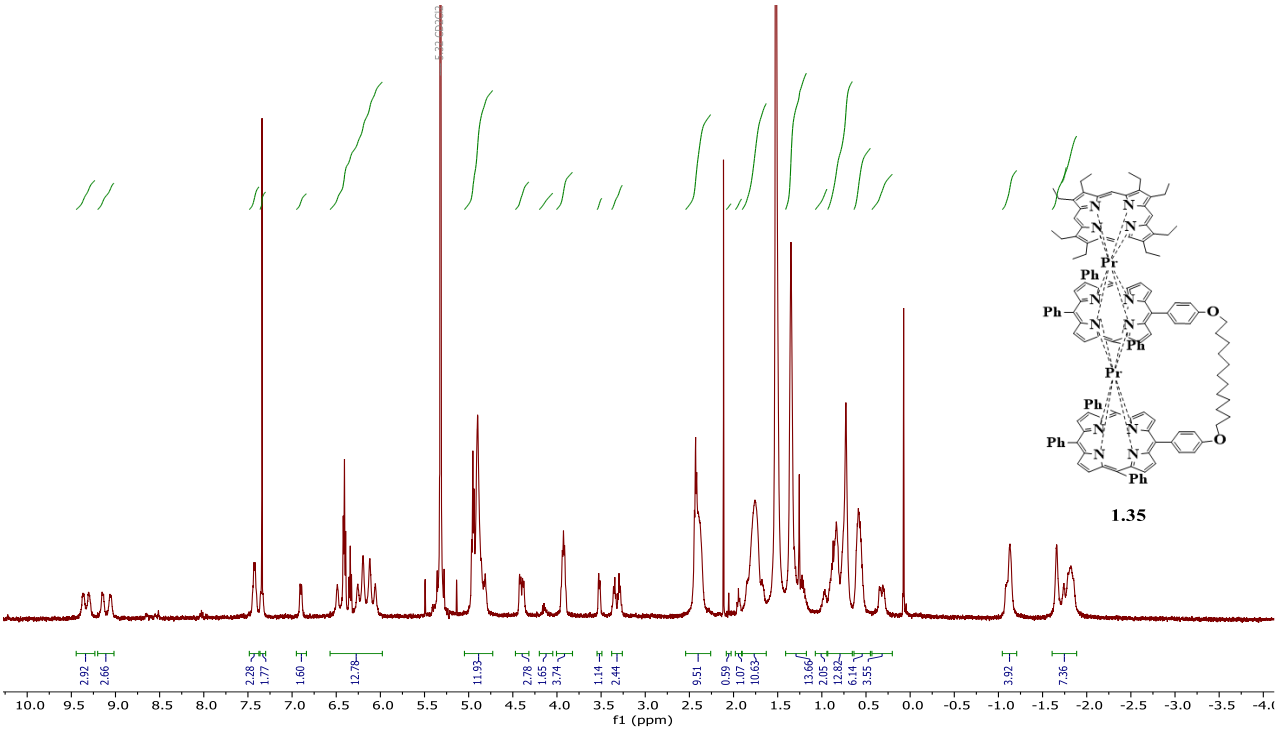

Figure 2.65: ^{1}H NMR of Pr-TD **2.35** in CD_2Cl_2.

We managed to grow a crystal from dichloromethane, methanol, and isopropanol through slow evaporation that confirmed the structure of Pr-TD **2.35,** and the XRD-structure of TD **2.35** (BAA) is shown in Figure 2.66.

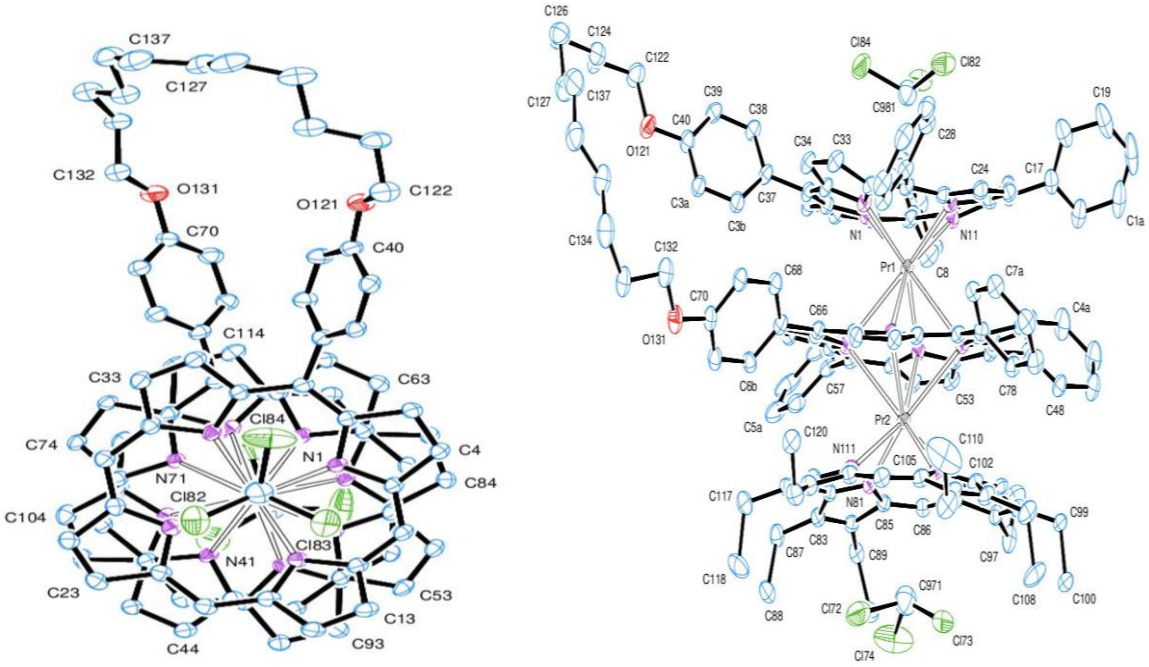

Figure 2.66: XRD structure for Pr-OEP-C_{12}-dyad triple-decker **2.35** (part structure shown in top view).

The X-ray crystal structure was analysed by our collaborator, Dr David Hughes, who provided the following comments. The triple-decker porphyrin molecule was clearly identified, as seen in Figure 2.66, from both the front and side aspects of the images. The three porphyrin molecules are organised on parallel planes, connected in a sandwich arrangement by praseodymium atoms. Each Pr atom is eight-coordinate, bonded to four central nitrogen atoms in porphyrin molecules.

Their coordination pattern is square antiprismatic, with the N4, N(1), N(11), N(21), N(31) square plane rotated approximately 10.8° about the Pr…Pr vector from the corresponding plane of N(81), N(91), N(101), N(111). The bridge connecting two porphyrin rings is located at the para position C(40) of one phenyl ring and the para position C(70) of a neighbouring phenyl ring, and the distance between O(121) and O(131) is 6.95 Å. The view along the Pr…Pr vector (showing the chloroform molecule of Cl(82-84) in the foreground, ethyl and phenyl substituent groups are not shown) clearly shows the offset arrangement of the three rings. MALDI-TOF-Ms of TD **2.35** showed a peak cluster at 2235.50 m/z (Figure 2.67).

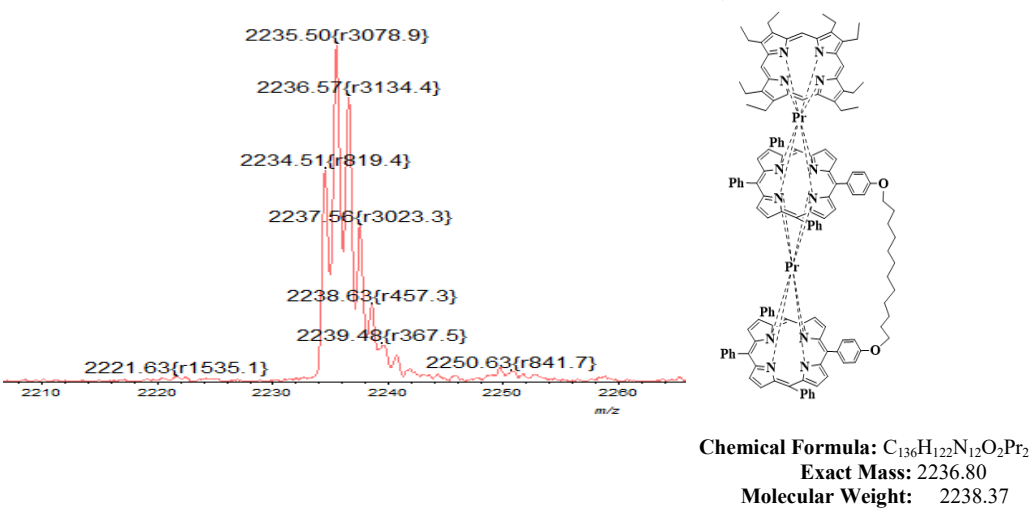

Figure 2.67: MALDI-TOF-MS of Pr-TD **2.35**.

2.11.4 Conclusion:

The synthesis of triple deckers with lanthanide paramagnetic metals has been achieved, but the characterisation was much more complicated than for the previous lanthanum triple decker. It appears that the twisted ethyl groups of the OEP ring in all the triple deckers we created make steric hindrance with porphyrin dimers **2.5** and **2.17**, and resulted in the BAA arrangement instead.

We thought that when we expanded the chains of porphyrin dimer, we might reduce the steric hindrance in the structure of the TDs, to enable formation of the ABA model, but this was not realised. The analysis of the crystallography proved the (BAA) model structure.

2.12 Attempts to produce triple deckers using other porphyrins with lanthanum metal:

We investigated different porphyrin cores, such as protoporphyrin (IX) **2.2**, protoporphyrin IX dimethyl ester **2.37**, octamethyl porphyrin **2.38**, and tetraphenyl porphyrin **2.10**, in attempts to make other triple-decker (ABA or BAA) structures.

2.12.1 Protoporphyrin (IX):

C_{10}-dyad **2.5**, 2 eq. $La(acac)_3H_2O$ and 1 eq. protoporphyrin (IX) **2.2** were mixed in pentanol in a sealed tube and heated at 165 ˚C (Scheme 2.19), and the reaction was monitored over 6 days. A mass corresponding to double-decker La-Dyad **2.25** was observed (olive-green spot with mass 1534.29 m/z, as shown in Figure 2.68), but there was never any evidence for a TD.

The same outcome was observed when we repeated the reaction using the same procedure but with the DBU as a base and when we changed the metal source from $La(acac)_3H_2O$ to $La(OTf)_3$.

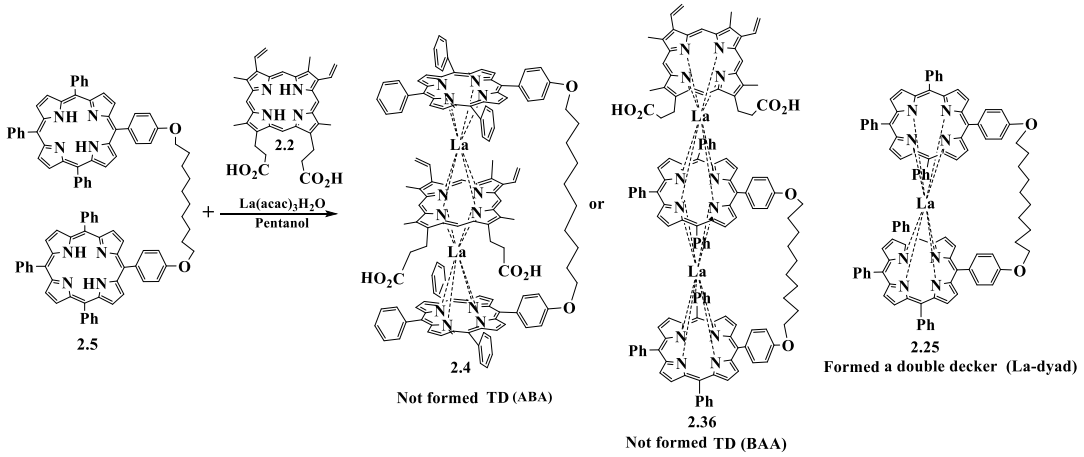

Scheme 2.19: Attempt to synthesise the desired La-TD **2.4** (ABA).

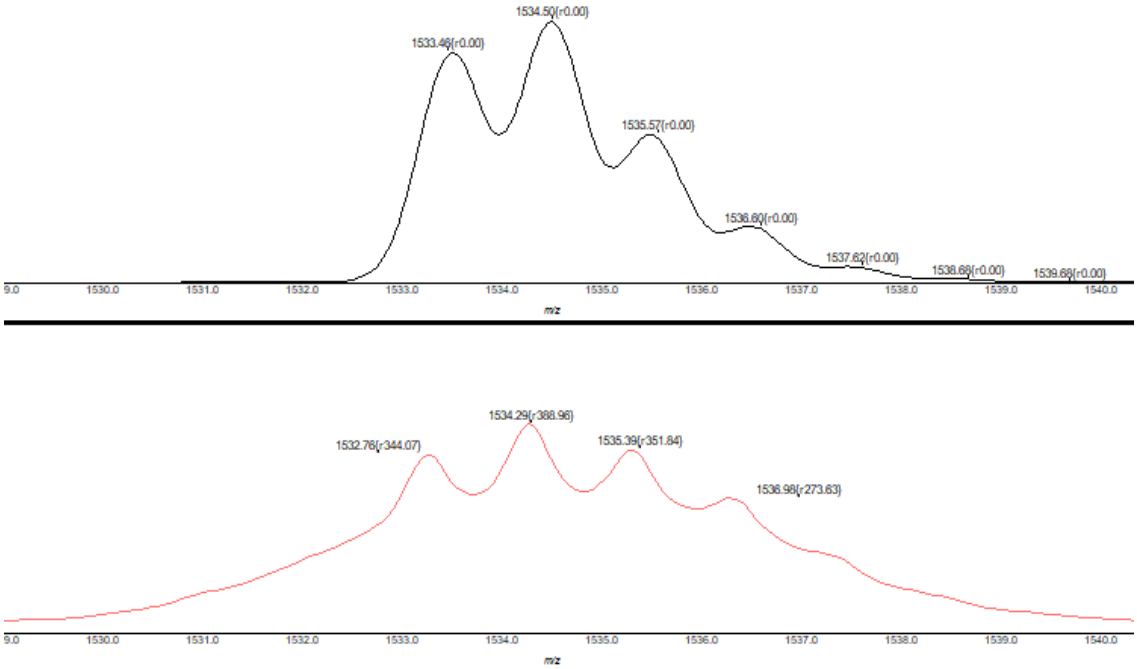

Figure 2.68: MALDI-TOF-MS of La-Dyad **2.25** (bottom) with its theoretical prediction (above).

2.12.2 Protoporphyrin IX dimethyl-ester:

We reacted C_{10}-dyad **2.5** with 2 eq. $La(acac)_3$ and 1 eq. of protoporphyrin IX dimethyl ester **2.37**, and the mixture was dissolved in 6 ml of pentanol in a sealed tube. The mixture was allowed to reflux at 180 °C for 5 days, monitoring throughout. Unfortunately, the outcome was the same as for protoporphyrin, with evidence for double-decker La-C_{10}dyad **2.25** but no TDs.

We noted in both cases the very low solubility of the protoporphyrin IX dimethyl ester, and it is possible that this prevents efficient TD formation.

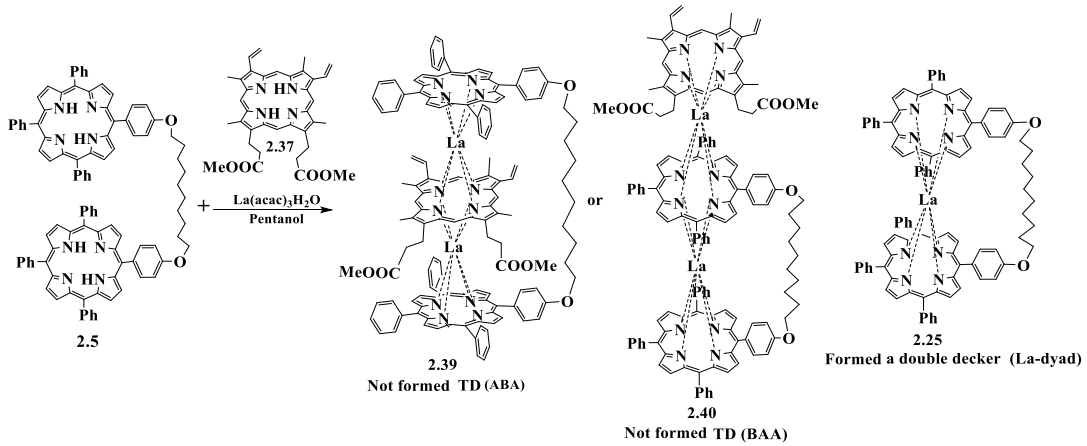

Scheme 2.20: Attempted synthesis of TD with protoporphyrin IX dimethyl ester and porphyrin dimer **2.5**.

2.12.3 Octamethyl porphyrin:

C_{10}-dyad **2.5**, 2 eq. of $La(acac)_3.H_2O$, and 0.9 eq. of octamethyl porphyrin **2.38** were dissolved in 6 ml of pentanol in a sealed tube and heated for 5 days at 180 °C, monitored by TLC. A new triple-decker spot was observed in TLC but in a low quantity.

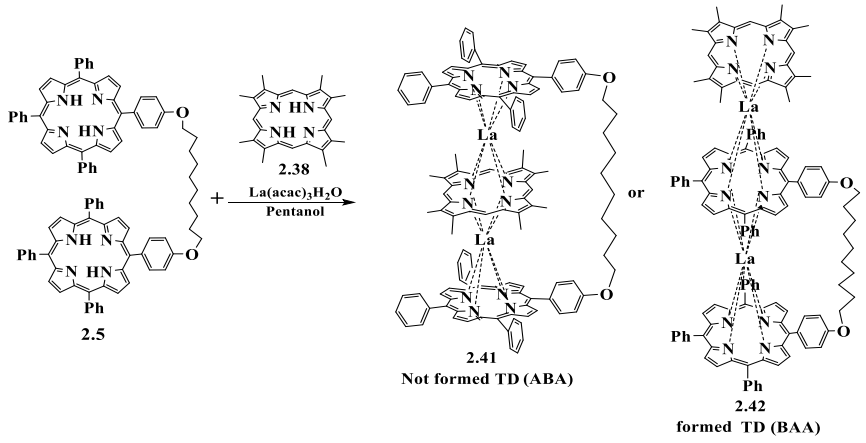

Scheme 2.21: Procedure to synthesise La-octamethyl porphyrin triple decker(s) with C_{10}-dyad **2.5**.

MALDI TOF-MS of the reaction mixture was taken (Figure 2.69), and the desired porphyrin TD mass was observed (2092.32 m/z). Unreacted OMP **2.38** (which also has low solubility) was observed at 421m/z **2.38**, and many unknown side products were also observed at 565 and 1588 m/z. The reaction showed no further improvement and was stopped.

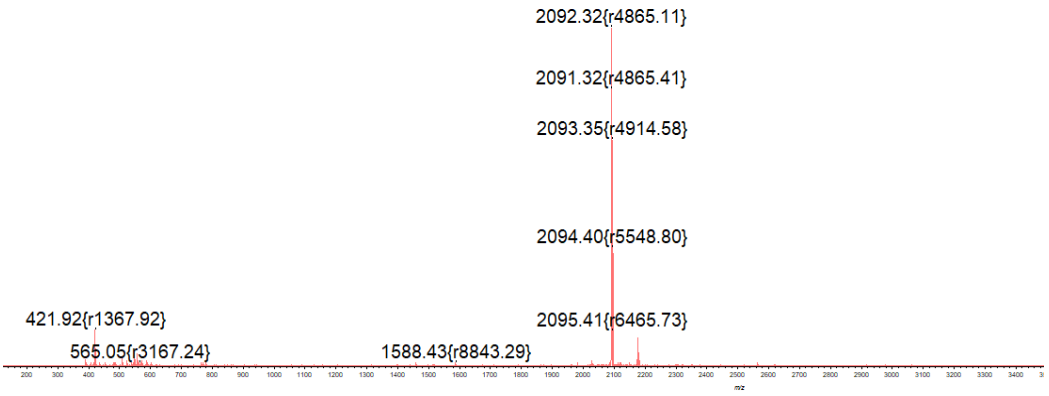

Figure 2.69: MALDI-TOF-MS of the sample of reaction after 5 days.

We isolated the TD by using DCM: Pet-ether (1:1 v/v) as the first solvent system for column chromatography, then changed the solvent system to (3:1) DCM: Pet-ether. The fourth fraction was the lanthanum TD, which was dark brown-green and gave a trace amount. The ^{1}H NMR spectrum (Figure 2.70) shows very broad signals and, at this stage, cannot be fully analysed. However, the signal at ≈ 4.56 ppm could be for OCH_2 as a triplet peak, indicating that the two extremities of the aliphatic chain have the same environment (symmetrical molecule). There was insufficient time to repeat this synthesis and obtain larger quantities of the TD.
However, this will be a valuable study for future work now that TD formation has been demonstrated.

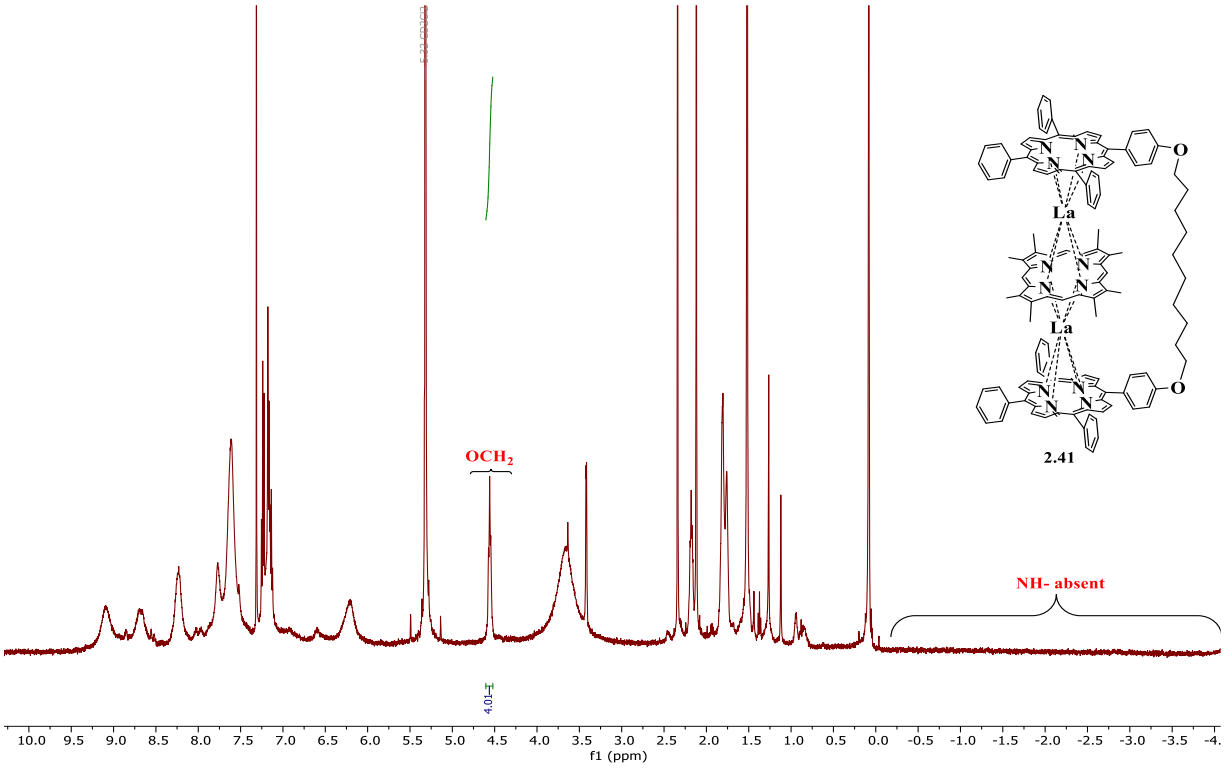

Figure 2.70: ^{1}H NMR spectrum OMP La-TD of octamethylporphyhrin with C_{10}-dyad **2.41** in methylene chloride-d2.

MALDI-TOF-MS shows a cluster at 2091.67 m/z, which proves that a La-TD was formed, as shown in Figure 2.71.

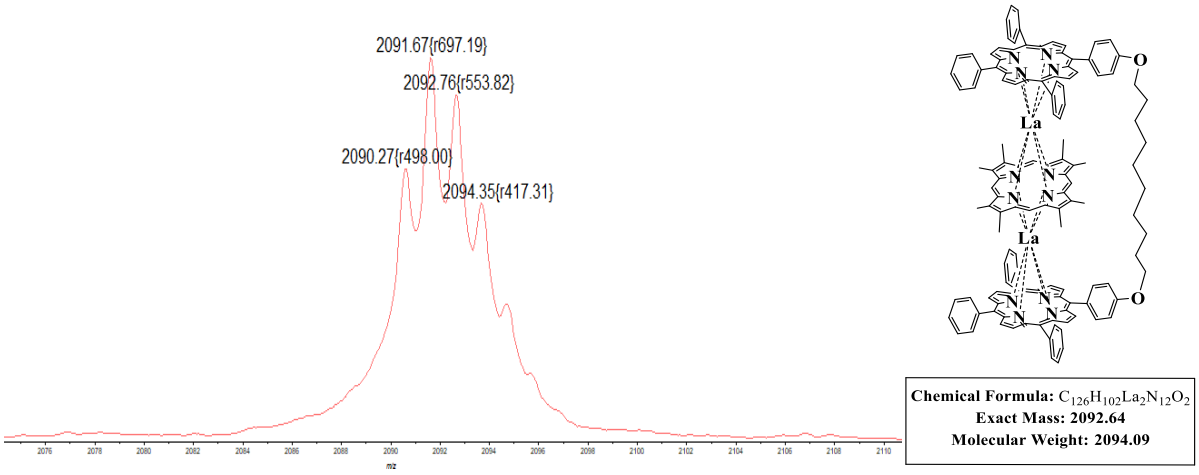

Figure 2.71: MALDI-TOF-MS of expected structure of OMP La-TD.

2.12.4 Tetraphenyl porphyrin:

Following the same process, we reacted C_{10}-dyad **2.5**, 0.9 eq. TPP **2.10** and 2 eq. of $La(acac)_3H_2O$ in 6 ml of pentanol at 180 °C in a sealed tube and refluxed the mixture for 5 days, monitored by TLC. MALDI-TOF-MS indicated the two starting materials, TPP **2.10** and C_{10}-dyad **2.5** plus unknown 751 m/z and homoleptic TD La_2TPP_3 **2.43** at 2115 m/z. The desired product of TD at 2286.18 m/z was also seen, as shown in Figure 2.72.

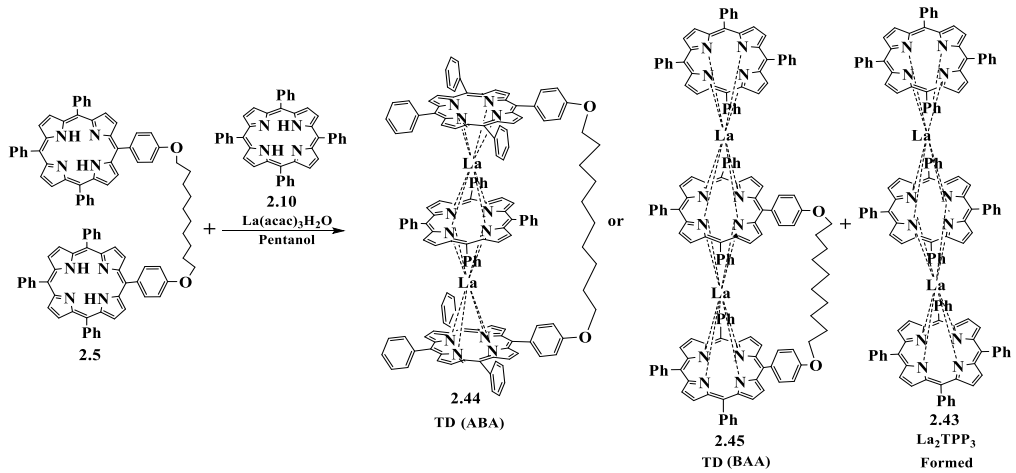

Scheme 2.22: Procedure to synthesise La-TD-TPP with C_{10}-dyad.

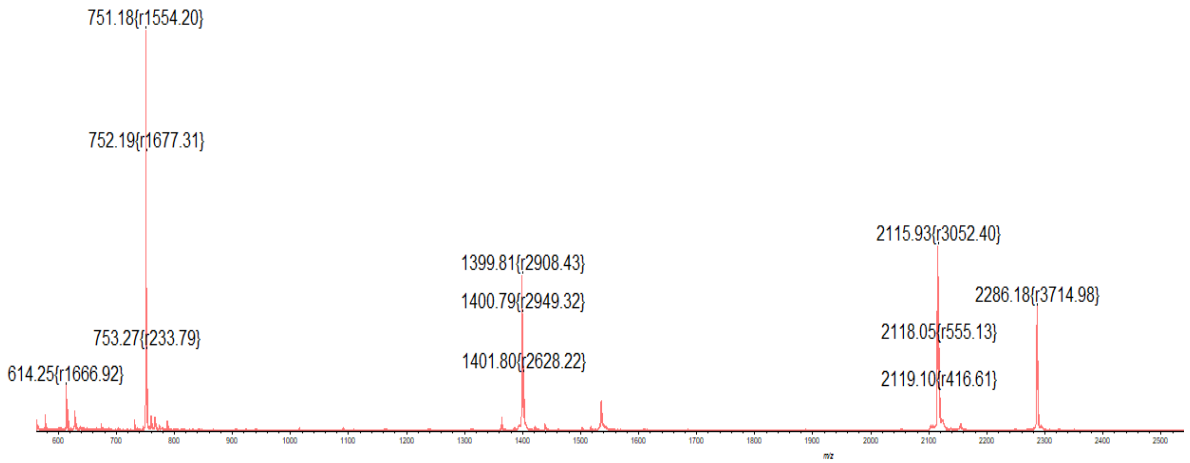

Figure 2.72: MALDI-TOF-MS of the reaction mixture after 12 hrs.

No further change was observed after 5 days. The crude dark brown-greenish solid was chromatographed on a silica gel column using DCM: Hexane (3:2 v/v), and the third main dark green-brown fraction contained the desired compound as indicated by the MALDI TOF-MS peak corresponding to 2287.42 m/z (Figure 2.73). However, there was insufficient time to purify this sample further and obtain clean NMR data to establish its structure.

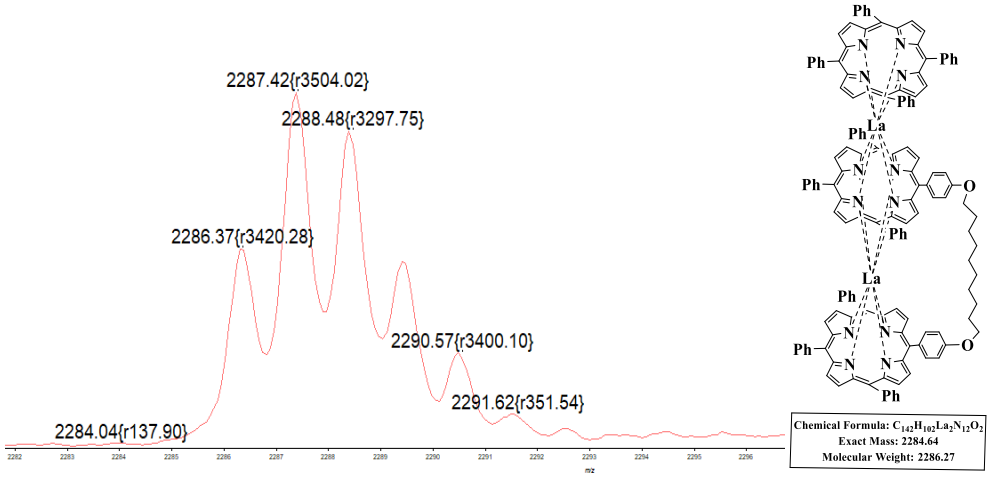

Figure 2.73: MALDI-TOF-MS of La-TD from TPP.

To conclude this part, we have identified that porphyrins like OEP behave differently to simple phthalocyanine in reactions with our linked porphyrin dimers: while Pc exclusively locates itself in the middle of the TD, the more hindered porphyrins lie only on the outside. Other porphyrin derivatives form TDs using the conditions developed in this work, but the low quantities and time restrictions have prevented their full characterisation.

2.13 Synthetic route for triad synthesis:

The project's second aim was a synthesis of triads for later use in triple-decker assemblies. We reasoned that the triad could be conveniently made by Steglich esterification between protoporphyrin (IX) **2.2** and TPP-OH **2.9**, as shown in Scheme 2.23.[33,34]

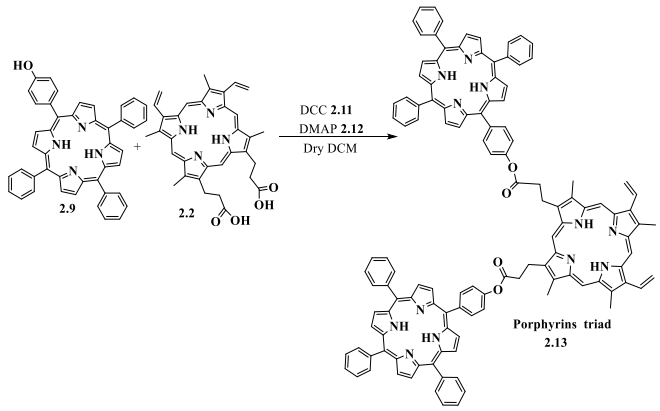

Scheme 2.23: Procedure to synthesise triad porphyrin **2.13**.

In this reaction, we used two methods, one at room temperature and another at 31–33 ℃, and we found similar results. In the first attempt, we reacted 1 eq. of protoporphyrin (IX) **2.2** with 2.2 eq. of TPPOH **2.9** and 0.1 eq. of DMAP with 2 eq. DCC in dry DCM at room temperature for 3 days under nitrogen. The reaction formed many unknown side products – 554, 1134, 1179, and 1819 – and unreacted starting material at 634 **2.9**, while there was a trace amount of porphyrin triad **2.13**, which was indicated by the MALDI-TOF-MS 1789.58 m/z.

In the second attempt, we used the same eqs of reactants, but we increased the reaction temperature from room temperature to ~30 ℃ for 15 min. After that, we changed the temperature to 38 ℃ for 3 hrs, then left the reaction between 31–33 ℃ overnight. The outcome was similar, with a faint spot corresponding to the desired trimer visible on TLC. However, all attempts to isolate it proved unsuccessful, in part because of the difficulty in separating from urea side products.

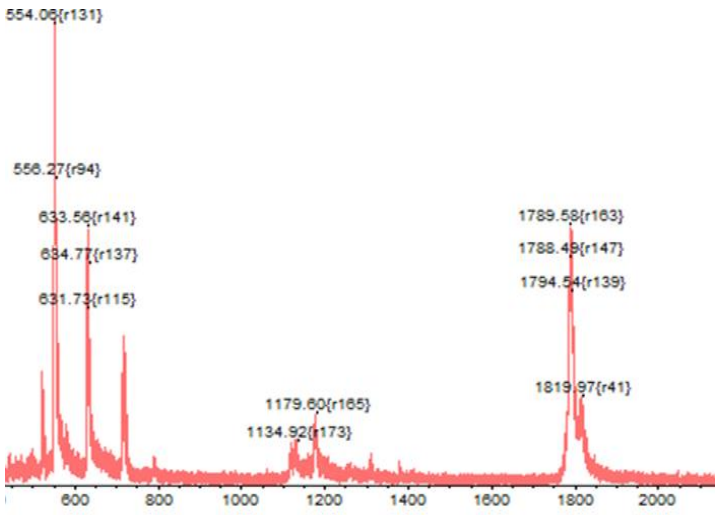

Figure 2.74: MALDI-TOF-MS of triad porphyrin reaction at 31–33 ℃.

2.14 Conclusions and future work:

We developed a procedure for the formation of lanthanide porphyrin triple deckers by using (2, 1, 0.9) equivalents for lanthanide, a dimer of porphyrin, and octaethylporphyrin, respectively; overall, this appears to be a very promising strategy for building up more complex arrays of TDs. In the synthesis of the starting materials, such as TPPOH **2.9** and dyad **2.5** or **2.17** (where a large part of this project's time was committed), it proved somewhat challenging to achieve adequate yield and isolation of the products, but the results are sufficiently conclusive to give confidence that TD formation is smooth and that unsymmetrical TD is formed with OEP **2.1**. This BAA arrangement is in direct contrast to the previously obtained results employing Pc, where the ABA arrangement is exclusively observed.

As we mentioned, the TD with the TPP **2.10** ring was produced, but in a trace amount and with the likely BAA arrangement due to steric hindrance, while the lanthanum triple-decker with OMP **2.38** ring could be the ABA isomer, indicated by the two extremities of the aliphatic chain having the same environment (symmetrical molecule). There was insufficient time to repeat this synthesis and obtain larger quantities of the TD, but the demonstration of TD formation and arrangement will provide a valuable pathway for future research. Also, we formed the porphyrin triad **2.13**, but we struggled to isolate it, and we failed to achieve a pure sample. For future work on the porphyrin triad, we suggest changing the conditions of the reaction, especially by using DIC instead of DCC, because it was challenging to remove DCU from the product. Also, we suggest using two solvents, such as dimethyl sulfoxide and dichloromethane (1:1, V/V DMSO: DCM[35]), to try to dissolve the protoporphyrin (IX) reactant because, as we mentioned previously, protoporphyrin (IX) **2.2** has a very low solubility

Chapter (3): Experimental Methods

3. Experimental Methods:

3.1 Physical measurement:

^{1}H NMR spectra were recorded either at 400 MHz on an Ultrashield Plus^{TM} 400 spectrometer or 500 MHz on a Bruker Ascend^{TM} 500 spectrometer in 5 mm diameter tubes using deuterated Chloroform, DCM, DMSO, Acetone, Toluene, and TCE. Signals are recorded using residual solvent as a reference and are expressed in ppm. The coupling constant J is provided in Hertz (Hz). All spectra were taken at ambient temperature, apart from the octaethylporphyrin triple-decker with Pr which used three different temperatures to improve the signal of the product. Column chromatography was performed at ambient temperature using Fluka or Merck silica gel 60 (70-230 mesh) at ambient or low pressure, and the ratios were given as v/v. Thin layer chromatography (TLC) was performed on Merck aluminium-backed silica gel 60 F254 coated plates and visualised by a UV light at 254 nm. Direct sample deposition was used to record mass spectra on am Axima MALDI-TOF device. Melting points were observed and recorded using a Reichert Thermovar microscope with thermobaric-based temperature control. UV-Vis spectra were collected using a Perkin-Elmer UV-Vis spectrometer Lamda XLS.

3.2 Reagents, solvents and reaction conditions:

Unless otherwise noted, all reagents and solvents were analytical grade, commercially received, and used without purification. Unless otherwise noted, SLR-grade solvents were used without drying. Magnesium sulphate dried organic layers. A reduced-pressure Büchi rotatary evaporator evaporated solvent.

3.3 Synthesis 5-(p-hydroxyphenyl)- 10, 15, 20 triphenyl porphyrin[4,5] 2.9:

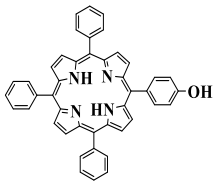

2.9

The technique proposed by Adler,[4,5] was followed using a combination of aldehydes but with several modifications. Both p-hydroxybenzaldehyde **2.7** (1eq, 7.0 g, 57 mmol) and benzaldehyde **2.6** (3eq, 17.5 g, 172 mmol) were dissolved in propionic acid (460 ml) and subjected to reflux. Freshly distilled pyrrole **2.8** (4eq, 15 g, 215 mmol) was added once to the refluxing liquid and refluxed for 1.5 h. Upon reaching room temperature, the crude mixture was selectively precipitated with MeOH (400ml) and filtered under suction to provide a purple solid. The crude precipitate underwent purification using column chromatography, employing a column length of < 8 cm. Isolation was achieved by using (3:1) DCM: Pet-ether to remove TPP **2.10** fraction, then by increasing the polarity of the solvent system gradually to (4:1 then 100% DCM) to remove all TPPOH **2.9** to gain (1.836 g, 5.1%) yield. **M.P.** >350 ℃.

^{1}H NMR (400 MHz, Chloroform-*d*) δ 8.88 (d, *J* = 4.5 Hz, 2H), 8.84 (d, *J* = 4.5 Hz, 6H), 8.23 – 8.19 (m, 6H), 8.08 (d, *J* = 8.5 Hz, 2H), 7.80 – 7.71 (m, 9H), 7.22 (d, *J* = 8.5 Hz, 2H), 5.18 (s, 1H) -OH, -2.77 (s, 2H) -NH.

MS (MALDI-TOF) : m/z = 630.94 [M^+]. UV-vis (DCM)/nm: 418, 515, 550, 591 and 648. Chemical Formula: $C_{44}H_{30}N_4O$.

3.4 Synthesis of tetraphenyl porphyrin 2.10:

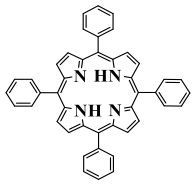

2.10

The compound was collected as a side product from a previous reaction and obtained as a purple solid at (6.450 g, 18 %).^{1}H NMR (400 MHz, Chloroform-*d*) δ 8.85 (s, 8H), 8.22 (d, *J* = 7.8 Hz, 8H), 7.80 – 7.72 (m, 12H), -2.77 (s, 2H). **M.P.** > 350 ℃. (MALDI-TOF): m/z = 614.22 [M^+]. Chemical Formula: $C_{44}H_{30}N_4$. UV-vis (DCM)/nm: 417, 514, 549, 590, 648.

3.5 Synthesis of porphyrin C_{10} dyad (TPP-O-$(CH_2)_{10}$-O-TPP) 2.5:

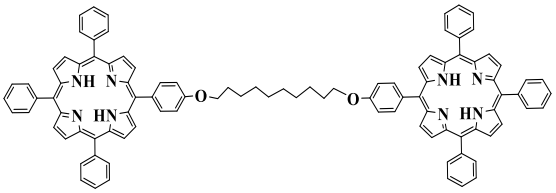

2.5

Two good methods to prepare **2.5** were found, the first condition gave the best yield with a long time, around two weeks and needed only recrystallisation to get a pure product of **2.5,** while the second condition gave a good yield with a short time but needed a column chromatography to collect a pure C_{10}-dyad.

1. A mixture of 1,10-dibromodecane (1eq, 0.24g, 0.79 mmol) and TPP-OH **2.9** (2eq, 1.0 g, 1.6 mmol) was prepared in dry acetone (12 ml). K_2CO_3 (0.44 g, 3.1 mmol) was added to the solution, and the combination was heated at 70 ℃ for 12 days in a sealed tube. Subsequently, the solvent was removed, and the residue was dissolved in DCM and washed with water. The organic layer was evaporated and purified by two slow and careful recrystallisation from a mixture of DCM: MeOH, resulting in the pure product **2.5** as a solid with a purple colour (0.984g, 88%).

2. A mixture of 1,10-dibromodecane (1eq, 0.38 g, 1.3 mmol) and TPP-OH **2.9** (1.6 g, 2.5 mmol) was prepared in DMF (23 ml) and K_2CO_3 (1.5eq, 0.52g, 3.7 mmol) was added, and the combination was heated at 70 ℃ for 2 hrs and 90 ℃ for another 2 hrs. In this reaction, we noticed the reaction is finished when the colour of the reaction changes from reddish brown to bright purple. The crude reaction was mixed with 250 ml of water and 25 ml of MeOH, and the solid was sonicated for 15-30 min. After filtering, we recovered the solid and purified the C_{10}-dyad using (3:2) DCM: Pet-ether. ($TPPOC_{10}H_{19}$) **2.16** was the first fraction, and the target product **2.5** was the second (1.15 g, 64%). **M.P.** > 300 °C.

^{1}H NMR (500 MHz, $CDCl_3$): δ 8.89 (d, *J* = 4.5 Hz, 4H) and 8.83 (d, *J* = 4.5 Hz, 12H) Hβ; 8.21 (dd, *J* = 7, 2 Hz, 12H) *HoPh*; 8.12 (dd, *J*= 7, 2 Hz, 4H) *HoPh'*; 7.78 – 7.71 (m, 18H) *HmPh* and *HpPh*; 7.29 (dd, *J*= 7, 2 Hz, 4H) *HmPh'*; 4.28 (t, *J* = 6.5 Hz, 4H) O-CH_2-; 2.05 – 1.99 (m, 4H); 1.71– 1.65 (m, 4H); 1.53 (s, 8H) ; -2.76 (s, 4H) NH. MS (MALDI-TOF): m/z =1399.59 [M^+]. UV-vis, (DCM)/nm: 419, 516, 551, 591 and 648. Chemical Formula: $C_{98}H_{78}N_8O_2$.

3.6 Synthesis of 5-(10'-bromo-decyloxyphenyl)-10,15,20-triphenyl porphyrin (TPP-OC$_{10}$Br) 2.15:

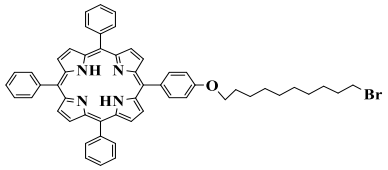

2.15

TPP-OH **2.9** (1eq, 0.1 g, 0.159 mmol) and (1.2eq, 0.057 g, 0.190 mmol) 1,10-dibromodecane and K_2CO_3 (2.5eq, 0.055 g, 0.3975 mmol) were dissolved in dry-acetone (15 ml) and the mixture reacted together at 70 ℃ for 34 hrs in a sealed tube. The crude mixture was then precipitated with 50 ml of distilled water and filtered. The solids obtained were washed with MeOH to recover a purple solid. After column chromatography of the solid over silica gel using THF: Pet-ether (1:3) (v/v) as eluent and recrystallisation from DCM/MeOH, the title compound was obtained pure (0.0576 g, 42%). **M.P.** > 300 °C.

^{1}H NMR (500 MHz, $CDCl_3$) δ 8.89 (d, *J* = 4.5 Hz, 2H) and 8.84 (s, 6H) Hβ; 8.22 – 8.19 (m, 6H), 8.12 (dd, *J* = 2.0, 6.5 Hz, 2H) H_{oPh}; 7.82 – 7.70 (m, 9H) and 7.28 (dd, *J* = 2.0, 6.5 Hz, 2H) H_{pPh} and H_{mPh} ; 4.25 (t, *J* = 7 Hz, 2H) O-CH_2, 3.44 (t, *J* = 7 Hz, 2H) -CH_2-Br , 2.01 – 1.96 (m, 2H), 1.91 – 1.86 (m, 2H), 1.64 – 1.60 (m, 2H), 1.50 –1.35 (m, 10H), -2.75 (s, 2H) -NH. MALDI-TOF: m/z= 850.53 [M^+]. UV-vis, (DCM)/nm: 418, 516, 551, 593 and 651 nm. Chemical Formula $C_{54}H_{49}BrN_4O$.

3.7 Synthesis of porphyrin C$_{12}$-dyad (TPP-O-(CH$_2$)$_{12}$-O-TPP) 2.17:

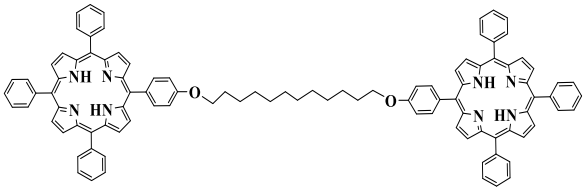

2.17

A mixture of 1,12-dibromododecane (1eq,0.244g, 0.744 mmol) and TPPOH **2.9** (2eq, 0.937g, 1.487 mmol) was dissolved in MEK (25 mL). An excess of potassium carbonate (7eq, 1.44 g, 10.41 mmol) and a catalytic amount of potassium iodide (2eq, 0.494 g, 2.974 mmol) was added to the mixture and refluxed under N_2 for 67 hrs. The product was purified by column chromatography on silica gel using DCM: Pet-ether (3:2) (v/v) as eluent. The second fraction was C_{12}-

dyad **2.17** and recrystallization from DCM/MeOH gave the titled compound as a purple solid (0.754 g, 70%). **M.P.** 312-315 ℃.

^{1}H NMR (500 MHz, $CDCl_3$) δ 8.89 (d, *J* = 4.5 Hz, 4H) and 8.83 (d, *J* = 4.5 Hz, 12H) H_β; 8.21 (dd, *J* = 8.5, 1.6 Hz, 12H) H_{oPh}; 8.11 (d, *J* = 8.5 Hz, 4H) H_{oPh}'; 7.80 –7.68 (m, 18H) H_{mPh} and H_{pPh}; 7.28 (d, *J*= 8.5 Hz, 4H) H_{mPh}'; 4.26 (t, *J* = 6.4 Hz, 4H) -O-CH_2 ; 2.02 – 1.96 (m, 4H) -CH_2-; 1.68 – 1.62 (m, 4H); 1.53 (s, 12H) -CH_2-; -2.76 (s, 4H) -NH. (MALDI-TOF-MS): m/z = 1428.65[M^+]. UV-Vis (DCM)/nm: 418, 515, 550, 591 and 647. Chemical Formula: $C_{100}H_{82}N_8O_2$.

3.8 Synthesis of metal-free phthalocyanine[15,16] 2.21:

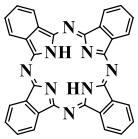

2.21

Using lithium as a template, a standard method is followed. A solution of phthalonitrile **2.20** (0.5 g, 4 mmol) in 1-pentanol (6 ml) was heated to 120 °C, then lithium (0.05 g, 7.2 mmol) was added, and the reaction proceeded for 1 hr. Next, (10 ml) of acetic acid was added and refluxed for another hour. Next, the reaction mixture was cooled to room temperature, methanol (110 ml) was added to precipitate the result, and the pure phthalocyanine solid was recovered by vacuum filtering (0.253g, 49%).

M.P. > 300 ℃. MS (MALDI-TOF): m/z = 514.15 [M^+]. UV-Vis, (THF) / nm: 377, 654, 690. Chemical Formula: $C_{32}H_{18}N_8$. Further characterisation was not possible because of the significant insolubility in organic solvents.

3.9 Synthesis of triple-decker[1,6] 2.22:

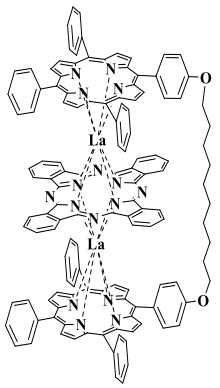

2.22

In use **2.5** (0.123 g, 0.0879 mmol), with 2 eq. of La(acac)$_3$H$_2$O (0.0767 g, 0.1758mmol) and 1 eq. of phthalocyanine **2.21** (0.045 g,0.0879 mmol) in octanol at 200 °C under N_2, all mixture refluxed together for 3 days and 10 hrs. The solvent was evaporated by distillation under a vacuum. The resultant products were then isolated using column chromatography, employing silica gel as the stationary phase. The obtained solids were then isolated using column chromatography using silica gel and eluted with a mixture of dichloromethane and hexane (3:2 v/v) as eluent, the first fraction containing the title product of **2.22** and it has a greenish-brown colour. Discovered a new solvent system (1:1) Toluene: Hexane as eluent in alumina oxide that isolates Lanthanum triple-decker **2.22**. The TD was the first greenish brown fraction containing the desired product **2.22**, and we recovered all a dark greenish brown solid (0.1g, 50%).

^{1}H NMR (500 MHz, $CDCl_3$) δ 10.08 (d, *J* = 7.2 Hz, 2H) H_{oiPh}'; 9.99 (t, *J* = 7 Hz, 6H) H_{oiPh}; 9.36 (dd, *J* = 5, 3 Hz, 8H) Hpc1; 8.48 – 8.40 (m, 6H) H_{ooPh}; 8.29 (dd, *J* = 5, 3 Hz, 8H) Hpc2; 7.98 (d, *J* = 6.5 Hz, 2H) H_{ooPh}'; 7.86 – 7.77 (m, 6H) H_{miPh}; 7.31 (d, *J* = 4 Hz, 4H) Hβ; 7.26 – 7.21 (m, 18H) Hβ and H_{pPh} ; 6.87 (d, *J* = 6.0 Hz, 2H) H_{miPh}'; 6.73 (d, *J* = 7Hz, 2H) H_{moPh}'; 6.64 (t, *J* = 7 Hz, 6H) H_{moPh}; 4.59 (t, *J* = 7 Hz, 4H) -O-CH_2- ; 2.33 – 2.23 (m, 4H) -CH_2-; 1.92 (s, 8H) -CH_2- ; 1.81 (s, 4H) -CH_2-. MS (MALDI-TOF): m/z = 2184.42. UV-vis, (DCM)/nm: 360, 423, 486, 549, 603. Chemical formula: $C_{130}H_{90}La_2N_{16}O_2$.

3.10 Synthesis of lanthanum double-decker 2.25:

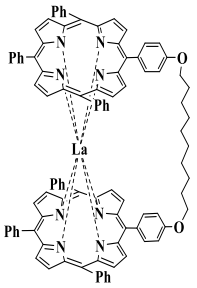

2.25

We prepared La-C_{10}-Dyad **2.25** by using 1 eq. of dyad **2.5** (0.12 g, 0.0858 mmol), 1.1 eq. of La(acac)$_3$.H_2O (0.045g, 0.0943 mmol), 1 ml from DBU in 5 ml pentanol in a sealed tube at 180 °C, reacted together for 5 days. The solvent was evaporated by distillation under a vacuum. ^{1}H NMR & UV-vis are not achieved due to the low solubility of the compound **2.25**, as a dark olive-green solid (0.769 g, 58%). MALDI-TOF: m/z =1534.46 [M^+]. $C_{98}H_{75}LaN_8O_2$.

3.11 Synthesis of homoleptic porphyrin triple-decker[27,28,29] 2.27:

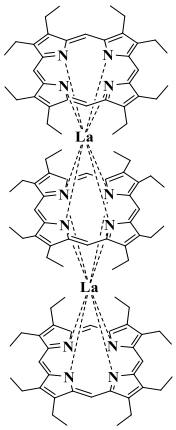

2.27

Octaethyl porphyrin **2.1** (0.3 g, 0.561 mmol) and $La(acac)_3H_2O$ (0.96 g, 2.2 mmol) were reacted in TCB (50 ml) at reflux together for 1 hr. We observed that the colour of the reaction changed from burgundy to brown, and left the reaction to reflux for 41 hrs as the total reaction time. Stopped the reaction after it got cold, then added MeOH and left it overnight. After that, the solid was filtered off and collected, which mainly consisted of unreacted **2.1** and side products, while the solution was a mixture of **2.27** and a tiny amount of OEP. The solvent system was (3:2) DCM: Pet-ether as eluent to isolate La_2-OEP_3 by column chromatography on silica gel. The third fraction was the desired compound TD, which has a dark burgundy colour. Recrystallised **2.27** by using (1:1) DCM: MeOH and gave a dark black crystal (0.09 g, 5%).

^{1}H NMR (500 MHz, Toluene-d_8) δ 8.50 (s, 8H) external-meso-H, 8.41 (s, 4H) internal-meso-H, 4.25 (q, J = 7.8 Hz, 16H) internal-8-CH_2, 3.93 (dq, J = 15.8, 7.8 Hz, 16H) internal-CH, 3.48 (dq, J = 15.6, 7.8 Hz, 16H) external-CH, 2.75 (t, J = 8.0 Hz, 24H) internal-CH_3, 1.15 –1.04 (t, 48H) external-CH_3. MS-(MALDI-TOF): m/z = 1874.87. Chemical formula: $C_{108}H_{132}La_2N_{12}$.

3.12 Synthesis of Lanthanum porphyrin triple-decker 2.29:

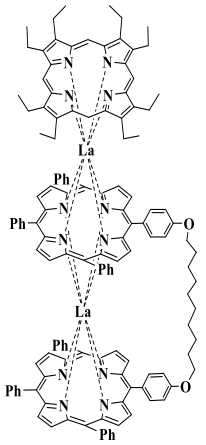

2.29

Prepared using procedure (A) for La-porphyrin triple-decker:

C_{10}-dyad **2.5** (0.114 g, 0.0814 mmol) was mixed with 2 eq. (0.077 g, 0.163 mmol) of lanthanum (III) acetylacetonate hydrate and 0.9 eq. of Octaethyl porphyrin **2.1** (0.039 g, 0.073 mmol) in 5 ml pentanol at 180 °C for 5 days in a sealed tube. After that, the solvent was removed under a stream of nitrogen. The crude was separated by column chromatography through silica gel using EtOAc/Hexane (3.3:100 v/v) as eluent, and the third fraction was a desired product of **2.29** containing the title product was collected as a reddish brown solid (0.021g, 12%).

Prepared using procedure (B) for La-porphyrin triple-decker:

C_{10} porphyrin dyad **2.5** (0.1055 g, 0.0754 mmol) was mixed with 2 eq. (0.0712 g, 0.151 mmol) of lanthanum (III) acetylacetonate hydrate and 0.9 eq. of OEP **2.1** (0.0363 g, 0.0678 mmol) in 5 ml pentanol at 165 °C for a week in a sealed tube. Then, the solvent was removed under a stream of nitrogen. The crude separated by column chromatography through silica gel using EtOAc/Hexane or EtOAc/Pet-ether (3.3:100 v/v) as eluent, and the third fraction was a desired product of **2.29** containing the title product was collected as reddish brown solid (0.0117 g, 7%). Recorded the ^{1}H NMR sample of **2.29** in two different solvents, Chloroform-*d* & Methylene Chloride-d_2, as shown below:

^{1}H NMR (500 MHz, Chloroform-*d*) δ 8.82 (d, *J* = 7.3 Hz, 2H), 8.78 (d, *J* = 7.3 Hz, 1H), 8.71 (dd, *J* = 8.1, 2.4 Hz, 1H), 8.59 (br s, 4H), 8.45-8.28 (m, 13H), 8.25 (d, *J* = 7.3 Hz, 3H), 8.18 (dd, *J* = 8.1, 2.4 Hz, 1H), 8.12 – 8.08 (m, 1H), 8.05 (dd, *J* = 7.3, 2.6 Hz, 3H), 8.03 (d, *J* = 3.0 Hz, 1H), 7.95 – 7.89 (m, 3H), 7.89 (d, *J* = 2.7 Hz, 1H), 7.85 (t, *J* = 7.2 Hz, 3H), 7.63 – 7.50 (m, 8H), 7.49 (d, *J* = 2.7 Hz, 1H), 7.47 (d, *J* = 2.9 Hz, 1H), 7.46 – 7.38 (m, 4H), 7.18 (t, *J* = 7.5 Hz, 3H), 6.79 – 6.76 (m, 1H), 6.53 (t, *J* = 8.6 Hz, 4H), 4.65 (t, *J* = 6.2 Hz, 2H), 4.33 (br s, 1H), 4.27

(br s, 1H), 3.57 (d, *J* = 13.5 Hz, 7H), 3.27 (dq, *J* = 15.6, 7.8 Hz, 8H), 2.37 – 2.26 (m, 2H), 2.06 (br s, 2H), 1.95 (br s, 2H), 1.79 (br s, 4H), 1.71 (br s, 6H), 0.95 (br s, 24H).

^{1}H NMR (500 MHz, Methylene Chloride-d_2) δ 8.83 (d, *J* = 7.1 Hz, 2H), 8.80 (s, 1H), 8.71 (d, *J* = 7.6 Hz, 1H), 8.53 (s, 4H), 8.45 – 8.16 (m, 14H), 8.15 – 7.76 (m, 14H), 7.71 – 7.31 (m, 14H), 7.23 (t, *J* = 7.4 Hz, 3H), 6.83 (d, *J* = 8.1 Hz, 1H), 6.65 – 6.50 (m, 4H), 4.65 (t, *J* = 6.5 Hz, 2H), 4.35 (br s, 1H), 4.28 (br s, 1H), 4.12 – 2.76 (br s, 16H), 2.30 (d, *J* = 9.8 Hz, 2H), 2.05 (br s, 2H), 1.94 (br s, 2H), 1.79 – 1.71 (2 x br s, 10H), 1.27 – 0.84 (br s, 24H).
A compound of **2.29** (118 protons) was observed. (MALDI-TOF): m/z = 2204.48 m/z. Chemical formula: $C_{134}H_{118}La_2N_{12}O_2$. UV-vis, (DCM)/nm (log ε): 398(5.8), 506(4), 595(3.8), 654(3.7), 730(3.9).

3.13 Synthesis of Lanthanum porphyrin triple-decker 2.30:

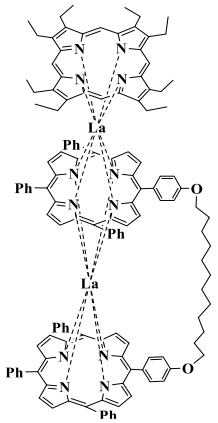

2.30

C_{12} porphyrin dyad **2.17** (0.078 g, 0.055 mmol) was mixed with 2 eq. (0.052 g, 0.11 mmol) of lanthanum (III) acetylacetonate hydrate and 0.9 eq. of octaethylporphyrin **2.1** (0.026 g, 0.05 mmol) in 5 ml from pentanol at 180°C for 3 days and 16 hrs in a sealed tube. Then, the solvent was removed under a stream of nitrogen. The crude was separated by column chromatography through silica gel using EtOAc/Hexane (3.3:100 v/v) as eluent, and the third fraction was a desired product of **2.30** containing the title product was collected as a reddish brown solid (0.0211g, ≈ 17%).
^{1}H NMR (500 MHz, Methylene Chloride-d_2) δ 8.79 (s, 3H), 8.66 (s, 2H), 8.60 – 8.18 (m, 16H), 8.14 (d, *J* = 7.7 Hz, 1H), 8.10 (d, *J* = 7.7 Hz, 1H), 8.04 (d, *J* = 8.5 Hz, 2H), 7.99 – 7.81 (m, 8H), 7.71 – 7.29 (m, 16H), 7.23 (d, *J* = 8.4 Hz, 4H), 6.78 (s, 1H), 6.58 – 6.46 (m, 4H), 4.63 (t, *J* = 6.3 Hz, 2H), 4.28 (2 x br s, 2H), 3.89 – 2.60 (br s,16H), 2.27 (br s, 2H), 2.01 (br s, 2H), 1.92 (br s, 2H), 1.75 (d, *J* = 7.1 Hz, 4H), 1.60 (br s, 10H), 1.07 (br s, 24H).

A compound **2.30** (122 protons) was observed. (MALDI-TOF): m/z = 2232.58 m/z). Chemical formula: $C_{136}H_{122}La_2N_{12}O_2$.

3.14 Synthesis of Neodymium porphyrins triple-decker 2.31:

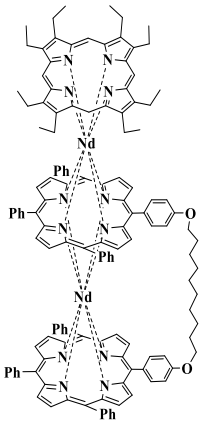

2.31

C_{10}-porphyrin dyad **2.5** (0.1g, 0.071 mmol) was mixed with 2 eq. (0.063 g, 0.14 mmol) of $Nd(acac)_3H_2O$ and 0.9 eq. of octaethylporphyrin **2.1** (0.0343 g, 0.064 mmol) in 5 ml pentanol at 180°C for 5 days in a sealed tube, solvent was removed under a stream of nitrogen. The crude was separated by column chromatography through silica gel using EtOAc/Hexane (3.3:100 v/v) as eluent, and the third fraction was a desired product of **2.31** containing the title product was collected as a reddish brown solid (0.011 g, ≈ 7%).

^{1}H NMR (500 MHz, Methylene Chloride-d_2) δ 8.49 (2x br s, 3H), 8.17 (s, 1H), 8.07 (s, 3H), 7.77 (s, 1H), 7.71 (s, 2H), 7.64 (s, 1H), 7.31 (s, 3H), 7.01 (s, 3H), 6.86 (s, 1H), 6.63 (s, 3H), 6.52 (d, *J*=10.7 Hz, 5H), 6.19 (s, 1H), 6.05 (s, 1H), 5.98 (s, 3H), 5.56 (s, 1H), 5.28 (s, 1H), 5.22 (s, 5H), 4.60 (s, 4H), 4.47 (s, 2H), 3.91 (s, 4H), 3.85 (br s, 2H), 3.76 (s, 3H), 3.67 (s, 2H), 3.57 (br s, 2H), 3.48 (s, 3H), 3.23 (br s, 8H), 2.66 (br s, 8H), 2.04 (s, 4H), 1.67 (s, 4H), 1.41 (br s, 10H), 1.21 – 1.11 (br s, 24H).

A compound of **2.31** (118 protons) was observed. Chemical formula: $C_{134}H_{118}Nd_2N_{12}O_2$. MS-(MALDI-TOF-MS): m/z = 2212.13 [M^+]. UV-vis, (DCM)/nm (log ε) :398(4.8), 506(4.2), 593(3.8), 649(3.6), 776(3.4).

3.15 Synthesis of homoleptic Neodymium triple-decker 2.32:

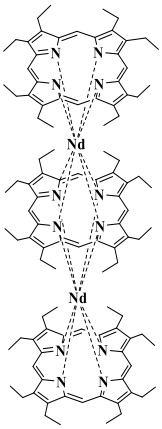

2.32

Compound **2.32** was collected as a side product from a previous reaction and obtained as a burgundy solid as a first fraction by column chromatography through silica gel using EtOAc/Hexane (3.3:100 v/v) as eluent in 10%. ^{1}H NMR (500 MHz, Toluene-d_8) δ 5.53 (s, 8H), 3.21 (dq, J = 15.5, 7.8 Hz, 16H), 3.01 (s, 4H), 2.62 (dq, J = 14.8, 7.6 Hz, 16H), 1.92 (q, J = 5 Hz, 16H), 1.40 (t, J = 7.2 Hz, 48H), 0.54 (t, J = 7.0 Hz, 24H). MALDI-TOF MS m/z 1879.59 [M^+]. Chemical formula: $C_{108}H_{132}Nd_2N_{12}$.

3.16 Synthesis of praseodymium triple-decker 2.33:

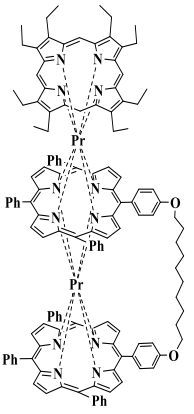

2.33

C_{10} porphyrin dyad **2.5** (0.1 g, 0.071 mmol) was mixed with 2 eq. (0.063 g, 0.14 mmol) of Pr $(acac)_3H_2O$ and 0.9 eq. of octaethylporphyrin **2.1** (0.0344 g, 0.06 mmol) in 5 ml pentanol at 180°C for 5 days, solvent was removed under a stream of nitrogen. The crude was separated by column chromatography through silica gel using EtOAc/Hexane (3.3:100 v/v) as eluent, and the third fraction was a desired product of **2.33** containing the title product was collected

as a reddish brown solid (0.011 g, 7%). ^{1}H NMR (500 MHz, Methylene Chloride-d_2) δ 9.29 – 9.12 (m, 3H), 8.97 (d, J = 8.5 Hz, 1H), 7.74 (s, 1H), 7.37 (t, J = 9.9 Hz, 3H), 6.87 (d, J = 8.4 Hz, 1H), 6.44 – 6.31 (m, 5H), 6.17 (s, 1H), 6.04 (s, 2H), 4.95 (d, J = 6.9 Hz, 3H), 4.89 – 4.75 (m, 8H), 4.40 (d, J = 7.5 Hz, 2H), 3.93 (s, 2H), 3.52 (d, J = 7.7 Hz, 1H), 3.38 (d, J = 7.1 Hz, 2H), 2.48 – 2.42 (m, 2H), 2.33 (2x br s, 7H), 2.06 – 1.98 (m, 2H), 1.67 (s, 14H), 1.30 (s, 12H), 1.25 (s, 13H), 0.89 – 0.81 (m, 8H), 0.78 – 0.67 (m, 7H), 0.63 – 0.50 (m, 5H), 0.45 (s, 1H), 0.38 (s, 1H), -0.97 – 1.16 (m, 4H), -1.57 – - 1.91 (m, 7H).

(MALDI-TOF): m/z = 2208.77 m/z. Chemical formula: $C_{134}H_{118}Pr_2N_{12}O_2$. UV-vis,(DCM)/nm (log ε) :399(5.8), 506(3.98), 595(3.81), 645(3.30), 753(3.5).

3.17 Synthesis of praseodymium triple-decker 2.35:

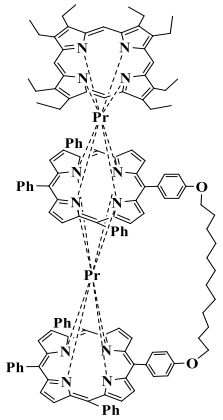

2.35

C_{12} porphyrin dyad **2.17** (0.1021g, 0.072 mmol) was mixed with 2 eq. (0.063g, 0.14 mmol) of Pr (acac)$_3$H$_2$O and 0.9 eq. of octaethyl porphyrin **2.1** (0.0345 g, 0.064 mmol) in 5 ml of pentanol at 180°C for 5 days. The solvent was removed under a stream of nitrogen. The crude was separated by column chromatography through silica gel using EtOAc/Hexane (3.3:100 v/v) as eluent, and the third fraction was a desired product of **2.35** containing the title product was collected as a reddish brown solid (0.020 g, 13%).

^{1}H NMR (500 MHz, Methylene Chloride-d_2) δ 9.36 – 9.30 (2 x br s, 3H), 9.14 – 9.05 (2 x br s, 3H), 7.43 – 7.41 (2 x br s, 2H), 7.34 (s, 2H), 6.90 (d, J = 8.5 Hz, 2H), 6.56 – 5.97 (m, 13H), 5.05 – 4.73 (m, 12H), 4.40 (dd, J = 17.3, 7.4 Hz, 3H), 4.14 (s, 2H), 4.01 – 3.82 (m, 4H), 3.52 (d, J = 7.7 Hz, 1H), 3.38 – 3.26 (m, 2H), 2.43 (t, J = 6.6 Hz, 10H), 2.05 (s, 1H), 1.93 (s, 1H),1.76 (s, 11H), 1.41 – 1.17 (m, 14H), 0.97 (s, 2H), 0.39 - 0.58 (m, 13H), 0.58 (s, 6H), 0.34 – 0.31 (2 x br s, 4H), -1.13 (s, 4H), -1.62 – -1.90 (m, 7H). MS (MALDI-TOF):m/z= 2235.50 [M$^+$]. Chemical formula: $C_{136}H_{122}Pr_2N_{12}O_2$.

3.18 Synthesis of Lanthanum triple-decker 2.41:

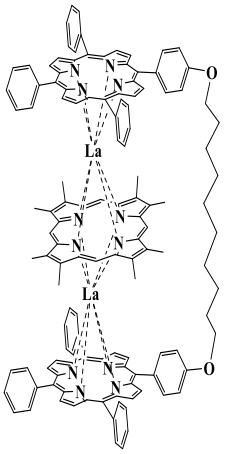

2.41

C_{10} porphyrin dyad **2.5** (1g, 0.071 mmol) was mixed with 2 eq. of La (III) acetylacetonate hydrate (0.068 g, 0.14 mmol) and 0.9 eq. of octamethyl porphyrin **2.38** (0.027g, 0.064 mmol) all dissolved in 6 ml of pentanol in a sealed tube. The mixture was set up to reflux at 180 ºC for 5 days the solvent was removed by distillation under reduced pressure, and the crude was separated by column chromatography through silica gel using (1:1), increased to (3:1) DCM: Pet-ether respectively to collect the fourth fraction was a desired product **2.41** in a small amount. We collect the desired product of TD **2.41** (trace) as reddish-brown material.^{1}H NMR is not achieved due to a trace amount of desired product **2.41**. MS(MALDI-TOF): m/z = 2091.67 [M^+]. Chemical Formula: $C_{126}H_{102}La_2N_{12}O_2$.

3.19 Synthesis of Lanthanum triple-decker 2.45:

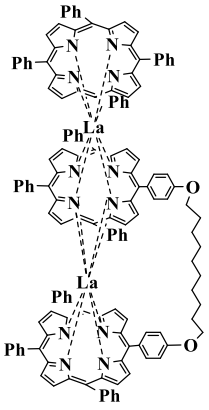

2.45

C_{10}-dyad **2.5** (0.1g, 0.071 mmol) was mixed with 2 eq. of La (III) acetylacetonate hydrate (0.068g, 0.14 mmol) and 0.9 eq. of tetraphenyl porphyrin **2.10** (0.0394g, 0.064 mmol), all dissolved in 6 ml of pentanol in a sealed tube. The mixture was set up to reflux at 180 ºC for 5

days then solvent was removed by distillation under reduced pressure, and the crude was separated by column chromatography through silica gel using (3:1) DCM: Pet-ether to collect the third fraction of desired product **2.45** a dark greenish brown material in trace yield. ^{1}H NMR is not achieved due to complicated signals in the diluted sample and very broad signals, especially in the aromatic range in the spectrum. MS(MALDI-TOF): m/z = 2287.42 [M^{+}]. Chemical Formula: $C_{142}H_{102}La_2N_{12}O_2$.

References:

(1). González-Lucas, D.; Soobrattee, S.C.; Hughes, D.L.; Tizzard, G.J.; Coles, S.J.; Cammidge, A.N. Straightforward and Controlled Synthesis of Porphyrin–Phthalocyanine–Porphyrin Heteroleptic Triple-Decker Assemblies. Chemistry -A European Journal, **2020**, 26 (47), 10724-10728.

(2). Jiang, J.; Ng, D.K. A Decade Journey in the Chemistry of Sandwich-Type Tetrapyrrolato−Rare Earth Complexes. Accounts Chem. Res, **2009**, 42 (1), 79-88.

(3). Shi, Y.; Zhang, F.; Linhardt, R.J. Porphyrin-based compounds and their applications in materials and medicine. Dyes Pigments, **2021**, 188, 109136.

(4). Adler, A.D.; Longo, F.R.; Finarelli, J.D.; Goldmacher, J.; Assour, J.; Korsakoff, L. A simplified synthesis for meso-tetraphenyl porphine. J. Org. Chem, **1967**, 32 (2), 476.

(5). Little, R.G. The mixed-aldehyde synthesis of difunctional tetraarylporphyrins. J. Heterocyclic Chem, 1981, 18 (1), 129-133.

(6). González Lucas, D., **2014**. Molecular machines constructed from multi-chromophore arrays (Doctoral dissertation, University of East Anglia).

(7). Aljuhani Ateyatallah., **2014**. Covalently linked dyads and Triads of Phthalocyanines and Porphyrins (Doctoral dissertation, University of East Anglia).

(8). Camilla Soobratte.S., **2016**. Controlled synthesis of lanthanide-bridged porphyrin -phthalocyanine triple deckers (Master Dissertation), University of East Anglia.

(9). Gouterman, M. Study of the effects of substitution on the absorption spectra of porphin. The Journal of Chemical Physics, **1959**, 30(5), pp.1139-1161.

(10). Gouterman, M. Spectra of porphyrins. Journal of Molecular Spectroscopy, **1961**, 6, pp.138-163.

(11). Whitten, D.G., Lopp, I.G. and Wildes, P.D. Fluorescence of zinc and magnesium etioporphyrin. I. Quenching and wavelength shifts due to complex formation. Journal of the American Chemical Society, **1968**, 90(26), pp.7196-7200.

(12). Rubio, M., Roos, B.O., Serrano-Andrés, L. and Merchán, M. Theoretical study of the electronic spectrum of magnesium-porphyrin. The Journal of Chemical Physics,**1999**, 110(15), pp.7202-7209.

(13). Sun, X.; Li, D.; Chen, G.; Zhang, J. A series of new porphyrin dyads: The synthesis and photophysical properties. Dyes Pigments, **2006**, 71 (2), 118-122.

(14). Wang, D.; Cheng, X.; Shi, Y.; Sun, E.; Tang, X.; Zhuang, C.; Shi, T. Synthesis and different substituent effects on spectral and electrochemical properties of porphyrin nicotinic acid binary compounds. Sol. State Sci, **2009**, 11, 195-199.

(15). McKeown, N.B. Phthalocyanine materials: synthesis, structure and function (No.6). Cambridge university press, **1998**.

(16). Breloy, L., Yavuz, O., Yilmaz, I., Yagci, Y. and Versace, D.L. Design, synthesis and use of phthalocyanines as a new class of visible-light photoinitiators for free-radical and cationic polymerizations. Polymer Chemistry, **2021**,12(30), pp.4291-4316.

(17). Martynov, A.G., Zubareva, O.V., Gorbunova, Y.G., Sakharov, S.G. and Tsivadze, A.Y. Synthesis, spectral properties and supramolecular dimerisation of heteroleptic triple-decker phthalocyanignato complexes with one outer crown-substituted ligand. Inorganica Chimica Acta, **2009**, 362(1), pp.11-18.

(18). Birin, K.P., Gorbunova, Y.G. and Tsivadze, A.Y. Efficient scrambling-free synthesis of heteroleptic terbium triple-decker (porphyrinato)(crown-phthalocyaninates). Dalton Transactions, **2012**, 41(32), pp.9672-9681.

(19). Birin, K.P., Gorbunova, Y.G. and Tsivadze, A.Y. Selective one-step synthesis of triple-decker (porphyrinato)(phthalocyaninato) early lanthanides: the balance of concurrent processes. Dalton Transactions. **2011**, 40(43), pp.11539-11549.

(20). Birin, K.P.; Poddubnaya, A.I.; Gorbunova, Y.G.; Tsivadze, A.Y. Revisiting the One-Step Synthesis of Heteroleptic Lanthanide (III) (Porphyrinato)(Phthalocyaninates): Opportunities and Limitations. Макрогетероциклы, **2017**, 10 (4-5), 514-519.

(21). Mironov, A.F. Lanthanide porphyrin complexes. Russian Chemical Reviews, **2013**, 82(4), p.333.

(22). Spyroulias, G.A., De Montauzon, D., Maisonat, A., Poilblanc, R. and Coutsolelos, A.G. Synthesis, UV-visible and electrochemical studies of lipophilic and hydrophilic lanthanide (III) bis (porphyrinates). Inorganica chimica acta, **1998**, 275, pp.182-191.

(23). Muhammed Alhunayhin.S., **2017**. Triple-decker assemblies based on porphyrins (Master Dissertation), University of East Anglia.

(24). Zhang, J.X., Chan, W.L., Xie, C., Zhou, Y., Chau, H.F., Maity, P., Harrison, G.T., Amassian, A., Mohammed, O.F., Tanner, P.A. and Wong, W.K. Impressive near-infrared brightness and singlet oxygen generation from strategic lanthanide–porphyrin double-decker complexes in aqueous solution. Light: Science & Applications, **2019**, 8(1), p.46.

(25) . Chandran, K., Nithya, R., Sankaran, K., Gopalan, A. and Ganesan, V. Synthesis and characterization of sodium alkoxides. Bulletin of Materials Science, **2006**, 29, pp.173-179.

(26). Binnemans, K. Rare-earth beta-diketonates. Handbook on the physics and chemistry of rare earths, **2005**, 35(5), pp.123.

(27). Buchler Johann;Acian Andre et al. Cerium (IV) Bis (Octaethylporphyrinate) and Dicerium (III)Tris (Octaethylporphyrinate): parents of New Family of Lanthanoid Double - Decker and Triple Decker, American Chemical Society. **1986**, 108,3652-3659.

(28). Buchler, J.; Acian, A.; et al. Cerium(IV) Bis(octaethylporphyrinate) and Dicerium(III) Tris(octaethylporphyrinate): Parents of a New Family of Lanthanoid Double-Decker and Triple-Decker Complexes. J. Am. Chemical. Society. **1986**, 108 (10), 3652–3659.

(29). Buchler, J.W., Kihn-Botulinski, M., Loeffler, J. and Wicholas, M. Metal complexes with tetrapyrrole ligands. Hydrogen-1 NMR spectrum of dicerium (III) tris (octaethylporphyrinate), Ce_2 $(OEP)_3$: evidence for alkyl group steric interaction. Inorganic Chemistry. **1989**, 28(19), pp.3770-3772.

(30). Jin, H.G., Jiang, X., Kuhne, I.A., Clair, S., Monnier, V., Chendo, C., Novitchi, G., Powell, A.K., Kadish, K.M. and Balaban, T.S. Microwave-mediated synthesis of bulky lanthanide porphyrin–phthalocyanine triple-deckers: Electrochemical and magnetic properties. Inorganic Chemistry. **2017**, 56(9), pp.4864-4873.

(31) Milgrom, L. R. The Colours of Life: An Introduction to the Chemistry of Porphyrins and Related Compounds; Oxford University Press: Oxford, **1997**.

(32). Duchowski, J.K. and Bocian, D.F. Spectroscopic characterization of triple-decker lanthanide porphyrin sandwich complexes. Effects of strong π π interactions in extended assemblies. Journal of the American Chemical Society. **1990**,112(24), pp.8807-8811.

(33). Sheehan, J. C.; Hess, G. P., A New Method of Forming Peptide Bonds. Journal of the American Chemical Society **1955**, 77 (4), 1067-1068.

(34). Neises, B.; Steglich, W., Simple Method for the Esterification of Carboxylic Acids. Angewandte Chemie International Edition in English.**1978**, 17 (7), 522-524.

(35). Gharibi, N.; Kailass, K.; Beharry, A. A. Exploiting the Cellular Redox-Control System for Activatable Photodynamic Therapy. ChemBioChem.**2019**, 20 (3), 345–349.

4. Appendices:

Crystal structure analysis of $[C_{10}H_{20}O_{20})$-$(C_{44}H_{27}N_4La)_2$-$(C_{36}H_{44}N_4)]$, *ca* C_2

Crystal data: $C_{134}H_{118}La_2N_{12}O_2$, *ca* C_2, M = 2230.24. Triclinic, space group P-1 (no. 2), a = 15.9006(7), b = 16.9764(8), c = 21.3450(11) Å, α = 80.029(4), β = 85.050(4), γ = 71.193(4) °, V = 5368.9(4) $Å^3$. Z = 2, Dc = 1.380 g cm^{-3}, F (000) = 2296, T = 99.97(12) K, μ(Cu-Kα) = 65.4 cm^{-1}, λ(Cu-Kα) = 1.54184 Å.

The crystal was a purple cuboid. From a sample under oil, one, *ca* 0.16 x 0.21 x 0.37 mm, was mounted on a small loop and fixed in the cold nitrogen stream on a Rigaku Oxford Diffraction XtaLAB Synergy diffractometer, equipped with Cu-Kα radiation, HyPix detector and mirror monochromator. Intensity data were measured by thin-slice ω-scans. Total no. of reflections recorded to θ_{max} = 72.5°, was 11127 of which 7455 were unique (Rint = 0.025); 6423 were 'observed' with $I > 2\sigma_I$. Note: the number of possible reflections is 20205; only a minor portion of the complete dataset has been recorded.

Data were processed using the CrysAlisPro-CCD and -RED (1) programs. The structure was determined by the intrinsic phasing routines in the SHELXT program (2A) and refined by full-matrix least-squares methods, on F^2's, in SHELXL (2B). Most of the non-hydrogen atoms were refined with anisotropic thermal parameters; there are regions of disorder in the molecule, e.g., in the bridging $O(CH_2)_{10}O$ group and in two of the ethyl groups, where atoms were refined isotropically. Very few hydrogen atoms were located in difference maps; all hydrogen atoms were included in idealised positions and their Uiso values were set to ride on the Ueq values of the parent carbon atoms. At the conclusion of the refinement, wR_2 = 0.147 and R_1 = 0.058 (2B) for all 7455 reflections weighted $w = [\sigma^2(F_o^2) + (0.1003\ P)^2 + 6.1691\ P]^{-1}$ with $P = (F_o^2 + 2F_c^2)/3$; for the 'observed' data only, R_1 = 0.051.

In the final difference map, the highest peak (*ca* 0.6 $eÅ^{-3}$) was near La (2).

Scattering factors for neutral atoms were taken from reference (3). Computer programs used in this analysis have been noted above and were run through WinGX (4) on a Dell Optiplex 780 PC at the University of East Anglia.

References

1) Programs CrysAlisPro, Rigaku Oxford Diffraction Ltd., Abingdon, UK (2018).
2) G. M. Sheldrick, Programs for crystal structure determination (SHELXT), *Acta Cryst.* (2015) A**71**, 3-8, and refinement (SHELXL), *Acta Cryst.* (2008) A**64**, 112-122 and (2015) C**71**, 3-8.
3) *'International Tables for X-ray Crystallography'*, Kluwer Academic Publishers, Dordrecht (1992). Vol. C, pp. 500, 219 and 193.
4) L. J. Farrugia, *J. Appl. Cryst.* (2012) **45**, 849–854.

Legends for Figures

Figure 1. View of a molecule of the La_2-triple-deck complex, indicating the atom numbering scheme. Thermal ellipsoids are drawn at the 50% probability level.

Figure 2. Details of the 'loop' between adjacent porphyrin planes; the disorder in this region has not been fully resolved.

Notes on the structure

The molecule is very similar in shape to that of the praseodymium complex below.

Crystal structure analysis of (Pr_2 triple-decker porphyrin with $O(CH_2)_{12}$-O link), plus solvent molecules

Crystal data: $C_{136}\,H_{122}\,N_{12}\,O_2\,Pr_2$, *ca* ($C_{8.39}\,N_{3.06}\,Cl_{7.29}$), M = 2640.16. Monoclinic, space group $P2_1/c$ (no. 14), a = 24.9526(2), b = 24.080(3), c = 21.5688(3) Å, β = 100.0578(10) °, V = 12,761.1(3) $Å^3$. Z = 4, Dc = 1.378 g cm^{-3}, F(000) = 5422, T = 100(2) K, μ(Cu-Kα) = 77.0 cm^{-1}, λ(Mo-Kα) = 1.54184 Å.

The crystal was a purple block. From a sample under oil, one, *ca* 0.05 x 0.08 x 0.17 mm, was mounted on a small loop and fixed in the cold nitrogen stream on a Rigaku Oxford Diffraction XtaLAB Synergy diffractometer, equipped with Cu-Kα radiation, HyPix detector and mirror monochromator. Intensity data were measured by thin-slice ω-scans. Total no. of reflections recorded, to θ_{max} = 70.0 °, was 94,481 of which 23,815 were unique (Rint = 0.055); 19,448 were 'observed' with $I > 2\sigma_I$.

Data were processed using the CrysAlisPro-CCD and -RED (1) programs. The structure was determined by the intrinsic phasing routines in the SHELXT program (2A) and refined by full-matrix least-squares methods, on F^2's, in SHELXL (2B). In the principal (porphyrin) molecule, the non-hydrogen atoms were refined with anisotropic thermal parameters. Hydrogen atoms were included in idealised positions and their Uiso values were set to ride on the Ueq values of the parent carbon atoms. Solvent molecules, mostly chloroform, were located, disordered, at each end of the triple-decker complex molecule and many more difference peaks were observed and included as partially occupied carbon or nitrogen atoms in the refinement process, but their parent molecules were not fully identified. At the conclusion of the refinement, wR_2 = 0.186 and R_1 = 0.075 (2B) for all 23,815 reflections weighted $w = [\sigma^2(F_o^2) + (0.1206\ P)^2 + 12.658\ P]^{-1}$ with $P = (F_o^2 + 2F_c^2)/3$; for the 'observed' data only, R_1 = 0.062.

In the final difference map, the highest peak (*ca* 1.5 $eÅ^{-3}$) was near Pr(2).

Scattering factors for neutral atoms were taken from reference (3). Computer programs used in this analysis have been noted above, and were run through WinGX (4) on a Dell Optiplex 780 PC at the University of East Anglia.

References

1) Programs CrysAlisPro, Rigaku Oxford Diffraction Ltd., Abingdon, UK (2023).

2) G. M. Sheldrick, Programs for crystal structure determination (SHELXT), *Acta Cryst.* (2015) A**71**, 3-8, and refinement (SHELXL), *Acta Cryst.* (2008) A**64**, 112-122 and (2015) C**71**, 3-8.
3) *'International Tables for X-ray Crystallography'*, Kluwer Academic Publishers, Dordrecht (1992). Vol. C, pp. 500, 219 and 193.
4) L. J. Farrugia, *J. Appl. Cryst.* (2012) **45**, 849–854.

Legends for Figures

Figure 1. View of the Pr_2 triple-decker porphyrin with an $O(CH_2)_{12}O$ link, with adjoining chloroform solvent molecules, indicating the atom numbering scheme. Thermal ellipsoids are drawn at the 20% probability level.

Figure 2. View along the Pr…Pr vector showing the chloroform molecule of Cl(82-84) in the foreground and the Cl(72-74) molecule almost hidden in the background. The ethyl and phenyl substituent groups are not shown.

Notes on the structure

The triple-decker porphyrin molecule was clearly identified and refined and is shown in Figures 1 and 2. The three porphyrin derivative molecules are arranged in parallel planes which are linked in a sandwich arrangement and connected through the praseodymium atoms. Each Pr atom is eight-coordinate, bonded to the four central nitrogen atoms of a pair of porphyrin molecules; the coordination pattern of both Pr atoms is square antiprismatic; the N_4 square plane of N(1),N(11),N(21),N(31) is rotated *ca* 10.8 ° about the Pr…Pr vector from the corresponding plane of N(81),N(91),N(101),N(111).

The loop linking two of the porphyrin rings runs from the para position C(40) of one phenyl ring to the para position C(70) of a phenyl ring of a neighbouring porphyrin ring. The $O(CH_2)_{12}O$ link appears well defined and consists of a chain with a *trans-(cis-trans-trans)$_3$-cis* conformation.

The solvent molecules have not all been identified; most show disorder. There are partially occupied chloroform molecules at each end of the stack of porphyrin molecules, each arranged with the C-H bond directed towards the centre of the N_4 group of the porphyrin molecule and the Pr atom; the C(971)…Pr(2) and C(981)… Pr(1) distances are 4.353 Å and 4.261 Å and the shortest C(chloroform)…N distances are C(971)…N(91) at 3.469 Å and C(981)…N(1) at

3.425 Å. These major $CHCl_3$ molecules are overlaid by minor chloro compounds, either more chloroform or perhaps CH_2Cl_2 molecules. And beyond these molecules there is a further partially occupied $CHCl_3$ molecule and an assortment of lighter atoms designated as either C or N atoms, with a range of occupancy factors, but of unrecognised molecules.